comptes rendus
palevol
2024 • 23 • 23

The remarkable record of mustelids from Hunas (Bavaria, Germany)

Adrian MARCISZAK, Brigitte HILPERT & Dieta AMBROS

art. 23 (23) — Published on 4 September 2024
www.cr-palevol.fr

PUBLICATIONS SCIENTIFIQUES

Couverture / Cover :
Credits: Marc Pascual, Pixabay: https://pixabay.com/fr/photos/belette-mostela-must%C3%A9lido-regardez-4412559/

Comptes Rendus Palevol est indexé dans / Comptes Rendus Palevol *is indexed by:*
– Cambridge Scientific Abstracts
– Current Contents® Physical
– Chemical, and Earth Sciences®
– ISI Alerting Services®
– Geoabstracts, Geobase, Georef, Inspec, Pascal
– Science Citation Index®, Science Citation Index Expanded®
– Scopus®.

Les articles ainsi que les nouveautés nomenclaturales publiés dans *Comptes Rendus Palevol* sont référencés par / *Articles and nomenclatural novelties published in* Comptes Rendus Palevol *are registered on:*
– ZooBank® (http://zoobank.org)

Comptes Rendus Palevol est une revue en flux continu publiée par les Publications scientifiques du Muséum, Paris et l'Académie des sciences, Paris
Comptes Rendus Palevol *is a fast track journal published by the Museum Science Press, Paris and the Académie des sciences, Paris*

Les Publications scientifiques du Muséum publient aussi / *The Museum Science Press also publish:*
Adansonia, ***Geodiversitas***, ***Zoosystema***, ***Anthropozoologica***, ***European Journal of Taxonomy***, ***Naturae***, ***Cryptogamie*** **sous-sections** ***Algologie***, ***Bryologie***, ***Mycologie***.

L'Académie des sciences publie aussi / *The Académie des sciences also publishes:*
Comptes Rendus Mathématique, ***Comptes Rendus Physique***, ***Comptes Rendus Mécanique***, ***Comptes Rendus Chimie***, ***Comptes Rendus Géoscience***, ***Comptes Rendus Biologies***.

Diffusion – Publications scientifiques Muséum national d'Histoire naturelle
CP 41 – 57 rue Cuvier F-75231 Paris cedex 05 (France)
Tél. : 33 (0)1 40 79 48 05 / Fax : 33 (0)1 40 79 38 40
diff.pub@mnhn.fr / https://sciencepress.mnhn.fr

Académie des sciences, Institut de France, 23 quai de Conti, 75006 Paris.

ISSN (imprimé / *print*) : 1631-0683/ ISSN (électronique / *electronic*) : 1777-571X

The remarkable record of mustelids from Hunas (Bavaria, Germany)

Adrian MARCISZAK
Department of Paleozoology, University of Wrocław,
Sienkiewicza 21, 50-335 Wrocław (Poland)
adrian.marciszak@uwr.edu.pl (corresponding author)

Brigitte HILPERT
Dieta AMBROS
GeoZentrum Nordbayern, Paleobiology, Friedrich-Alexander University Erlangen-Nürnberg,
Loewenichstrasse 28, 91054 Erlangen (Germany)
brigitte-hilpert@gmx.de
dieta.ambros@fau.de

Submitted on 13 April 2024 | Accepted on 25 June 2024 | Published on 4 September 2024

urn:lsid:zoobank.org:pub:315BC2E8-5F5D-4F57-A265-B625969F5A3A

Marciszak A., Hilpert B. & Ambros D. 2024. — The remarkable record of mustelids from Hunas (Bavaria, Germany). *Comptes Rendus Palevol* 23 (23): 339-383. https://doi.org/10.5852/cr-palevol2024v23a23

ABSTRACT
The mustelid assemblage from Hunas is represented by seven species: *Gulo gulo gulo* (Linnaeus, 1758), *Meles meles* (Linnaeus, 1758), *Lutra lutra groissii* Heller, 1983, *Martes martes* (Linnaeus, 1758), *Mustela putorius* Linnaeus, 1758, *Mustela erminea* Linnaeus, 1758 and *Mustela nivalis* Linnaeus, 1766. Most species have been found in the G1-G3 complex, while their remains in other layers are rare. The guild is dominated by remains of *Mustela nivalis*, for which well-preserved and stratified material shows a large, robust weasel, with a notable predominance of males. The morphology of *Mustela nivalis*, together with the occurrence of *Lutra lutra* (Linnaeus, 1758), allowed us to estimate the age of the horizon at MIS 7.

KEY WORDS
Morphology, assemblage, biochronology, paleobiology.

RÉSUMÉ
Le remarquable signalement des mustélidés de Hunas (Bavière, Allemagne).
L'assemblage des mustélidés de Hunas est représenté par sept espèces : *Gulo gulo gulo* (Linnaeus, 1758), *Meles meles* (Linnaeus, 1758), *Lutra lutra groissii* Heller, 1983, *Martes martes* (Linnaeus, 1758), *Mustela putorius* Linnaeus, 1758, *Mustela erminea* Linnaeus, 1758 et *Mustela nivalis* Linnaeus, 1766. La plupart des espèces ont été trouvées dans le complexe G1-G3, tandis que leurs restes dans d'autres couches sont rares. La guilde est dominée par les restes de *Mustela nivalis*, pour lesquels un matériel bien conservé et stratifié montre une grande belette robuste, avec une prédominance notable de mâles. La morphologie de *Mustela nivalis*, ainsi que la présence de *Lutra lutra* (Linnaeus, 1758), nous ont permis d'estimer l'âge de l'horizon à MIS 7.

MOTS CLÉS
Morphologie, assemblage, biochronologie, paléobiologie.

INTRODUCTION

Small mustelids are good models to study inter-population morphological variation due to their extraordinary vast geographical range and extreme sensitivity to climate caused (Heptner & Naumov 1967; King & Moors 1979; King 1989). Size variation is mainly influenced by local climatic conditions, intraspecific variability and, particularly, expanded sexual dimorphism (King & Powell 2007; Marciszak & Socha 2014). Species from the genus *Mustela* Linnaeus, 1758 are cosmopolitan and do not follow Bergmann's rule (Kratochvíl 1951, 1977a, b; Erlinge 1975, 1979, 1987; King 1989; Abramov & Baryshnikov 2000; Marciszak *et al.* 2021). The smallest specimens are found on the northern fringes of the distribution range, while the largest ones occur in the Mediterranean regions (King & Powell 2007; Marciszak & Socha 2014).

While size variation of *Mustela erminea* Linnaeus, 1758 and *Mustela nivalis* Linnaeus, 1766 has been well documented for the extant populations (Abramov & Baryshnikov 2000; King & Powell 2007), so far little research has been done on the fossil material of the two species. The main problem is the small number of localities with sufficiently abundant, well-stratified material that would permit variation analysis. At present, only a few European sites are known to hold sufficient material, consisting of at least 30 or more individuals, for palaeoecological analysis. Among them are the Austrian Schusterlucke (Galik 1997a, b), French Aven I Abimes de la Fage (Hugueney 1975) and Baume de Gigny (Delpech 1989), Hungarian Istallöskö (Jánossy 1955) and Puskaporos (Kormos 1911), Polish Biśnik Cave (Marciszak & Socha 2014) and German Hunas (Heller 1983a, d, e). Mustelid material from some sites like Aven I Abimes de la Fage (Hugueney 1975), Baume de Gigny (Delpech 1989) or Biśnik Cave (Marciszak & Socha 2014) was studied in detail and published.

Mustelid remains from Hunas were never properly studied, which caused that many mistakes and incorrect determinations appeared. The mustelid faunal list presented by Heller (1965, 1966, 1983a-c) included some ancient species *Mustela* cf. *stromeri*, *Mustela* aff. *palerminea* and *Mustela* aff. *praenivalis*. Their presence is in clear contradiction with speleothem dates and the remaining faunal elements (Ambros 2006). The profile bottom in Hunas has been dated with 230Th/234U with a median age of *c.* 221 kya (Hennig *et al.* 1983). A new U-series age for the youngest speleothem generation falls again into a similar time window of *c.* 250 kya (J. Fietzke & M. López Correa pers. comm.), providing a theoretical maximum age constraint for the cave sediments. In this context the presence of a certain taxon should not related to chronostratigraphic setting of the site. If fossil remains are indicative of a specific species, should be referred to this taxon. Specific attribution should not be done based on chrononological ground. Following this line of conclusions, the main aim of this paper is a detailed morphometrical study of the fossil mustelid material from Hunas and clarification of their taxonomic determination. The obtained results are also discussed in broader European biochronological and paleoecological contexts.

Fig. 1. — Location of Hunas site within Germany.

SITE

The cave ruin of Hunas (49°30'17.0"N, 11°32'41.0"E, 520 m a.s.l.) is situated in the quarry of the Sebald Zement company, Hartmannshof, on the eastern slope of the Steinberg, in the central part of the Franconian Alb, about 40 km east of Nürnberg (Fig. 1). Colloquially it is known as the "Höhlenruine von Hunas" (Hunas for short) and is one from 23 caves with finds of Middle Palaeolithic age (mostly Neanderthals) in the Franconian Alb. The cave is embedded in the dolomite of Jurassic age, typical for the Franconian Alb, of the Middle Kimmeridgian (Malm Delta) (Hilpert 2005, 2006).

The cave was discovered in 1956 by Florian Heller. The northern part of the cave ruin was excavated between 1956 and 1964. The southern part, closer to the supposed entrances, was excavated between 1983 and 2012 (Heller 1983a-c; Hilpert 2005, 2006; Ambros & Hilpert 2023). The former cave of Hunas probably consisted of a single large cave room that was filled in with sediments. At the thickest point, these reached 12 m (Fig. 2). The base is formed by a speleothem with a few stalagmites and extensive floor sinter. Erosion blurred the traces of the entrances. The whole stratigraphic sequence was investigated (Ambros & Hilpert 2023). The sequence shows a series of sediments of various compositions (Fig. 3). The brown, grey and yellowish sediments are mainly built from fine-grained sands and silts, mixed with dolostone blocks of different size (Appendix 1; Fig. 2).

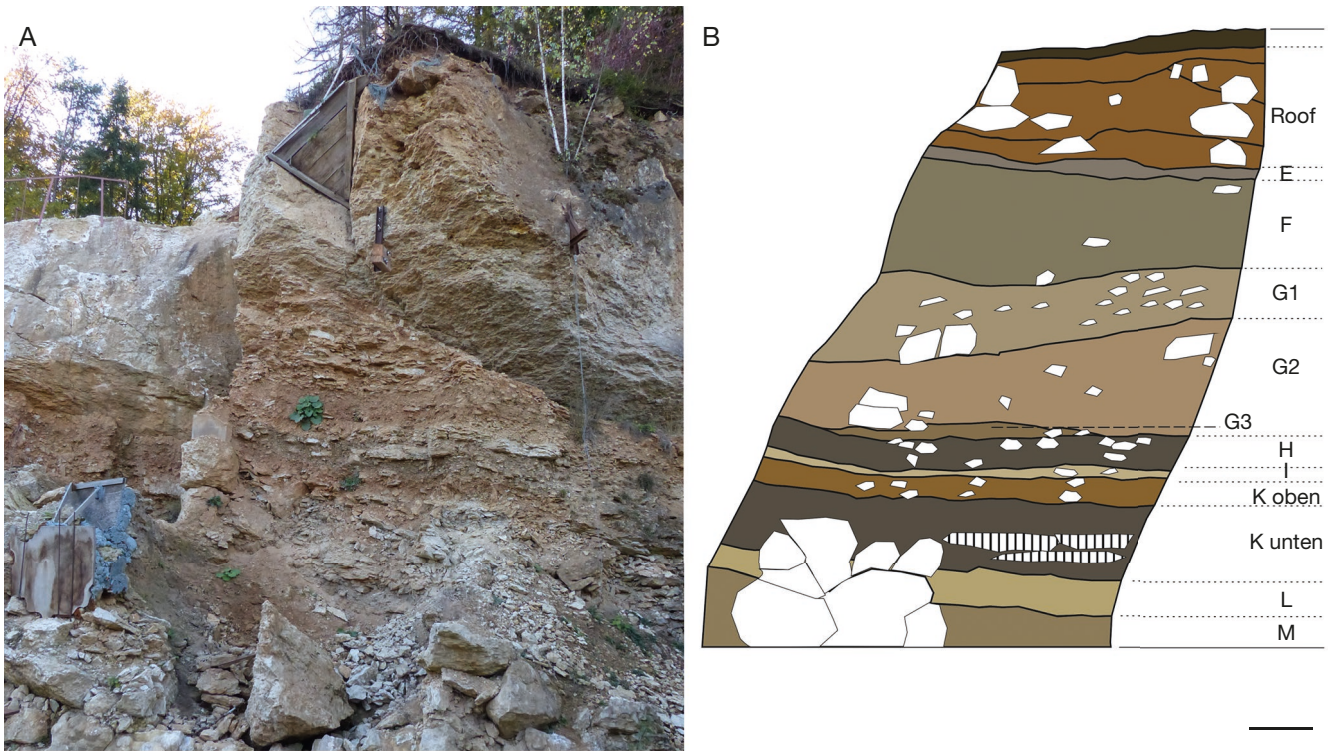

Fig. 2. — Profile of Hunas (**A**) and the sequence of layers in the profile (**B**). For détails of the separate layers in **B**, see Appendix 1. Scale bar: 1 m. Credits: B, P. Sessler 1964.

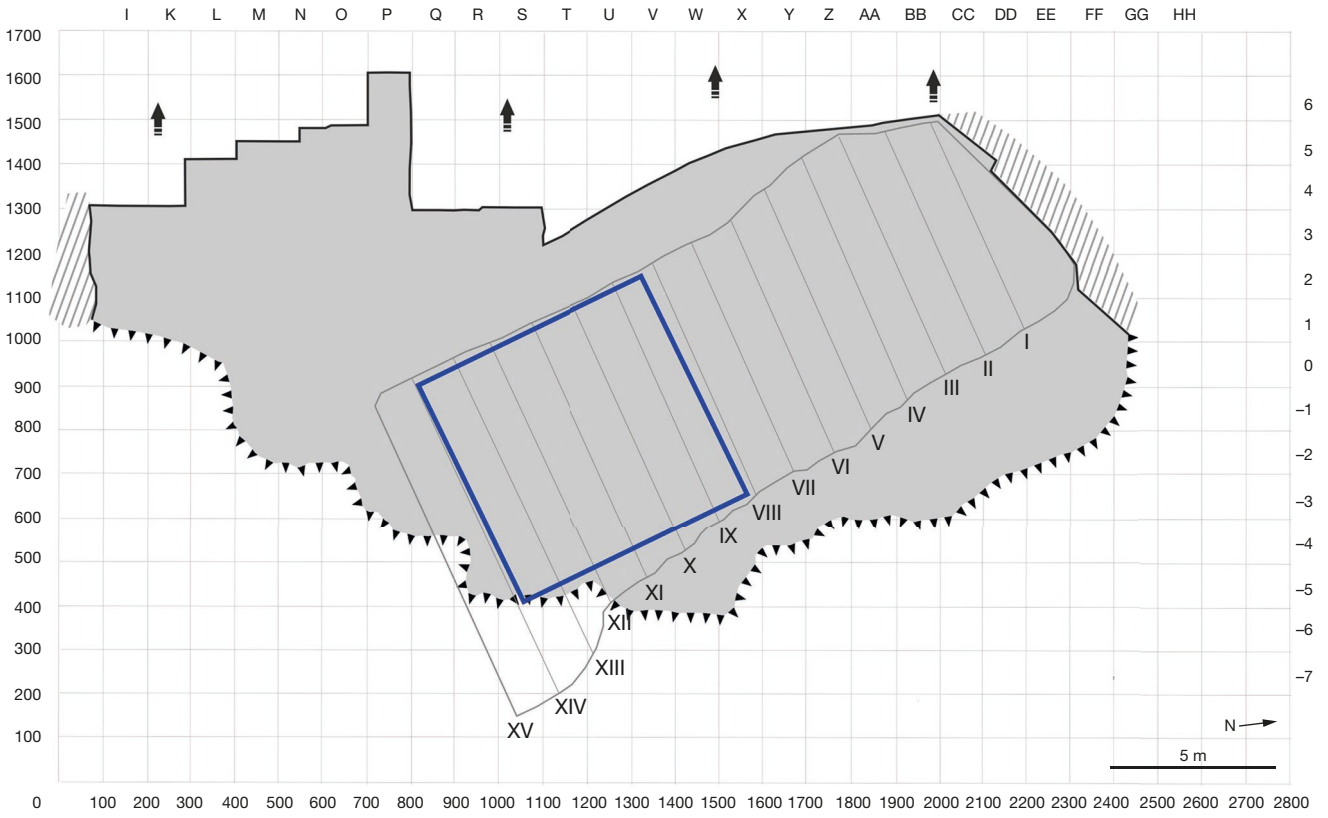

Fig. 3. — Horizontal profile of excavation and area of mustelid finds from Hunas: **I**-**XV**, profiles from the excavation of Florian Heller (1956-1964). **Grey area**, complete area of excavations (1956-1964 and 1983-2012); **blue square**, area of mustelid finds.

As a result of excavations, 148 taxa have been identified thus far: 14 snails, 5 fishes, 4 amphibians, 6 reptiles, 35 birds and 84 mammals (10 insectivores, 6 bats, 2 lagomorphs, 38 rodents, 2 primates, 14 carnivores, 3 perissodactyls and 9 artiodactyls (Appendix 2; Heller 1963a, b, 1965, 1966, 1983d, e; Schütt & Hemmer 1978; Groiss 1983, 1985, 1986; Jánossy 1983; Stadie 1983; Adam 1986; Carls 1986; Carls *et al.* 1988a, b; Fetscher 1996; Ehrlinger 1997; Karwath 1998; Koenigswald & Heinrich 1999; Kowalski 2001; Ambros 2003, 2006; Hilpert 2005, 2006; Ambros *et al.* 2005; Alt *et al.* 2006; Baumann 2011; Böhme 2011; Marciszak *et al.* 2019). The occurrence of small mustelids is almost exclusively restricted to the "G" complex in the overall Hunas stratigraphic sequence (Fig. 3). Mustelid remains, especially those of *M. nivalis*, were gathered in places where owl rests and nests. Due to the long-term accumulation of pellets, an unusually high number of *M. nivalis* remains have accumulated (Fig. 3)

MATERIAL AND METHODS

The mustelids material from Hunas is stored at the GeoZentrum Nordbayern, Lehrstuhl Paläoumwelt, Friedrich-Alexander-Universität Erlangen-Nürnberg. All available bones were re-examined during this study. A catalogue list was created with detailed descriptions of the specimens, including previous determinations (Appendix 3). For comparison, we used mustelid materials from various Central European sites, dated on the last 600 kya. Most were measured by the author A.M.; otherwise, it is indicated in the text with the appropriate citation. We also used for comparison remains of extant *Gulo gulo* Ambros, 2005, *Meles meles* (Linnaeus, 1758), *Lutra lutra* (Linnaeus, 1758), *Martes martes* (Linnaeus, 1758), *Mustela eversmanii (*Lesson, 1827), *Mustela putorius* Linnaeus, 1758,, *Mustela erminea* and *Mustela nivalis* from Europe, measured by A.M.

Measurements were taken point to point, with the landmark system, to the nearest 0.01 mm. The measurements included mandible (Appendices 4; 5), dentition (Appendices 6; 7) and and postcranial elements (Appendixces 8; 9). All measurements are given in mm, and those shown in brackets were estimated. Measurements were taken using a set for image analysis using an Olympus stereo microscope ZSX 12, camera Olympus DP 71, programme Cell D. This set, coupled with an Olympus TG4 camera, was used to take photographs. Throughout the text, upper teeth are referred to as capital letters (e.g. P4), while lower teeth are referred to as lowercase letters (e.g. p4). Osteological and dental terminology and tooth morphotypes follow Gimranov & Kosintsev (2015) for *Martes* Pinel, 1792 and Rabeder (1976) for *Mustela*. Morphotype schemas and their descriptions are given in Appendix 10.

Abbreviations

B	bucco-lingual breadth;
Ba	mesial breadth;
Bp	distal breadth;
L	mesio-distal length;
M	mean;
mm	millimetre;
mc	metacarpal;
mt	metatarsal;
N	number in sample.

SYSTEMATIC PALEONTOLOGY

Remains of seven mustelid species have been found in the Hunas sediments: *Gulo gulo gulo* (Linnaeus, 1758), *Meles meles*, *Lutra lutra groissii* Heller, 1983, *Martes martes*, *Mustela putorius*, *Mustela erminea* and *Mustela nivalis* (Table 1). The mustelid assemblage is dominated by remains of *M. nivalis*, while other species are represented by relatively scant fossil material. All the species were found in the G1-G3 complex, while *M. nivalis* is also present in other layers, but in lower numbers. Only adult specimens were found, and except for *M. putorius* (only ♀♀) and *M. erminea* (♂ and ♀), a notable dominance of ♂♂ was found. The material is well preserved, although no complete skulls were found. The mustelids material from Hunas is represented mostly by maxillae and hemimandibles as well as their fragments, isolated teeth and long bones (humeri, ulnae, radii, femora, tibiae) and pelvis bones.

Class MAMMALIA Linnaeus, 1758
Order CARNIVORA Bowdich, 1821
Suborder CANIFORMIA Kretzoi, 1943
Infraorder ARCTOIDEA Flower, 1869
Family Mustelidae Fischer, 1817
Genus *Gulo* Pallas, 1780

Gulo gulo gulo (Linnaeus, 1758)

Gulo gulo Ambros, 2006: 39; fig. 49; tab. 52. – Döppes 2005: 421; tab. 7. – Rosendahl, Ambros, Hilpert, Hambach, Alt, Knipping, Reisch & Kaulich 2011: 19; tab. 3/2. – Baumann 2011: 8.

Referred material. — Metacarpal 4 and pisiform.

Description

A single mc 4 lacking a distal epiphysis, but the total length of the bone can be estimated to *c.* 53 mm. The bone is elongated and slim, with a gracile proximal end. The proximal epiphysis is flattened laterally and narrows into the ventral side. The outer border of the surface articulating with the hamatum curves into the ventral border. Viewed from the dorsal side, the hamatum surface forms a distinct angle with a plane of the articulation for mc 3. The narrow shaft is equally wide along its entire length.

Comparison and remarks

The moderately sized mc 4 from Hunas metrically and morphologically matches the mc 4 of *G. gulo*. The bone is much longer than the mc 4 of the Late Pleistocene and extant *M. meles* (Table 2). The mc 4 of *G. gulo* differs from those of *M. meles* in the larger size and in a more elongated and gracile build, mainly in an elongated shaft and slimmer proximal and distal

TABLE 1. — Occurrence of mustelids in Hunas site (quantity given as NISP/MNI). For détails of the separate layers, see Appendix 1.

	Layers				
Species	**L**	**K**	**H**	**G1-G3**	**Total**
Gulo gulo gulo (Linnaeus, 1758)	–	–	–	2/1	2/1
Meles meles (Linnaeus, 1758)	–	–	–	2/1	2/1
Lutra lutra groissii Heller, 1983	–	–	–	2/1	2/1
Martes martes (Linnaeus, 1758)	–	–	–	3/1	3/1
Mustela putorius Linnaeus, 1758	–	–	–	10/3	10/3
Mustela erminea Linnaeus, 1758	–	–	–	8/2 (1 ♂/1 ♀)	8/2 (1 ♂/1 ♀)
Mustela nivalis Linnaeus, 1766	3/2 (1 ♂/1 ♀)	52/10 (5 ♂♂/5 ♀♀)	1/1 (1 ♀)	494/132 (98 ♂♂/34 ♀♀)	551/169 (120 ♂♂/49 ♀♀)

TABLE 2. — Size comparison of mc 4 of *Gulo gulo* (Linnaeus, 1758) (different subspecies) and *Meles meles* (Linnaeus, 1758) (data from Döppes 2001, 2005; Ambros 2006; Marciszak 2012; Marciszak *et al.* 2017a, b and own measurements). The measurements are in centimetres.

	L			pB			dB		
Species	**M**	**min-max**	**N**	**M**	**min-max**	**N**	**M**	**min-max**	**N**
Hunas	[53]	–	1	7.50	–	1	7.00	–	1
Gulo gulo spelaeus (Goldfuss, 1818)	56.84	51.94-62.76	49	9.57	7.79-11.59	49	11.75	9.87-14.46	49
Gulo gulo gulo (Linnaeus, 1758) ♂♂	51.33	47.40-56.30	20	7.56	6.25-8.40	6	9.74	8.90-10.10	15
Gulo gulo gulo ♀♀	47.49	45.50-51.20	15	7.00	6.40-7.60	4	9.04	8.30-9.80	16
Meles meles (Linnaeus, 1758)	29.89	25.80-32.50	29	5.88	5.00-7.78	35	6.37	5.80-7.00	28

epiphyses. Toward the ventral side, the proximal epiphysis of the mc 4 from Hunas is narrower than that of *M. meles*. The outer border of the surface articulating with the hamatum curves less considerably into the ventral border. The inner border of the proximal epiphysis is deeply notched near the middle, while in *M. meles* the indentation is not so distinct. Viewed from the dorsal side, the plane of the hamatum surface forms a gentle angle with a plane of articulation for mc 3. The elongated shaft is much narrower and equally wide along its entire length. In *M. meles* the shaft of mc 4 is proportionally much shorter and robust and broadens proximally and distally.

Within the evolutionary lineage of *G. g. schlosseri* => *gulo* an increasing in body size is observed. Within this lineage, the late Middle Pleistocene individuals, e.g. Aven 1 (MIS 8-7) and Aven 2 of La Fage (MIS 6) (Hugueney 1975; Bourgeois & Philippe 2017), layers 19ad of Biśnik Cave (MIS 9-8; Marciszak 2012), layers 1-4 of Deszczowa Cave (MIS 9-8; Krajcarz 2012; Marciszak 2012) and Moggaster Cave (MIS 11; Döppes 2001) are characterised by medium-sized individuals, comparable with extant *G. g. gulo*. They are smaller than the robust Late Pleistocene *G. g. spelaeus*, which was on average 15-20% larger than the extant *G. gulo* (Döppes 2001, 2005; Marciszak *et al.* 2017b). In this context, dimensions of the Hunas individual corroborated with the other late Middle Pleistocene European specimens.

Genus *Meles* Brisson, 1762

Meles meles (Linnaeus, 1758)

Meles sp. Heller, 1983: 209; pl. 8/10-11. – Groiss 1983: 354; table 48. – Koenigswald & Heinrich 1999: 96. – Ambros 2006: 54. – Baumann 2011: 8. – Rosendahl, Ambros, Hilpert, Hambach, Alt, Knipping, Reisch & Kaulich 2011: 19; table 3/2.

Meles meles Ambros, 2006: 54; table 75.

REFERRED MATERIAL. — Mandible with p4-m1 and metatarsal 3.

DESCRIPTION

The mandibular body is long and stout. Its height measured behind m1 is larger than m1's length. On the buccal side, under the teeth row, a shallow, wide depression runs, which reduces in distally. Three rounded mental foramina are moderately spaced and located under the distal roots of p2, p3 and p4. The first and the second are situated on similar levels, while the third is placed slightly below. The mandibular body has a moderately convex lower margin, with the maximum convexity under m1. The teeth row is straight, and the teeth are set close to each other. Alveoles of the missing p2 and p3 show the presence of large, two-rooted teeth, with their distal parts oriented slightly disto-lingually. Large and proportionally wide p4 is two-rooted and high crowned. It possesses an asymmetric protoconid in the lateral view, pushed slightly mesially. From its apex, running mesially and distally, two thin ridges, which end on contact with the cingulum. The crown widens distally, with strong, disto-lingual curvature. The mesial margin is rounded, and the buccal straight and distal margin is blunt. Stronger cingulums are present on the mesial and distal margins of the crown.

The elongated m1 has a short trigonid and long and relatively narrow talonid. The trigonid is curved buccally and concave lingually. From the base of the high protoconid arises a short, low ridge that runs disto-buccally to the mesial wall of the hypoconid. From the buccal side this ridge is separated by a small groove. The metaconid and the paraconid are equal in height, and are separated by a deep, U-shaped valley. From the paraconid apex runs two thin and sharp ridges in the buccal and distal directions. The deeply basined talonid is notably

TABLE 3. — Comparison of size and main indexes of m1 of *Meles meles* (Linnaeus, 1758) (different chronosubspecies) (data from Wolsan 2001; Madurell-Malapeira *et al.* 2011a, b; Marciszak 2012). The measurements are in millimetres.

	Hunas	Early-Middle Pleistocene			Extant		
Indexes	**M**	**M**	**min-max**	**N**	**M**	**min-max**	**N**
L m1	17.94	16.77	15.30-18.00	12	16.18	14.35-18.37	104
B ta m1	7.86	7.28	6.30-7.93	10	7.61	5.90-8.75	105
B ta/L m1	43.8	43.1	38.8-45.7	10	47.0	37.2-52.7	105

broader than the trigonid, with a lower distal wall. On its surface are many low enamel folds and wrinkles. The large, high hypoconid is elongated and bears two ridges, which run mesially and distally from the apex of the cusp. Distally to the hypoconid is situated a large hypoconulid, which also bears two ridges. It is separated from the distal wall of the talonid by a fine groove. On the lingual wall is situated a large, high entoconid, after which is situated a small, low postentoconulid. The weak cingulum is located mesio-buccally.

The incomplete mt 3 lacks proximal epiphysis and is a robust, short bone. The bone has a massive, curved diaphysis, front-distally flattened and rectangular. Distal articulation is relatively large, rounded and irregularly shaped. The medial epicondyle is more prominent than the lateral one. Metrically and morphologically, this mt 3 from Hunas is indistinguishable from the mt 3 of *M. meles* (Table 2).

REMARKS

Because of great morphological variability, the taxonomy of the Pleistocene badgers is still frequently discussed and uncertain. Previously for the European Early and early Middle Pleistocene as a characteristic subspecies was regarded *Meles meles atavus* (Kormos, 1914) (Kormos 1914; Wolsan 2001; Madurell-Malapeira *et al.* 2011a, b). The form was determined as a distinct species on the vague feature of a presence of an additional cuspid between the protoconid and the hypoconid on m1. However, the presence or absence of this supernumerary cuspid is within the normal range of variation of extant *M. meles*, which was already questioned by Kretzoi (1938, 1941a, b) and later by other authors (Wolsan 2001; Madurell-Malapeira *et al.* 2011a, b; Marciszak 2012; Marciszak *et al.* 2021). Cranial and mandibular characteristics have sometimes been used as diagnostic features for species determination (Arribas & Garrido 2007). These characters are sexually and ontogenetically highly variable and as such, these features should not be employed for taxonomic purposes (Madurell-Malapeira *et al.* 2011a, b; Mecozzi *et al.* 2019; Mecozzi 2022).

The Hunas badger has a long but proportionally narrow tooth (Table 3). The tooth falls into the range variability of Early and early Middle Pleistocene and the extant *M. meles*. In both dimensions the Hunas badger stayed closer to the mean of Early-Middle Pleistocene than to the mean of extant *M. meles* (Table 3; Madurell-Malapeira *et al.* 2011a). Also, the talonid breadth to the L m1 ratio of the Hunas badger (43.8) is closer to the mean of the Early Pleistocene (43.1) than to that of the extant *M. meles* (47.0) (Table 3). This index demonstrated the presence in Hunas of a less evolved form, with elongated and narrower m1 and with a well-developed talonid. Of course, a single specimen cannot be regarded as a decisive factor, but signals the presence of an individual that is morphologically intermediate between the primitive features displayed by the Early and early Middle Pleistocene and the more progressive morphology of the extant *M. meles* (Wolsan 2001; Madurell-Malapeira *et al.* 2011a, b). Early and early Middle Pleistocene *M. meles* cannot be readily encompassed within the range of variation of extant *M. meles* (Madurell-Malapeira *et al.* 2011a; Mecozzi *et al.* 2019; Mecozzi 2022). The large number of extant badger subspecies can be explained by the long divergence during the Plio-Pleistocene and by the wide, Eurasian distribution. *Meles meles* appeared around 1.5 mya and became the only badger present in European sites. The radiation of the genus *Meles* occurred during the general climatic changes that took place during between the 2.6-2.2 mya and resulting environmental shifts across Eurasia (Faggi *et al.* 2024)

Genus *Lutra* Brisson, 1762

Lutra lutra groissii Heller, 1983
(Fig. 4A)

Lutra lutra groissii Heller, 1983: 211; pl. 8/1. – Groiss 1983: 354; table 48. – Koenigswald & Heinrich 1999: 96. – Ambros 2006: 54. – Rosendahl, Ambros, Hilpert, Hambach, Alt, Knipping, Reisch & Kaulich 2011: 19; table 3/2.

Lutra lutra Ambros, 2006: 37; fig. 43; table 18. – Baumann 2011: 8.

REFERRED MATERIAL. — Maxilla with P4-M1 and phalanx 1.

DESCRIPTION

Both teeth are unworn and belonged to a relatively young animal. In the occlusal view, P4 has a rectangular triangle outline (Fig. 4). The crown is divided into two morphologically distinct parts, the trigon extending buccally and the talon lingually. All margins are rounded, with two considerable concaves. The mesial concave is situated on the median part, on the border between the parastyle and protocone. The buccal concavity is placed almost exactly in the medium of this margin. The elongated and large parastyle is a crescent, low cusp. Its apex and the mesial wall of the paracone are connected by a distinct, low, thick crest, which does not extend to the paracone apex. The high, conical paracone is oriented almost vertically. It is separated from the protocone by a wide, not very deep, V-shaped valley. This distinct cusp has three

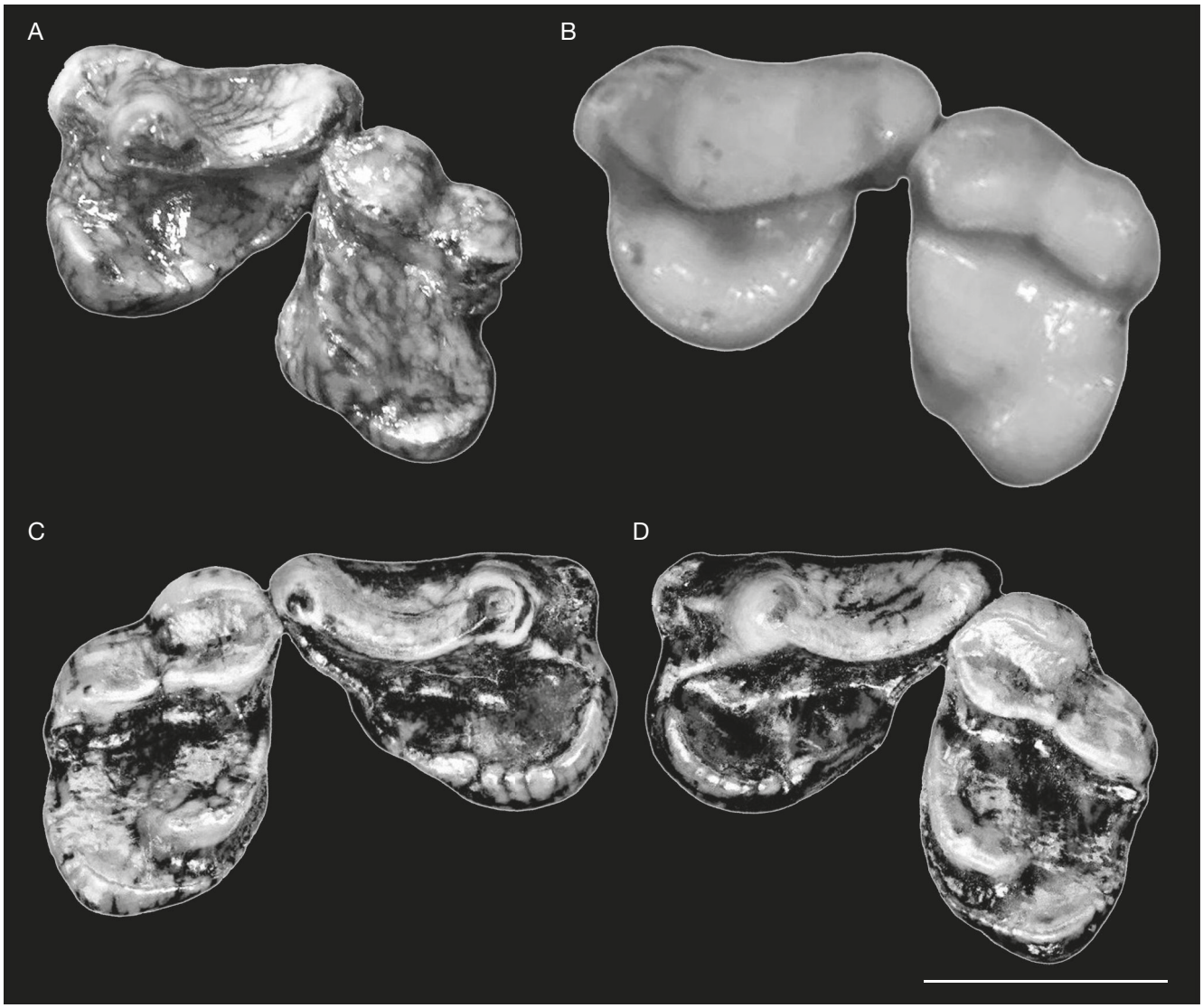

Fig. 4. — The P4-M1 of *Lutra* Brisson, 1762 species: **A**, *Lutra lutra groissii* Heller, 1983 from Hunas (HHu 4020); **B**, extant *Lutra lutra* (Linnaeus, 1758) from Silesia; **C**, **D**, *Lutra simplicidens* Thenius, 1965 from Voigtstedt (**C**, IQW 1966/7314 (Voi. 3532); **D**, IQW 1966/7313 (Voi. 3525); modified after Cherin (2017: 436; fig. 2). Scale bar: 10 mm.

crests, two mesial and one distal. The first mesial crest, low and flat, runs mesio-lingually from the top. The second, much thicker and stronger crest runs mesially toward a parastyle in the mesio-buccal margin of the crown as part of the mesial cingulum. The distal crest is orientated oblique-longitudinally, running from the top toward the metacone. The elongated and enlarged parastyle is pointed mesially and narrows distally. Its internal, broad surface forms an elongated, triangular, shallow basin, slightly deeper in the middle. The whole protocone is collared by a thick, high cingulum, especially strong on the mesial and mesio-lingual margins. The talon is mesio-distally enlarged and broad, and its distal margin does not reach the distal margin of the metacone in the occlusal view. The metacone is lower than the paracone and the crest that connects the two cusps is curved lingually. On the buccal wall of the talon a flat and relatively deep surface in the form of a concave meniscus is present. A stronger cingulum is present only on the disto-lingual margin (Fig. 4).

M1 has a bean-shaped occlusal outline, and the crown is oriented disto-lingually (Fig. 4). In relation to P4, it is situated more disto-lingually. There are two considerable concavities, buccal and distal. The buccal one is situated in the median part between the paracone and the metacone. The distal depression is located on the border between the trigon and talon. In the lateral view, the crown is strongly concave in the median part. The depression is a wide, flat, U-shaped valley, which runs transversally through the whole crown length. The trigon is slightly shorter than the talon, with two well developed, main cusps. Both cusps are relatively high and spherical, and the paracone is slightly higher and larger than the metacone. Both cusps are separated by a wide, not very deep, V-shaped valley. The elongated talon is broad, with rounded margins. The protocone is elongated and well developed, connected to the paracone by a strong and thin crest. The hypocone is on the disto-lingual corner of the talon and is crest-like. The central, extensive basin of

the talon is concave, shallow and smooth. The moderately developed cingulum is placed only on the disto-lingual margin of the talon (Fig. 4).

Remarks

The unique find of the otter from Hunas was studied by Heller (1983d, e). He compared the find with various lutrinae species and determined it as *L. lutra*. He also found some differences like an enlarged protocone of P4 and an M1 with a shallower median depression and less marked median, buccal concavity and talon oriented less disto-lingually. This allowed him to classify the Hunas otter as a new subspecies called *Lutra lutra groissii* (Heller 1983d, e). Potentially, three lutrinae species can be considered: *L. lutra*, *Lutra simplicidens* Thenius, 1965 and *Cyrnaonyx antiqua* (de Blainville, 1841). The differences between them are mostly in the premolars and molars. Morphologically, the Hunas otter considerably stood out from the dentition of *C. antiqua*. In the occlusal view, the P4 from Hunas is a rectangular triangle, while the P4 of *C. antiqua* is an irregular quadratic (Fig. 4). The parastyle is smaller and less distinct in the Hunas specimen.

The most noticeable two features distinguishing the Hunas otter from *C. antiqua* are the shape of the protocone and the talon of P4. The protocone of *C. antiqua* is extremely large, long and broad, with a deep, crescent inner surface. It is collared, as the rest of the crown (except the buccal margin) by a very thick and strong cingulum wall. Secondly, the buccal median concavity is much more strongly developed, the talon is oriented particularly disto-buccally, far beyond the main axis of the tooth. Both features in the Hunas otter are less developed (Fig. 4). Also, the M1 of the Hunas otter differs from that of *C. antiqua*. In this species the joint paracone-metacone is developed as a wide, blunt, medio-distal crest. The protocone is a flat, narrow, longitudinally elongated cusp, connected mesially with the paraconule. The distinct lingual and distal cingulum includes a blunt metaconule on the disto-lingual crown margin. A distinct cingulum developed on the buccal side of the tooth forms a marked mesio-buccal parastyle near the paracone. The central part of the crown consists of a shallow depression separating the buccal cusps and crests from the lingual ones.

If the Hunas otter cannot be assigned to *C. antiqua*, maybe it is *L. simplicidens*. Admittedly, the youngest records of this species are dated to 400-350 kya, however, the relict survival of this otter, as many other Eurasian carnivores, cannot be entirely rule out. Compared the Hunas maxilla with the material of *L. simplicidens* from Voigtstedt (800-700 kya; Cherin 2017), we found some similarities in the build of P4, which differed from the extant *L. lutra*. When comparing the P4s of the Hunas and Voigtstedt individuals with extant *L. lutra*, teeth of both fossil specimens have proportionally larger, semilunar parastyles, much longer and broader protocones, which is oriented noticeably more mesio-lingually and stronger developed paracone crests (Fig. 4).

The Hunas otter differs from Voigtstedt in a longer protocone with shallower internal basin and less expanded mesio-ligually, stronger buccal, median concavity and weak cingulum. The metacone of the P4 of *L. lutra* is a small blunt cusp in the disto-buccal crown margin. It is separated from the paracone on the buccal side by a distinct valley. A low protocone is included in the mesio-lingual margin of the crown as a crest-like wall running from the protocone toward the metacone. It forms the lingual border of one or two shallow depressions situated between the protocone, paracone and metacone. The depressions are separated from each other by a transverse wall. The external margin of the crown consists of a low cingulum visible in the buccal view. Also, an indistinct cingulum is situated below the parastyle (Fig. 4). Morphologically, the P4 from Hunas most closely resembles the P4 of *L. lutra* from Hoxne (Willemsen 1992; Mecozzi *et al.* 2022). Both teeth hold many morphological similarities like large, crescent parastyle, considerable buccal, median concavity, particularly enlarged protocone and weak cingulum.

When comparing the M1 of the Hunas otter with the *L. simplicidens* from Voigtstedt, it was found that they differ considerably (Fig. 4). The occlusal outline of both teeth is different. In the M1 from Hunas the crown curved considerably, with the distal walls of the trigon and talon directed strongly distally. In the M1 from Voigtstedt the main axis of the crown running from disto-buccally to the mesio-lingual side, with almost straight trigon and talon in the occlusal view. In relation to P4, it is pushed more buccally (Fig. 4).

In the Voigtstedt M1 the trigon and talon are of similar length, while in Hunas the talon is longer. The median concavity on the buccal margin of the trigon is stronger developed in Hunas M1. While in the Hunas otter the paracone is only slightly higher and larger than the metacone, in the Voigtstedt M1 the paracone is considerably larger and higher than the metacone. The transversal depression running through the whole crown length and separated trigon from the talon in Hunas M1 is much broader and shallower. The protocone and hypocone constriction is lower and shorter, ending on the mesial margin of the talon. In the Voigtstedt otter this structure is much longer, thicker and curved, reaching the central point of the internal talon basin (Fig. 4). The internal basin of the Hunas otter is more elongated, narrower and shallower than in the Voigtstedt otter. The lingual cingulum is more strongly developed.

Contrary to that, the M1 of the Hunas otter holds many similarities with the extant *L. lutra* like M1, in relations to the P4, pushed more lingually and less perpendicularly, similar size of paracone and metacone, broad and shallow depression separated trigon and talon, relatively short and low protocone and arched curved crown in the occlusal view. However, it simultaneously differs in the less arched trigon and talon, more strongly developed median concavity on the trigon buccal margin, higher para- and metacone and longer talon, with broader and more extensive internal basin, and stronger cingulum (Fig. 4).

Given the above features, it can be concluded that the Hunas otter showed some intermediate characteristics between *L. simplicidens* and *L. lutra*, and can suggest one evolutionary lineage or development of similar features during the evolution. According most authors, the derivation *L. lutra* from *L. simplicidens*

is hardly conceivable (Willemsen 1992, 2006; Mecozzi *et al.* 2022), but cannot be entirely ruled out. Our analysis showed the Hunas otter as something like a transitional form between these two species, and a possible link between them. There are morphometric differences between the two species that provide further support for a different derivation of *L. lutra*. The generally accepted chronological framework is that *L. lutra* dispersed into Europe from Asia during the late Middle Pleistocene and replaced *L. simplicidens* (Willemsen 1992, 2006; Mecozzi *et al.* 2022). In this scenario dated to *c.* 550-500 kya, otters from Cengelle, previously classified as *L. lutra* by Pasa (1947), with the trigonid broader than the talonid, can be re-determined as *L. simplicidens* (Mecozzi *et al.* 2022). This character has a high taxonomic value, which allows attribution of the Cengelle otter to *L. simplicidens* (Willemsen 1992).

The P4 from Hoxne, ascribed to *Lutra* sp. by Willemsen (1992), was recognised as having a strong resemblance to *L. lutra*. Given the absence of coeval maxillary Lutrinae material, attribution to *L. simplicidens* cannot be entirely ruled out. The comparison of the P4 shows slightly but significant morphological distinction between the Hoxne specimen and Voigtstedt ones. *L. simplicidens* has a characteristic talon profile, with a convexity along the distal margin, about half length, in the occlusal view (Cherin 2017). In the P4 from Hoxne, the profile of the distal margin is straight, not convex, which allows us to refer it to *L. lutra* (Mecozzi *et al.* 2022). If not for the whole European territory, locally *L. simplicidens* may be ancestral to some populations of *L. lutra*. The present work allows us to recognise several anatomical similarities as well as distinctions of the Hunas otter between *L. simplicidens* and *L. lutra*. The presence of such multiple, intermediate features in this specimen might suggest that *L. simplicidens* may be part of the same clade. Unfortunately, this cannot be supported by cladistic data until sufficiently complete cranial material of *L. simplicidens* are discovered. The same goes for the European late Middle Pleistocene *L. lutra* and the revision of the material from other, so far undescribed sites. New discoveries can also help clarify the taxonomic status of some of these otters, however most of these materials would require a taxonomic revision. In light of the observed similarities with *L. simplicidens*, the Hunas otter and *L. lutra*, the possible attribution of *L. simplicidens* in one evolutionary lineage with *L. lutra* is plausible, but further discoveries are needed to test this hypothesis. In view of the uniqueness of the Hunas find and its morphological separation from extant *L. lutra*, we also maintain subspecific status of the otter *L. l. groissii*, proposed by Heller (1983d, e).

Genus *Martes* Pinel, 1792

Martes martes (Linnaeus, 1758)
(Fig. 5A, B)

Martes sp. Heller, 1983: 209. – Groiss 1983: 354; table 48. – Koenigswald & Heinrich 1999: 96. – Ambros 2006: 54; table 92. – Baumann 2011: 8. – Rosendahl, Ambros, Hilpert, Hambach, Alt, Knipping, Reisch & Kaulich 2011: 19; table 3/2.

Martes martes Rosendahl, Ambros, Hilpert, Hambach, Alt, Knipping, Reisch & Kaulich 2011: 19; table 3/2.

REFERRED MATERIAL. — m1, proximal epiphysis of right ulna and distal half of left metapodium.

DESCRIPTION

The right m1 belongs to a large, old specimen, with strongly abraded cusps (Fig. 5). However, despite the wear, all features necessary for taxonomic determination are visible and morphometrical analysis is possible. The elongated m1 has a proportionally short, massive trigonid with a moderately high paraconid and prominent protoconid. The mesial margin of the trigonid is rounded, while the buccal margin is convex, and the lingual one is concave. The talonid possesses a straight lingual margin and blunt distal margin, while the buccal margin is slightly concave on the beginning and convex in the latter part. The oval metaconid is strong and well defined. The long and low talonid, with a low middle part, is broader than the trigonid. The internal talonid surface is shallow and smooth.

Together with this m1, a proximal epiphysis of a right ulna is also present. It is well preserved and belongs to an adult individual, with all sutures fused. The head is strongly curved latero-medially. The strong and short olecranon is square-shaped. Its apex is partly perforated by a small cavity surrounded by two fairly prominent tubercles. Its medial edge has a pronounced concavity. The trochlear notch for the humeral trochlea is broad and well developed and bears strongly pronounced medial expansion. The radial notch is also well marked. The lateral face is convex and has a clear interosseous border, which forms a shallow groove.

REMARKS

Morphologically, the m1 of the Hunas marten closely resembles *M. martes* and differs from that of *M. vetus* Kretzoi, 1942 and *Martes foina* (Erxleben, 1777) (Fig. 5). The Hunas specimen strongly resembles m1 of *M. martes* in the short and low trigonid, broad and long talonid, strong metaconid and lack of the paraconid edge. This structure falls from the paraconid diagonally in a disto-lingual direction. It causes the tooth base to bulge lingually and a clear inner cavity between the metaconid and the paraconid edge is developed. The m1 of *M. foina* is characterised by a proportionally high and long trigonid, small metaconid, presence of well-developed paraconid edge, and short and narrow talonid, with breadth that is on average smaller than that of the trigonid (Fig. 5).

In all these features the m1 of *M. foina* is so distinct from the Hunas marten that the possibility that this individual can be classified as this species is rejected. When compared to two basic indexes used to determine marten material, the Hunas specimens showed clear affiliation to *M. martes*. The ratio of the talonid length to the trigonid length (L ta/L tr m1) in the Hunas specimen is 61.3 and stays closer to the mean of *M. martes* (61.9, 55.1-72.3, n = 138) than to the mean of *M. foina* (L ta/L tr m1 = 39.4, 33.3-47.5, n = 112). Also, the second index, the talonid to the trigonid breadth of m1 (B ta/B tr m1) in the Hunas marten (101.7) corroborates more

with the mean of *M. martes* (106.6, 103.2-113.7, n = 138) than the mean of *M. foina* (92.2, 87.5-96.3, n = 112). All metric and morphological features allowed us to determine that the m1 from Hunas is a *M. martes*.

The same was obtained for the proximal epiphysis of the right ulna since the shape of the proximal ulna end shows clear distinctions between *M. martes* and *M. foina* (Ambros & Hilpert 2005). In *M. martes*, the medial side of the olecranon process protrudes like a hook in front, while *M. foina* lack this structure. Also, the supervision of the processes olecranon also allows the two to be separated. In *M. martes* the two knot-shaped processes are approximately extended equally in the ventral direction, sometimes also the lateral one, and the process is somewhat more extensive. In *M. foina* the medial node extends significantly further ventrally than the lateral (Ambros & Hilpert 2005). Both features can be easily recognised on the Hunas marten. Finally, the distal half of the metapodium was attributed to *M. martes*. The taxonomic attribution is unequivocally supported by its strong morphologic and morphometric affinities with the other metacarpals and metatarsals of *M. martes*, especially by a notably elongated and slim build. Although the described metapodium is incomplete, we can state with reasonable certainty that HHu 4525 belongs to this species. *Martes martes* is the only marten reported at Hunas.

Genus *Mustela* Linnaeus, 1758

Mustela putorius Linnaeus, 1758
(Fig. 5C, D)

Putorius cf. *stromeri* Heller, 1983: 207; fig. 44; pl. 6/9-15; table 27. – Groiss 1983: 354; table 48. – Koenigswald & Heinrich 1999: 95. – Rosendahl, Ambros, Hilpert, Hambach, Alt, Knipping, Reisch & Kaulich 2011: 19; table 3/2.

Mustela cf. *stromeri* Ambros, 2006: 36; fig. 42-1/2/3; table 53.

Mustela putorius Ambros 2006: 36.

Putorius stromeri Baumann, 2011: 8.

Referred material. — 2 C1, maxilla fr., 3 mandibles, baculum, 2 × metacarpal 4 and metacarpal 5.

Description
Among the 10 bones assigned to *M. putorius*, the most interesting and informative are two mandibles and one mandible fragment. The mandibular body is elongated and high, the corpus height decreasing slightly distally, and is the smallest in the middle length of m1. The body is relatively high and thick, and the thickness increases slightly into the distal direction. The ventral margin deviates dorsally, with a constant lateral thickness along most of its length. The margin is slightly curved, with maximum convexity under m1. The symphyseal area is elongated and relatively robust. Starting from the symphysis, on the mandibular body running moderately developed, longitudinal, lingual furrow. Two oval-shaped mental foramina are located on the buccal side. The larger mesial one is below p2, while the smaller, distal one is below the distal root of p4. The mesial edge of the masseteric fossa reaches m2, and it is rounded and rather deep. The tooth row is straight in the occlusal view, with only the p2 crown forming an angle of 50-60° with the rest of the teeth. Distal parts of p3 and p4 are oriented disto-buccally. They are tightly spaced to each other.

The c1 tooth is flattened laterally and relatively short mesio-distally, with a well-developed cingulum. The oval, two-rooted p2 is large and weakly reduced. The two-rooted p3 is low and narrow and bears an elongated, weakly developed distal cingular projection. It has a strong, irregular shape in the lateral view. Its lingual margin is convex, mesial and distal margins are rounded, while on the buccal margin occurs a moderate concavity. The p4 tooth is two-rooted and narrow, with a high, prominent protoconid, which is separated from the surrounding cingulum by a shallow, V-shaped valley. A stronger cingulum is present in the mesial and distal margins of the crown. In the p4 of the HHu 4605 individual, the mesial margin of the tooth is blunt, buccal straight, while the distal margin is arched. The first half of the lingual margin is straight, but the second half is strongly widened disto-lingually, and a well-developed convexity occurs on this part.

The occlusal outline of the HHu 4606 p4 is similar, but the convexity is better developed on the buccal side, and the lingual bulge is well marked. The well preserved m1 of HHu 4605 is elongated and robust, with rounded mesial and blunt distal margins. The buccal margin is concave, while most of the lingual margin is straight, with a prominent, median bulge. The m1 tooth has an elongated and low paraconid and prominent protoconid. Both the main cusps are separated by a deep valley, and the distal wall of the paraconid and mesial wall of the protoconid form an open angle. The trigonid is relatively long and high in relation to the tooth length, while the talonid is trenchant, moderately long and narrow. The talonid bears a large and dominant hypoconid, which is slightly connected with the distal cingulum.

Remarks
The Hunas polecats were small, robust individuals. Heller (1983d, e) conducted detailed morphometrical analysis of both mandibles and concluded that they represented the Early Pleistocene species *Mustela stromeri* Kormos, 1934 (*Putorius* cf. *stromeri* according to Heller 1983d, e). He compared the Hunas polecat with the material of *Mustela eversmanii* (Lesson, 1827) from Hohlefels, Mauer, Sirgenstein and Weimar-Ehringsdorf (Soergel 1917) and *M. stromeri* from Villány 5 and Beremend 5 (Kormos 1934). For comparison, he used 14 individuals of the extant *M. eversmanii* and 89 extant specimens of *M. putorius* from Silesia (SW Poland), taken from Soergel (1917).

Kormos (1934) described *M. stromeri* as a small polecat, with elongated, narrow and tear-shaped infraorbital foramen, straight upper teeth row, large P2, M1 with broad trigon, elongated and slender mandibular body, narrow m1 with a small bulge in the place of the non-existing metaconid and with a high, broad and long talonid. Heller (1983d, e) described

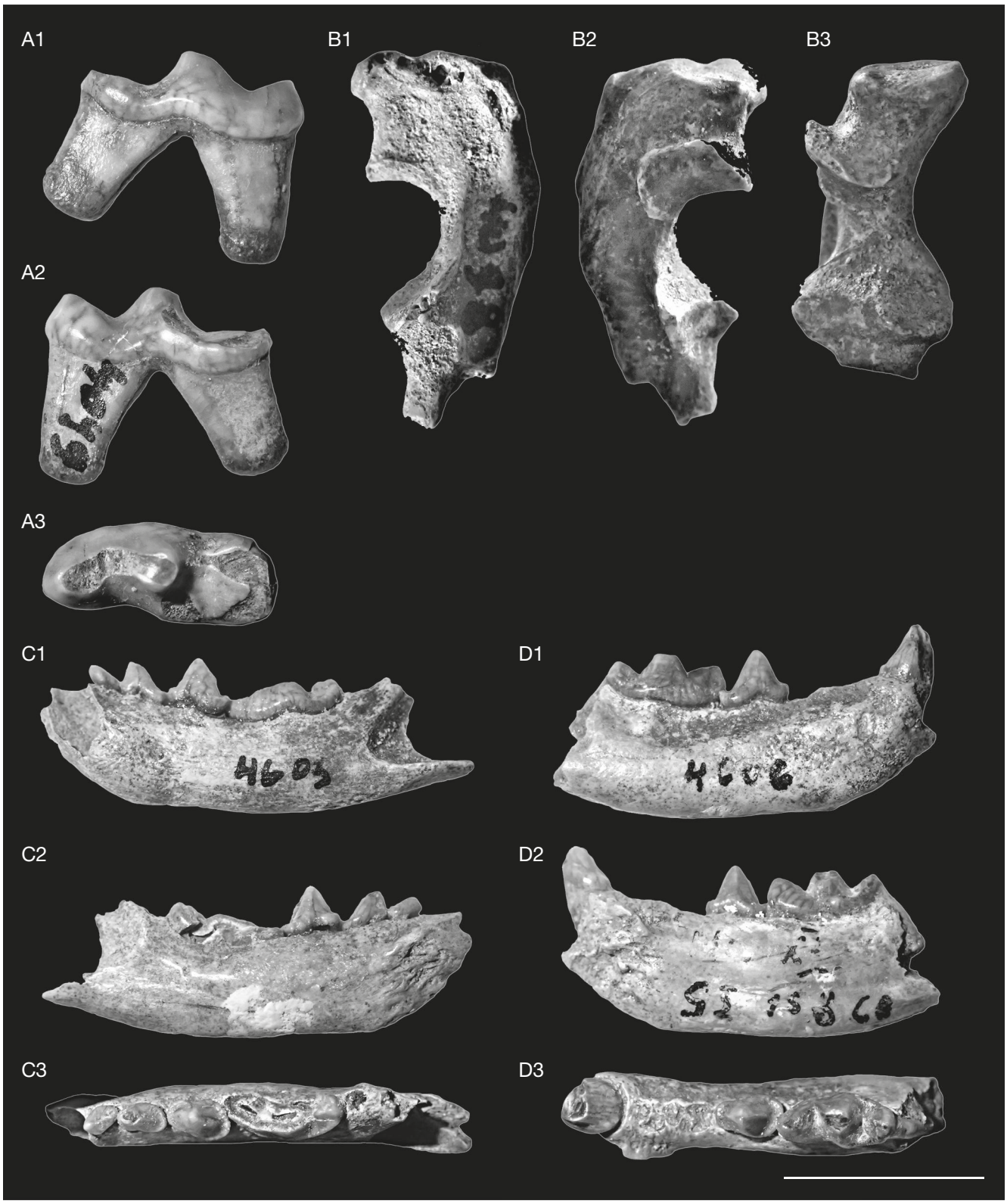

FIG. 5. — Medium sized mustelids from Hunas: **A**, **B**, *Martes martes* (Linnaeus, 1758): **A**, right m1 (HHu 4099); **B**, right ulna (HHu 4098); **C**, **D**, *Mustela putorius* Linnaeus, 1758: **C**, left mandible (HHu 4605); **D**, right mandible (HHu 4606). Numbers: **1**, buccal view; **2**, lingual view; **3**, occlusal view. Scale bar: 10 mm.

TABLE 4. — Main indexes of the mandible and lower dentition, distinguishing different species of European polecats (*, mandibular body height after m1).

	Hunas		*Mustela stromeri* (Kormos, 1934)			*Mustela eversmanii* Lesson, 1827		*Mustela putorius* Linnaeus, 1758	
ratio	M	min-max (n)	M	min-max (n)	Sex	M	min-max (n)	M	min-max (n)
H m1	7.58	7.49-7.66 (2)	6.74	6.34-7.06 (6)	♂♂	10.89	9.23-13.67 (86)	8.89	7.97-9.98 (225)
					♀♀	8.57	7.56-9.14 (54)	7.43	6.65-8.04 (144)
L m1/H m1*	107.4	104.9-109.9 (2)	90.6	85.2-96.2 (6)	♂/♀	92.1	82.4-102.6 (144)	114.6	97.6-126.4 (332)
Bp/L p4	61.6	60.0-63.1 (2)	53.2	48.1-57.2 (6)	♂/♀	72.4	63.9-79.4 (249)	60.7	54.5-66.7 (378)
L m1	8.14	8.04-8.23 (2)	7.62	7.34-7.88 (6)	♂♂	9.86	8.45-11.56 (86)	8.97	7.84-9.98 (305)
					♀♀	7.97	7.17-8.66 (54)	7.46	6.63-8.15 (144)
L ta/ L tr m1	31.1	30.7-31.5 (2)	47.8	45.8-49.2 (6)	♂/♀	19.7	16.9-25.7 (245)	26.4	18.9-29.7 (449)
B ta/B tr m1	81.2	79.8-82.5 (2)	94.5	91.9-96.8 (6)	♂/♀	61.4	55.6-68.7 (245)	72.1	63.9-77.8 (449)

two mandibles as belonging to this species. He determined them as *M. stromeri* based on their small size, slender but thick body mandible (especially strong thickening under m1), strong cingulum on p3, p4 and m1, and narrow m1 with broad, long and less trenchant talonid. However, revision of the European occurrence of *M. stromeri* showed that some specimens, previously assigned to this species might in fact represent *Mustela plioerminea* Stach, 1957, *Mustela strandi* Kormos, 1934 or even other, related forms. Such a statement was found, e.g. for the material from Osztramos 7 (Jánossy 1978). On the other hand, material from Erpfingen 3 seems to belong to some intermediate form.

The elongated symphyseal area is moderately massive, as in *M. putorius*, and stronger in HHU 4606. It is intermediate between very robust symphysis of *M. eversmanii* and elongated, rather weak symphyseal area in *M. stromeri*. In Hunas polecats, the masseteric fossa is quite deep, with a rounded mesial margin, reaching the m1/m2 boundary (HHU 4606) or only m2 (HHU 4605) (Fig. 5). Although variable, such morphology of the masseteric fossa is characteristic for *M. putorius*. In *M. stromeri* it is shorter and shallower, maximally reaching m2, with a triangular mesial margin. In *M. eversmanii* it is noticeably deep and long, and its mesial margin is rounded. The lower surface is extended and forms a flat surface of a rectangular shape for the attachment of powerful muscles. *Mustela eversmanii* also possesses a strong longitudinal, lingual furrow of the mandibular body. This structure in the form of a gentle arc runs from the symphysis along the whole mandibular body. In *M. putorius* this lingual furrow is weaker, however, the degree of development of this structure in this species is variable. Together with individuals with a strong lingual furrow, many specimens show weak development. In *M. stromeri* this structure is usually absent, and if already present, is noticeably weakly developed. In both Hunas specimens the furrow is moderately developed (Fig. 5).

Also, analysis of the dental material shows strong affinities of Hunas polecats to *M. putorius*, like in the moderately massive p4 and m1 with long and moderately robust trigonid and short and reduced talonid. The values of the two main indexes describing m1, the talonid breadth/length to the trigonid breadth/length, are above those characterised *M. eversmanii* in both specimens, but corroborate with those of *M. putorius* (Table 4). Simultaneously, they are distinctly below the indexes of *M. stromeri*, and a low degree of evolution can be seen in the morphology of m1, with an elongated and low crown, proportionally short and weak trigonid and long and narrow talonid. A higher evolutionary level, also represented by specimens from Hunas, can be seen in *M. putorius*, for which indexes showed intermediate values between primitive *M. stromeri* and the most advanced and specialised *M. eversmanii*. The last polecat is characterised by particularly enlarged and robust lower carnassials, an adaptation to crushing skulls and bones of large prey (Rempe 1970). All those aforementioned features allow us to determine the Hunas polecats as *M. putorius*.

When comparing the Hunas specimens with three polecat species, it is clear that the individual strongly resembles *M. putorius* and differs from *M. stromeri* and *M. eversmanii* in many morphometrical features. The results are in clear opposition with Heller's (1983d, e) determination (Table 4). Metrical values showed that the Hunas individuals were small, comparable in size with ♀♀ of extant polecats and exceed values obtained for *M. stromeri*. The mandibular body of *M. stromeri* is elongated and slender, and the corpus height is roughly constant on the whole-body length. The body height after m1 for the Hunas specimens are 7.49 mm (HHu 4605) and 7.66 mm (HHu 4606), which exceeds values of *M. stromeri*, following the smallest ♀♀ of *M. eversmanii*, but well corroborated with the values of *M. putorius* ♀♀ (Table 4).

Among three polecats, *M. eversmanii* possesses a particularly high and thick mandibular body. The body height measured after m1 (measurement no. 14) is very useful in species identification. Values below 8.0 mm almost always indicate *M. putorius*, while values greater than 9.5 mm almost exclusively allow classification of the specimen as *M. eversmanii* (Marciszak 2012; Crégut-Bonnoure *et al.* 2018).Research on large samples of both species showed that the measurement is also correlated with age and individual variation. On rare occasions, some huge individuals with comparatively not very high mandible bodies are also known (Marciszak 2012). An index of L m1 to the mandible body height measured after m1 is also useful. Its mean value for *M. eversmanii* is 92.1, while for *M. putorius* the mean is 114.6 (Table 4). The data showed that ratios of both polecats overlap very little. The Hunas specimens with ratios of 104.9 and 109.9 are much closer to the mean of *M. putorius* than to *M. eversmanii* (Table 4). The low value of this index in *M. stromeri* is not related to the massive mandibular body like in *M. eversmanii*, but to its slender and elongated build.

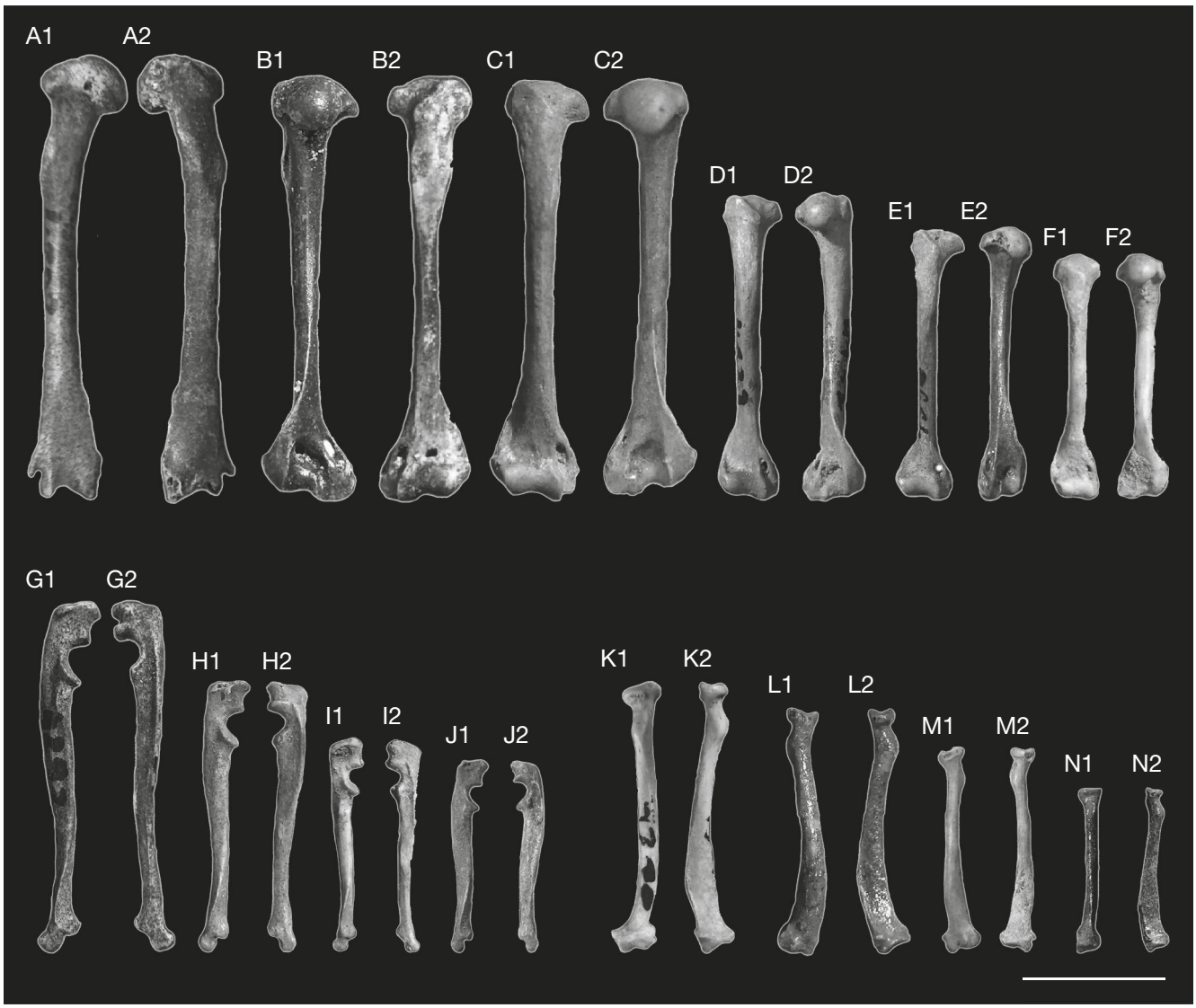

Fig. 6. — Long bones of the forelimb of the two smallest mustelids from Hunas: **A**, *Mustela erminea* Linnaeus, 1758, right humerus (♂, Hu/4207); **B**-**N**, *Mustela nivalis* Linnaeus, 1766: **B**, left humerus (♂, Hu/4569); **C**, right humerus (♂, Hu/4217); **D**, right humerus (♂, Hu/4393); **E**, right humerus (♀, Hu/4481); **F**, right humerus (♀, Hu/4431); **G**, left ulna (♂, Hu/4408); **H**, left ulna (♂, Hu/4510); **I**, left ulna (♀, Hu/4487); **J**, left ulna (♀, Hu/4425); **K**, left radius (♂, Hu/4310); **L**, right radius (♂, Hu/4519); **M**, left radius (♀, Hu/4182); **N**, left radius (♀, Hu/4434). Numbers: **1**, dorsal view; **2**, ventral view. Credits: photo by B. Hilpert. Scale bar: 10 mm.

Mustela erminea Linnaeus, 1758
(Fig. 7A)

Mustela aff. *palerminea* Heller, 1983: 200; fig. 44; pl. 6/5-8; table 26. – Groiss 1983: 354; table 48. – Koenigswald & Heinrich 1999: 94. – Ambros 2006: 35; fig. 41-3/7/8; tables 47, 78, 85. – Rosendahl, Ambros, Hilpert, Hambach, Alt, Knipping, Reisch & Kaulich 2011: 19; table 3/2.

Mustela palerminea Baumann, 2011: 8.

Referred material. — Humerus, ulna, femur, tibia, 3 metapodials.

Description

Long and narrow humerus has a flat and narrow head. The greater tubercle extends distally along the side of the articulation surface (Fig. 6). The well-marked neck is directed distally. The lesser tubercle is well-developed. The rugose area on the inner surface of the shaft for the attachment of the inner humeral head of the triceps muscle is prominent. The lateral epicondylar crest is strongly developed towards the lateral epicondyle from the last distal fourth. The medial epicondylar crest is prominent and has a narrow supracondylar foramen. The strong medial condyle is situated slightly back, while the lateral condyle is deeper in the mesio-distal direction. A rounded and shallow coronoid fossa does not connect with the wide and deep olecranon pit (Fig. 6). The radius is thin and flattened dorso-ventrally, and it has a slightly concave ventral surface (Fig. 6). The moderately large head has a shallow and rounded articular surface. It is mesially collared by a moderately prominent coronoid process.

The articulation surface for the lesser sigmoid cavity is relatively large. The distal end is widened laterally, with a well-marked elliptical glenoid cavity, framed by a rough condyle on the ventral and medial sides. The facet for the ulna is small, while the styloid process is well-developed. The grooves for

TABLE 5. — Dimensions of long bones of different small, European *Mustela* Linnaeus, 1758 species.

		Hunas		*Mustela erminea* Linnaeus, 1758		*Mustela nivalis* Linnaeus, 1766	
Bone	**Sex**	**M**	**min-max (n)**	**M**	**min-max (n)**	**M**	**min-max (n)**
humerus L	♂♂	22.63	19.94-26.14 (19)	36.69	34.10-39.76 (72)	23.72	20.49-26.89 (124)
	♀♀	17.10	16.42-18.02 (14)	30.52	26.04-33.16 (69)	18.06	15.84-19.32 (112)
humerus dB	♂♂	4.81	4.06-5.66 (19)	7.39	6.39-7.94 (72)	4.72	4.27-5.51 (124)
	♀♀	3.48	3.09-4.16 (21)	5.93	5.17-6.63 (69)	3.31	2.98-3.68 (112)
radius L	♂♂	16.22	15.46-17.56 (12)	27.09	24.48-28.97 (72)	16.83	14.68-18.17 (124)
	♀♀	12.57	11.36-13.75 (4)	21.30	19.51-22.97 (69)	12.20	11.18-13.44 (112)
ulna L	♂♂	19.91	17.66-21.26 (4)	33.52	29.97-37.14 (72)	21.76	19.14-23.97 (124)
	♀♀	14.61	13.27-16.84 (5)	25.99	24.18-28.81 (69)	15.21	14.28-16.48 (112)
femur L	♂♂	23.45	20.04-26.74 (29)	41.88	36.59-44.46 (72)	25.15	21.39-28.15 (124)
	♀♀	16.33	13.00-19.50	33.01	30.39-35.51 (69)	17.95	16.25-19.31 (112)
femur dB	♂♂	4.40	3.64-5.02 (28)	7.65	6.99-7.99 (72)	4.73	4.18-5.21 (124)
	♀♀	2.88	1.15-3.48 (13)	6.04	5.61-6.59 (69)	3.33	3.13-3.56 (112)
tibia L	♂♂	24.77	21.22-27.06 (21)	44.97	39.57-48.25 (72)	25.94	22.29-28.77 (124)
	♀♀	17.73	16.44-18.67 (10)	34.66	31.37-36.89 (69)	19.40	17.64-20.78 (112)

the extensor muscle tendons, extensors carpi radialis longior and brevior muscles are broad and deep. The scapholunar articulation area is relatively short and broad (Fig. 6). The ulna is massive, with a strong but short proximal end (Fig. 6). The surface for attachment of the scapular head of the triceps muscle is broad and strongly rugose. The olecranon has a quadrilateral shape with its apex hollowed out in part of a small cavity bordered by two fairly prominent tubercles. The shaft is curved in the lateral and medial view and massive in its longitudinal extent. The articulating surface for the radius is large, while the articulating surface for the pisiform is quite narrow. The distal end is characterised by a significant protrusion of the ulnar styloid process (Fig. 6).

The long, cylindrical femur possesses a spherical head with a prominent neck (Fig. 7). The trochanteric fossa is narrow and deep. The lesser trochanter is a slight conical prominence. The shaft is slightly bowed in its longitudinal extent. The greater trochanter rises distinctly above the head level and is obliquely truncated on its lateral side. The surface of the trochanter extends further down the proximal extremity of the femur. The tibial articulations are nearly equal in size. At the distal end, the condyles are separated by a broad and deep groove. The lateral condyle is slightly more developed than the medial one (Fig. 7). The body of the long and thin tibia is triangular in its proximal third, slightly convex medially, with a large tibial fossa from the lateral side (Fig. 7). The distal surface below the head is narrow and shallow. The tibial crest is well marked but relatively short. At the distal end, the articular surface consists of two separate grooves. The medial throat is deeper than the lateral one. The grooves for tendons of the flexor longus digitorum and tibialis posticus muscles are well defined at the distal epiphysis. The notch incising the mesial border of the distal surface is quite small (Fig. 7).

REMARKS

A permanent problem in faunistic analyses is distinguishing small species of the genus *Mustela*. Many authors made several attempts, resulting in the conclusion that the only reliable criterion is size. This was largely the case with the rich material from Hunas, where Heller (1983d, e) also attempted to classify this material. No cranial material of *M. erminea* was found in Hunas. Apart from the abundant cranial material, attributed exclusively to *M. nivalis*, even more numerous postcranial skeletal elements in Hunas were found. It is represented mainly by long bones, but also some pelvis and metapodials. They are well preserved and about one-third are complete. No substantial differences between *M. erminea* and *M. nivalis* were found in the morphology of the postcranial bones. The variability of the features is so high that it is impossible to establish any characteristics for that species. In this context, the only reliable criteria for distinguishing the postcranial elements of small *Mustela* species are dimensions.

A similar situation was found for the material of the Early and early Middle Pleistocene *M. palerminea* and *M. praenivalis*, where size was the only criteria for their classification (Rabeder 1976; Wiszniowska 1989; Marciszak *et al.* 2021). Long bones are recognisable and measurable markers for species determination. Small mustelids are characterised by extreme sexual dimorphism, with ♂♂ 1.5 times larger than ♀♀ (Kratochvíl 1977a, b; King 1989; King & Powell 2007). The metrical analysis of sexes' long bones of *M. erminea* and *M. nivalis* from Hunas is based on the differences in size of ♂♂ and ♀♀ in extant, Silesian populations. These differences were shown in all long bones, and the most important was greatest length (L). This value was lower in ♀♀ than ♂♂ in all analysed bones (Table 5). The long bones differ significantly in size like in extant forms, where size ranges of *M. erminea* ♀♀ and *M. nivalis* ♂♂ do not overlap (Table 5). Since the individuals of *M. erminea* and *M. nivalis* from Hunas are comparable in size with the extant, Silesian populations, respectively, it is possible to track sexual dimorphism based on long bones. It is possible even in the case of incomplete bones, since the proportions of bone parts are quite constant (Reichstein 1986; Marciszak 2012; Marciszak *et al.* 2021). It allows us to estimate the total length of such bones and also use them in the analysis (Table 5).

The analysis of the dimensions of the numerous postcranial materials allowed to include for *M. erminea* only a few bones. Between two humeri, the larger (HHu 4207, L 34.44 mm) was determined as ♂, while the smaller (HHu 4569, L 27.81 mm)

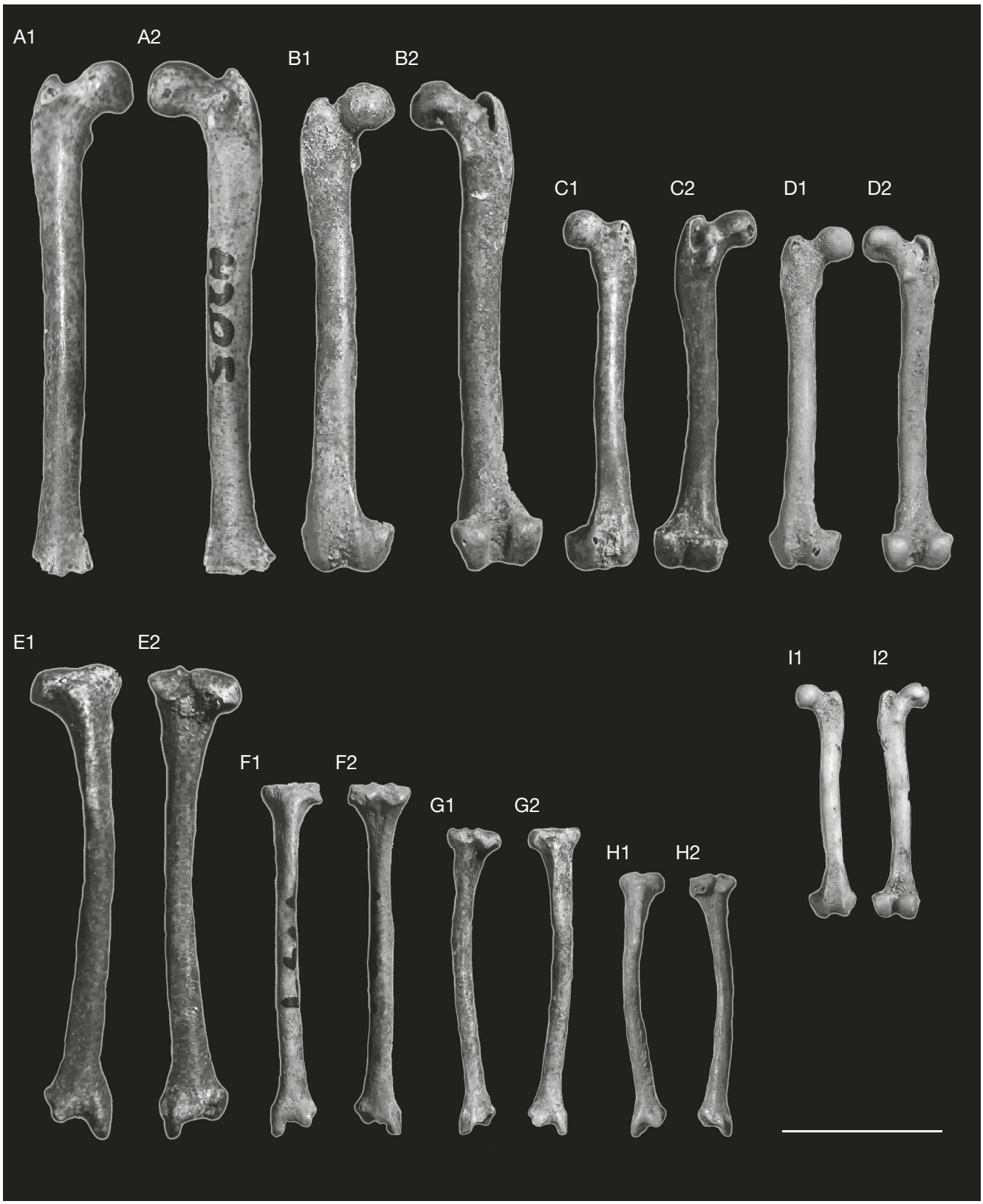

Fig. 7. — Long bones of the hindlimb of the two smallest mustelids from Hunas: **A**, *Mustela erminea* Linnaeus, 1758, right femur (♂, Hu/4205); **B**-**I**, *Mustela nivalis* Linnaeus, 1766: **B**, right femur (♂, Hu/4226); **C**, left femur (♂, Hu/4475); **D**, right femur (♀, Hu/4419); **E**, left femur (♀, Hu/4493); **F**, right tibia (♂, Hu/4229); **G**, left tibia (♂, Hu/4151); **H**, right tibia (♀, Hu/4444); **I**, left tibia (♀, Hu/4170). Numbers: **1**, dorsal view; **2**,ventral view. Credits: photo by B. Hilpert. Scale bar: 10 mm.

was assigned as ♀. A single incomplete radius (HHu 4301) and three femora, one intact (HHu 4205, L = 35.02 mm) and two incomplete (HHu 4209 and HHu 4496), showed intermediate values, so they cannot be properly sexed. The proximal half of the sole tibia (HHu 4206) belongs to a moderately large individual, most probably ♀ (Table 5). Because metapodials of the extant *M. erminea* cannot be reliably sexed, we did do this for the material of this species from Hunas. The study of the postcranial material of *M. erminea* from Hunas does not show a predominance of ♂♂ or ♀♀ and shows the presence of medium-sized individuals (Table 5). Metrically and morphologically, they are indistinguishable from the extant Silesian population.

Mustela nivalis Linnaeus, 1766
(Fig. 7B-H)

Mustela aff. *praenivalis* Heller, 1983: 200; fig. 44; pl. 6/1-4, 16-18; table 25. – Groiss 1983: 354; table 48. – Koenigswald & Heinrich 1999: 94. – Ambros 2006: 54. – Rosendahl, Ambros, Hilpert, Hambach, Alt, Knipping, Reisch & Kaulich 2011: 19; table 3/2

Mustela praenivalis Baumann, 2011: 8.

Referred material. — 5 vertebrae, scapula, baculum, 15 canines, isolated P4 and m1, maxilla fragment, 169 hemimandibles (120 ♂♂, 49 ♀♀), 102 humeri (63 ♂♂, 37 ♀♀), 24 ulnae (15 ♂♂, 9 ♀♀), 21 radii (16 ♂♂, 3 ♀♀), 100 femora (52 ♂♂, 40 ♀♀), 81 tibiae (62 ♂♂, 19 ♀♀), 33 pelvis bones (551/169 - 120 ♂♂, 49 ♀♀).

Description
The elongated and low mandibular body has a constant lateral thickness for its whole length (Fig. 8). The lower margin is moderately curved and reaches the curvature peak below the m1 level. The symphysis is long and narrow. Two oval-shaped mental foramina are of similar size but are located on different levels. The mesial one is situated higher, below p2 and the distal one are located below the distal root of p3, and on a lower level than the first. Some specimens have a vestigial, longitudinal, lingual furrow of the mandibular body, but the degree of development varies substantially between individuals from weak to moderate. In most individuals this structure is absent. The strong ramus has a shape of rectangular triangle. Its mesial margin rises gently to the top, while the distal margin is almost vertical. The condylar process is massive and short, elongated laterally and inclined slightly downward on the medial side. It is positioned below the teeth row. The angular process is short and is shaped like a rectangular triangle. The deep masseteric fossa has a rounded mesial margin and reaches the m1/m2 boundary. The teeth row is straight in the occlusal view, with only the p2 crown placed at an angle of 30-40o to the rest of the teeth. The distal halves of p3-p4 are oriented disto-buccally. The teeth are positioned loosely to each other, and between them are visible small diastemas (Fig. 8).

The elongated and oval p2 is moderately reduced (Figs 8; 9). The two-rooted p3 is low and moderately massive. The protoconid is pushed strongly mesially and almost exactly to the axis of the tooth. The blunt mesial and rounded distal margins have a weak cingulum. The crown bears an elongated, well-developed, distal, cingular projection. The buccal edge is straight, while the lingual one is weakly convex. The two-rooted p4 is an elongated and robust tooth, with a prominent, medially positioned protoconid, which is moderately separated from the surrounding cingulum. Before the protoconid is a crescent, shallow valley. The stronger cingulum is situated on the distal margin. The mesial and distal margins are blunt, while the distal halves of the buccal and lingual edges are strongly convex. This bulge is more developed on the buccal side. The elongated and narrow m1 is moderately trenchant. The crown has a long and low paraconid and prominent, but relatively low protoconid. The trigonid is moderately long and low in relation to tooth length. The buccal margin is moderately convex. The lingual margin of the paraconid and talonid is straight, while the lingual edge of the protoconid is moderately convex. The short and moderately broad talonid bears a centrally positioned hypoconid. The reduced m2 is a moderately large, oval-shaped and one-rooted tooth with a low crown (Figs 8; 9).

Comparison with *Mustela erminea*
The morphometric analysis of the material of the smallest mustelids from Hunas was carried out based on the sex division, determined based on the combination of the length m1 and the height of the mandibular body after m1. By comparing with the sexually divided Silesian population of the extant *M. nivalis*, it was possible to separate the population into ♂♂ and ♀♀. The taxonomic analysis also included a comparison with the sexually divided Silesian population of the extant *M. erminea*, *M. palerminea* and *M. praenivalis*. Both ancient species have already been subjected to critical analysis (Marciszak *et al.* 2021), which showed that many of the previously reported distinguishing features are no longer valid. For this reason, the legitimacy of their designation was not discussed here, and the focus was on comparing the given characteristics of the Hunas population with other species. In particular, the most important similarities and differences were highlighted, which in the end allowed us to reach a credible conclusion.

Compared to *M. erminea*, cranial and dental material of the smallest mustelids from Hunas show differences in:

1) overall smaller size, well documented by the L m1, where the mean of *M. nivalis* ♂♂ from Hunas (4.43 mm, 4.02-4.97 mm, n = 103) is distinctly smaller than the mean of both sexes of *M. erminea* (♂♂ 5.84 mm, 5.51-6.36 mm, n = 151; ♀♀ = 5.19 mm, 4.65-5.57 mm, n = 177), even if slightly overlapping with ♀♀ *M. erminea* (Table 6);

2) on average shorter and shallower masseteric fossa, reaching maximally the m1/m2 boundary, with a more triangular, mesial margin, although some individuals from Hunas also have a more rounded, mesial margin. *Mustela erminea* possesses, longer ones on average, reaching m1/2 up to the trigonid/talonid m1 border, and deeper masseteric fossa, for which the mesial margin is almost always rounded;

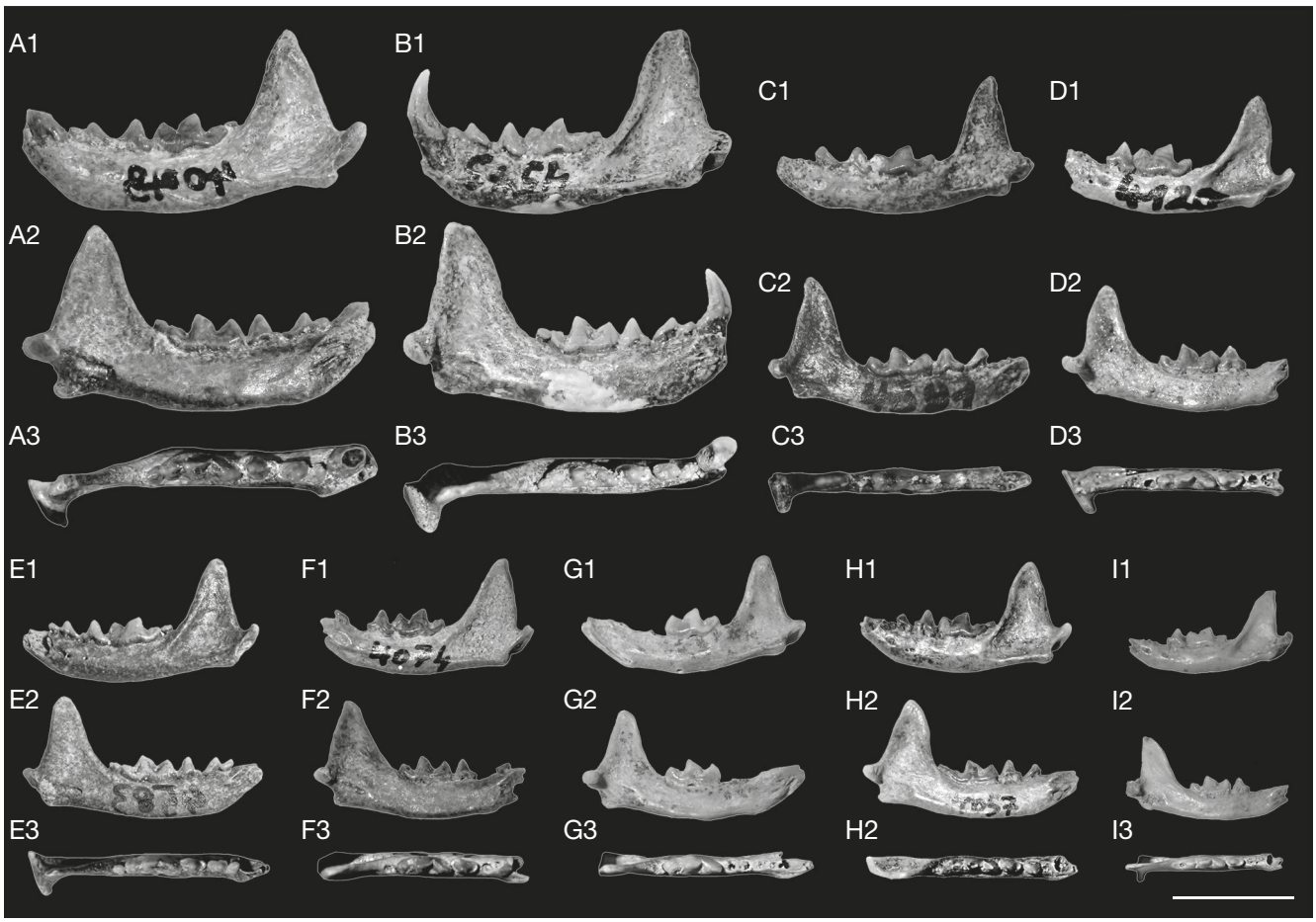

Fig. 8. — Mandibles of the largest and smallest individuals of *Mustela nivalis* Linnaeus, 1766 from Hunas as an example of strong sexual dimorphism: **A**, ♂ (Hu/4049, 4.97 mm); **B**, ♂ (Hu/45434.76 mm); **C**, ♂ (Hu/4581, 4.08 mm); **D**, ♂ (Hu/4120, 4.04 mm); **E**, ♀ (Hu/4583, 3.98 mm); **F**, ♀ (Hu/4074, 3.97 mm); **G**, ♀ (Hu/4602, 3.98 mm); **H**, ♀ (Hu/4057, 3.98 mm); **I**, ♀ (Hu/4587, 2.87 mm). In brackets together with collection number also L m1 in mm of particular specimens are given. Numbers: **1**, buccal view; **2**, lingual view; **3**, occlusal view (A and D reversed). Scale bar: 10 mm.

3) shape of the coronoid process. In *M. nivalis* from Hunas, the mesial and distal edges of this process are approximately of the same length and form the same angles with the longitudinal axis of the mandible. In *M. erminea*, the mesial edge is more inclined than the distal one, which is almost vertical and therefore considerably shorter;

4) presence of weakly to moderately marked, but still stronger than in *M. erminea*, longitudinal, lingual furrow of the mandibular body;

5) proportionally larger and less reduced p2, where p2 L/m1 L index of *M. nivalis* from Hunas (♂♂ 28.3, 22.9-31.9, n = 26; ♀♀ 29.4, 26.9-32.0, n = 5) is higher than that of *M. erminea* (♂♂ 23.1, 20.4-26.7, n = 151; ♀♀ 24.1, 20.5-27.0, n = 178). There is apparently some overlap, but the ratios differ notably;

6) narrower p3, which is well documented by ratios, but the ranges of variability strongly overlap: *M. nivalis* from Hunas (♂♂ 56.0, 43.2-69.2, n = 46; ♀♀ 56.0, 46.8-66.4, n = 18) is higher than this of *M. erminea* (♂♂ 61.5, 54.2-68.7, n = 197; ♀♀ 60.2, 50.7-69.1, n = 230). The morphotype analysis showed variable results in both species, and the higher proportion of more advanced morphotypes in ♂♂. In ♂♂ *M. nivalis* from Hunas the most common are morphotypes B (43.5%, wider distally than mesially, without a buccal protrusion) and C (37.0%, distally strongly widened and the occlusal crown outline is therefore strongly asymmetrical). For Hunas ♀♀ the more typical morphotypes are A2 (50.0%), distally also not widened, but with a mesio-buccal protrusion of the crown margin, and B (22.2%). Other morphotypes in both sexes of *M. nivalis* from Hunas are much less common (Table 7). In *M. erminea* one morphotype is clearly dominant, C (89.3%) in ♂♂ and B (74.3%) in ♀♀ (Table 7);

7) narrower p4, with less marked difference between the mesial and distal halves of the crown, where both the means and the ranges of variability of the Ba/Bp p4 indexes almost do not coincide: *M. nivalis* from Hunas (♂♂ 88.8, 83.8-93.7, n = 69; ♀♀ 90.3, 87.2-94.1, n = 29) is higher than that of *M. erminea* (♂♂ 74.6, 62.2-74.4, n = 248; ♀♀ 81.4, 68.3-85.8, n = 162) (Table 6). The morphotype analysis documented the distinctly wider (in relation to the mesial) distal half of p4 in *M. erminea*. In both sexes (♂♂ 94.3%, ♀♀ 82.1%) of this species the most advanced morphotype C dominated, where the crown is strongly widened bucco-lingually. In *M. nivalis* from Hunas (♂♂ 81.2%; ♀♀ 75.9%) the most common is morphotype B, where the buccal margin is still almost straight, while the lingual margin in the distal

TABLE 6. — Main indexes of the mandible and lower dentition, distinguishing different small, European *Mustela* Linnaeus, 1758 species. Abbreviations: **eMP**, early Middle Pleistocene; **EP**, Early Pleistocene.

		Hunas		*Mustela erminea* Linnaeus, 1758		*Mustela nivalis* Linnaeus, 1766			*Mustela palerminea* Baumann 2011		*Mustela praenivalis* Kormos, 1934	
ratio	**Sex**	**M**	**min-max (n)**	**M**	**min-max (n)**	**M**	**min-max (n)**	**Age**	**M**	**min-max (n)**	**M**	**min-max (n)**
p2 L/m1 L	♂♂	28.3	22.9-31.9 (26)	23.1	20.4-26.7 (151)	25.5	22.1-30.8 (304)	EP	31.1	28.1-33.8 (32)	30.9	28.7-34.7 (27)
	♀♀	29.4	26.9-32.0 (5)	24.1	20.5-27.0 (178)	26.1	22.2-30.9 (187)	eMP	28.9	24.3-32.4 (12)	31.4	26.5-37.4 (11)
B/L p3	♂♂	56.0	43.2-69.2 (46)	61.5	54.2-68.7 (197)	57.3	47.0-68.2 (290)	EP	54.6	45.8-62.1 (91)	52.5	46.2-64.1 (22)
	♀♀	56.0	46.8-66.4 (18)	60.2	50.7-69.1 (230)	57.8	42.1-73.4 (260)	eMP	57.7	52.4-63.2 (18)	53.6	49.7-60.1 (7)
Ba/Bp p4	♂♂	88.8	83.8-93.7 (69)	74.6	62.2-74.4 (248)	89.0	83.1-93.9 (206)	EP	89.3	82.2-95.9 (194)	94.7	89.6-96.9 (35)
	♀♀	90.3	87.2-94.1 (29)	81.4	68.3-85.8 (162)	88.9	82.2-93.5 (221)	eMP	88.1	82.3-92.5 (33)	91.9	86.5-96.7 (11)
L m1	♂♂	4.43	4.02-4.97 (103)	5.84	5.51-6.35 (151)	4.58	4.02-5.27 (304)	EP	5.46	4.49-6.12 (165)	4.23	3.27-5.09 (57)
	♀♀	3.55	2.87-3.98 (39)	5.19	4.65-5.57 (177)	3.59	3.09-4.14 (187)	eMP	5.23	4.46-5.97 (36)	3.81	3.12-4.76 (24)
L ta/ L tr m1	♂♂	40.6	30.5-51.2 (103)	23.9	18.6-32.4 (151)	39.6	28.7-44.7 (304)	EP	45.4	35.8-51.7 (165)	54.8	50.8-59.9 (57)
	♀♀	49.1	39.2-54.4 (39)	27.8	20.8-33.9 (177)	44.4	38.3-51.5 (187)	eMP	43.1	37.6-49.7 (36)	53.8	50.5-56.9 (24)
B ta/B tr m1	♂♂	90.6	87.1-95.8 (103)	78.1	66.5-87.1 (151)	90.2	86.8-99.3 (304)	EP	91.9	89.3-94.3 (165)	94.7	88.5-96.9 (57)
	♀♀	91.7	87.2-96.2 (39)	82.9	77.7-86.1 (177)	91.3	81.5-98.3 (187)	eMP	90.1	87.8-92.7 (36)	94.0	90.5-96.3 (24)

TABLE 7. — Number and percentage of particular morphotypes in small, European *Mustela* Linnaeus, 1758 species.

		Hunas		*Mustela erminea* Linnaeus, 1758		*Mustela nivalis* Linnaeus, 1766		*Mustela palerminea* Baumann 2011	*Mustela praenivalis* Kormos, 1934
Tooth	**Morph.**	♂♂	♀♀	♂♂	♀♀	♂♂	♀♀		
p3	A1	–	3 (16.7%)	–	10 (4.4%)	12 (4.1%)	31 (11.9%)	84 (81.6%)	6 (20.0%)
	A2	–	9 (50.0%)	4 (2.0%)	37 (16.1%)	28 (9.7%)	157 (60.4%)	11 (10.7%)	22 (73.3%)
	B	20 (43.5%)	4 (22.2%)	15 (7.6%)	171 (74.3%)	38 (13.1%)	35 (13.5%)	8 (7.8%)	2 (6.7%)
	C	17 (37.0%)	2 (11.1%)	176 (89.3%)	12 (5.2%)	51 (17.6%)	24 (9.2%)	–	–
	D	9 (19.5%)	–	2 (1.1%)	–	161 (55.5%)	13 (5.0%)	–	–
p4	A	10 (14.5%)	6 (20.7%)	–	–	12 (5.8%)	14 (6.3%)	145 (61.2%)	11 (21.2%)
	B	56 (81.2%)	22 (75.9%)	14 (5.7%)	29 (17.9%)	36 (17.5%)	193 (87.4%)	92 (38.8%)	41 (78.8%)
	C	2 (2.9%)	1 (3.5%)	234 (94.3%)	133 (82.1%)	158 (76.7%)	14 (6.3%)	–	–
m1	A	–	10 (25.6%)	–	–	–	19 (10.2%)	166 (79.4%)	82 (82.8%)
	B	2 (2.0%)	19 (48.7%)	–	–	–	117 (62.6%)	43 (20.6%)	17 (17.2%)
	C	25 (24.3%)	7 (18.0%)	8 (5.3%)	15 (8.5%)	36 (11.8%)	33 (17.7%)	–	–
	D	76 (73.8%)	3 (7.7%)	143 (94.7%)	162 (91.5%)	268 (88.2%)	18 (9.6%)	–	–

part holds a moderately developed convexity. In the Hunas population there is also the most primitive morphotype A, with a narrow and elongated crown, with the mesial and distal halves of similar width (♂♂ 14.5%; ♀♀ 20.7%) (Table 7);

8) m1 with a proportionally lower and shorter trigonid and longer and broader talonid, where the indexes of trigonid and talonid length and breadth of ♂♂ are higher than ♀♀ in both species, and where both the means and the ranges of variability of L ta/L tr m1 and B ta/B tr m1 indexes almost do not overlap. In *M. nivalis* from Hunas both ratios are as follows: L ta/L tr m1 (♂♂ 40.6, 30.5-51.2, n = 103; ♀♀ 49.1, 39.2-54.4, n = 39), while B ta/B tr m1 (♂♂ 90.6, 87.1-95.8, n = 103; ♀♀ 91.7, 87.2-96.2, n = 39). The values of both indexes in *M. erminea* are distinctly lower: L ta/L tr m1 (♂♂ 23.9, 18.6-32.4, n = 151; ♀♀ 27.8, 20.8-33.9, n = 177), while B ta/B tr m1 (♂♂ 78.1, 66.5-87.1, n = 151; ♀♀ 82.9, 77.7-86.1, n = 177) (Table 6);

9) much less developed m1 protoconid broadening, usually, where it is present, occurs in variable size on the lingual margin, while in *M. erminea* this crown bulging occurs on the buccal and lingual sides. It is well illustrated by the morphotype analysis, where for both sexes of *M. erminea* (♂♂ 94.7%, ♀♀ 91.5%) the evolutionarily most advanced morphotype D is dominant, broadened buccally and lingually, commonly with a lingual, additional, median root. In *M. nivalis* from Hunas the situation is totally different and more variable. In ♂♂ morphotype C is dominant (73.8%), only lingually widened, tending to form a lingual root under the metaconid ridge of the protoconid. About one-fourth (24.3%) are of the less advanced morphotype B, which is only buccally widened, and is dominant (48.7%) in ♀♀ *M. nivalis* from Hunas. There are fewer of morphotype C (18.0%) and the most primitive A (25.6%), with an elongated and narrow crown (Table 7).

COMPARISON WITH *MUSTELA NIVALIS*

When comparing *M. nivalis* from Hunas with the extant Silesian population of this species, we found few distinguishing features; the scale and degree of differentiation between the two groups is quite small, especially in comparison with *M. erminea*. The size and main indexes used in taxonomic analysis, like p2 L/m1 L, B/L p3, Ba/Bp p4, L ta/L tr m1 and B ta/B tr m1, differ very little. In most cases, indexes and the ranges of variation are almost identical, and the differences found between the sexes in both cases are almost the same.

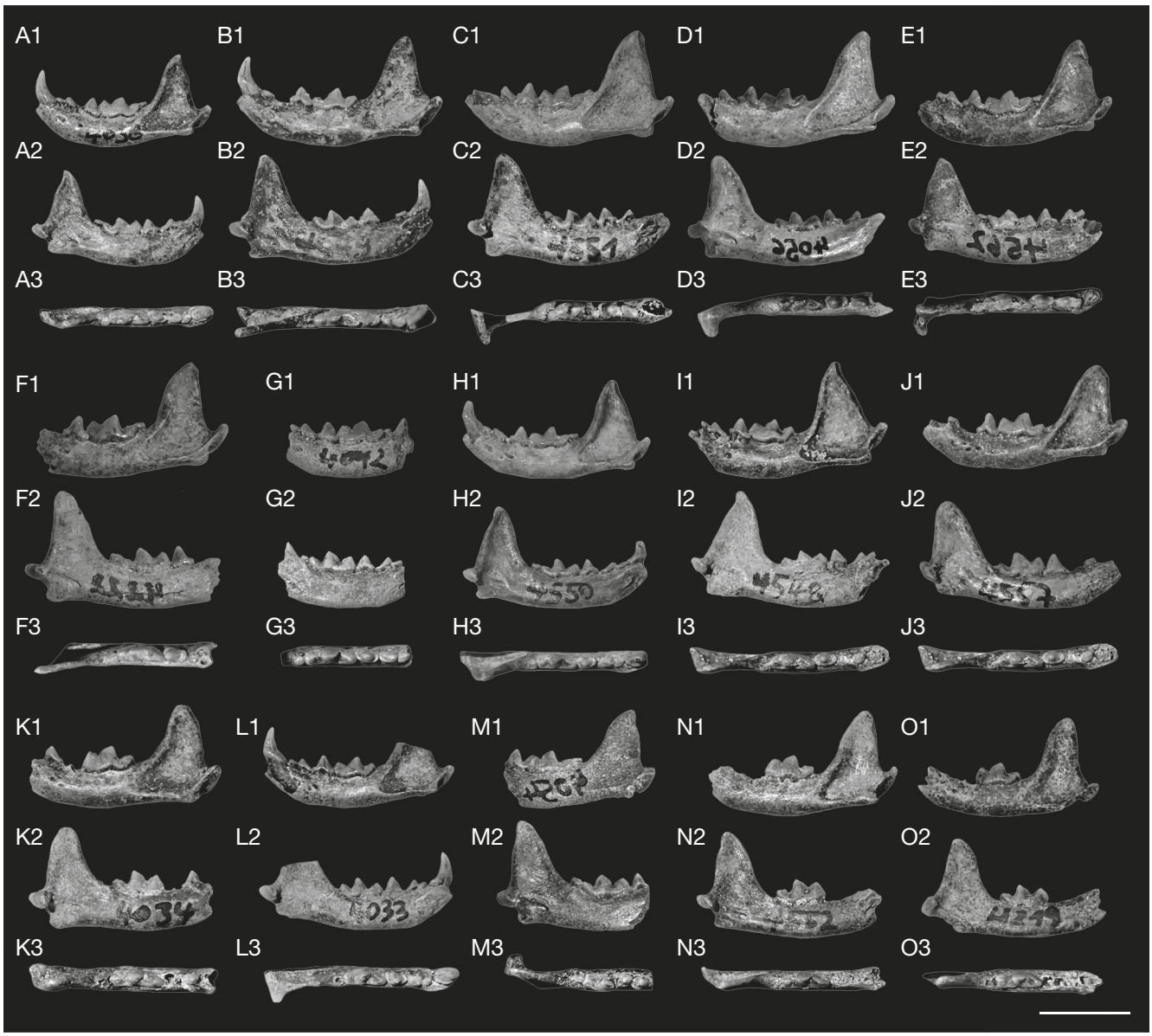

Fig. 9. — Mandibles of the average and large sized ♂♂ of *Mustela nivalis* Linnaeus, 1766 from Hunas: **A**, Hu/4036 (4.27 mm); **B**, Hu/4549 (4.27 mm); **C**, Hu/4551 (4.32 mm); **D**, Hu/4056 (4.47 mm); **E**, Hu/4562 (4.48 mm); **F**, Hu/4222 (4.57 mm); **G**, Hu/4042 (4.59 mm); **H**, Hu/4550 (4.38 mm); **I**, Hu/4548 (4.38 mm); **J**, Hu/4557 (4.37 mm); **K**, Hu/4034 (4.88 mm); **L**, Hu/4033 (4.52 mm); **M**, Hu/4054 (4.78 mm); **N**, Hu/4552 (4.69 mm); **O**, Hu/4219 (4.39 mm). In brackets together with collection number also L m1 in mm of particular specimens are given. Numbers: **1**, buccal view; **2**, lingual view; **3**, occlusal view (D, E, F, and M reversed). Scale bar: 10 mm.

The differentiating features presented below are highly differentiated and tend to be frequent rather than typical for a particular population. The only reliable difference is presence of weakly to moderately marked, but still stronger than in the extant *M. nivalis*, longitudinal, lingual furrow of the mandibular body.

Mentioned by Heller (1983d, e), considerable bulging of the pars alveolars below the teeth row and accompanying its trough-like depression in *M. nivalis* from Hunas occurred in such a large degree of diversification of development, it is impossible to find any regularity. Apart from individuals with a fairly strong structure (although not as much as Heller suggested), in most specimens this structure is absent or poorly marked. Moreover, a similar high variability was observed for the extant Silesian *M. erminea*, which absolutely excludes its usefulness in taxonomic analyses. The same was found for the extant Silesian population of *M. nivalis*.

Comparison with *Mustela palerminea* and *Mustela praenivalis*

Finally, the comparison with two ancestor species of small *Mustela*, *M. palerminea* and *M. praenivalis*, do not confirm the statement by Heller (1983d, e). Although the morphometric analysis showed the existence of a few weakly expressed, primitive features, they should rather be treated in the category of ancestral remnants. It is also an expression and proof of evolution within one evolutionary line. It also explains the presence of given features at different stages of advancement

from data, different in time and space. Evolution as a process is gradual and heterogeneous, so a given feature may appear earlier in one area, while at a contemporaneous but geographically distant site, it is still primordial. A similar suggestion that the material of the smallest *Mustela* from Hunas is an intermediate form and evidence of gradual evolution was already proposed by Heller (1983d, e).

Compared to *M. palerminea*, cranial and dental material of *M. nivalis* from Hunas shows the following differences:

1) smaller size, well-illustrated by the L m1, where the mean of *M. nivalis* ♂♂ from Hunas (4.43 mm, 4.02-4.97 mm, n = 103) is smaller than the mean of *M. palerminea* (EP 5.46 mm, 4.49-6.12 mm, n = 165; eMP 5.23 mm, 4.46-5.97 mm, n = 36). Overlap in the size class of *c.* 4.50-5.00 mm is observed, with the large *M. nivalis* ♂♂ from Hunas comparable with the small (probably ♀♀) *M. palerminea*;

2) on average deeper masseteric fossa, with a more triangular mesial margin. *Mustela palerminea* possesses on average shallower masseteric fossa, with a more rounded mesial edge;

3) shape of the condyloid process, which in *M. nivalis* from Hunas is more elongated and straighter, while in *M. palerminea* is usually shorter and hook-shaped;

4) the morphology of the angular process, longer and hooked in *M. palerminea*, contrary to the short and straight angular process as observed in *M. nivalis* from Hunas;

5) presence of a longitudinal, lingual furrow of the mandibular body, which is on average distinctly weaker than in *M. palerminea*. However, the degree of development of this structure in *M. palerminea* is variable. Together with individuals with a strong lingual furrow, many specimens show a weakly developed structure, similar to that of *M. erminea*. In larger series from Deutsch Altenburg 2 and Żabia Cave, about 70% of individuals have at most a moderately strong lingual furrow.

The main indexes, like p2 L/m1 L, B/L p3, Ba/Bp p4, L ta/L tr m1 and B ta/B tr m1, differ slightly between *M. nivalis* from Hunas and *M. palerminea*. Their variability ranges generally largely overlap, with the means indicating a slightly higher level of evolutionary development in *M. nivalis* from Hunas. This is not due to evolutionary advancement of *M. nivalis* from Hunas, but rather to the primitivism of the features characterising *M. palerminea*. The evolutionary lineage *M. palerminea* => *M. erminea* is characterised by a stronger development of progressive features compared to the lineage *M. praenivalis* => *M. nivalis*, which is visible in the comparison shown above (Figs 10; 11).

The comparison of *M. nivalis* from Hunas with *M. praenivalis* showed similar morphological differences like those noted in comparison with *M. palerminea*. In relation to *M. praenivalis*, *M. nivalis* from Hunas has a deeper and longer masseteric fossa, which reaches the m1/m2 boundary, weaker lingual furrow, more elongated and straighter angular and condyloid processes, proportionally more reduced p2, broader p3, stronger marked difference between the mesial and distal halves of the p4 crown, and m1 with proportionally higher and longer trigonid and shorter and narrower talonid (Table 6). There is apparently some overlap, but the ratios differ. The comparison of indexes, starting from the Early Pleistocene through the early Middle Pleistocene, both represented by *M. praenivalis*, populations of *M. nivalis* from Hunas (MIS 7), up to the extant *M. nivalis*, shows a slow but clearly marked increase in the progressiveness of cranial and dental features. However, it is clearly less pronounced than in the evolutionary line of *M. erminea* => *M. palerminea*. The above conclusion is additionally confirmed by analyses of the frequency of occurrence of given morphotypes. In the lineage presented above, *M. praenivalis* => *M. nivalis*, we observe an increasing share of evolutionarily advanced morphotypes (Table 7).

Comparison of the postcranial material

Numerous and well-preserved postcranial skeletal elements, mainly long bones, but also vertebrae or pelvis, of *M. nivalis* from Hunas, are morphologically similar to those of *M. erminea*, but they differ metrically in their smaller size. They are also indistinguishable from bones of extant *M. nivalis*, which shows great sexual dimorphism, where ranges of variation of sexes almost do not overlap. All long bones of *M. nivalis* from Hunas are metrically comparable with those of the extant *M. nivalis*, and the material of this species from Hunas can therefore be sexed. The analysis showed a predominance of ♂♂ and documented presence of only adult, moderately to large-sized individuals.

Considering all the given information, the analysis allowed us to determine the whole cranial and dental material of the smallest *Mustela* from Huans as *M. nivalis*. Certain insignificant morphological differences found in relation to extant *M. nivalis* are a remnant of its ancestor, *M. praenivalis*. These primary features, expressed to varying degrees in different individuals from Hunas, are already quite weakly expressed. In principle, they should be treated in terms of frequency in terms of the entire population, rather than as the occurrence of a given feature characterizing the population. Thus, Hunas is unique on an Eurasian scale in terms of it allowing the study of a *M. nivalis* population (Figs 10; 11) deposited in one spatially limited place, in a relatively short time and in good condition.

In addition, it allows us to capture the already faintly expressed, but still present, primitive features that are no longer present in stratigraphically younger populations. This is direct evidence of the evolution of the phylogenetic lineage of *M. praenivalis* => *M. nivalis*. In this lineage, the population of *M. nivalis* from Hunas documents one of the last accords immediately preceding the appearance of the extant *M. nivalis*. Ambros (2006) also pointed out the absence of ancient species like *M. palerminea* and *M. praenivalis*. She found no distinguishing features *M.* cf. *palerminea* from Hunas (in fact, *M. nivalis*) and *M. erminea*. Also, the analysis of postcranial material did not allow her to clarify this problem (Ambros 2006).

DISCUSSION

The abundant mustelid fauna from Hunas is typical of the late Middle-Late Pleistocene time interval. Their uniqueness lies primarily in the presence of very rare species in the fossil

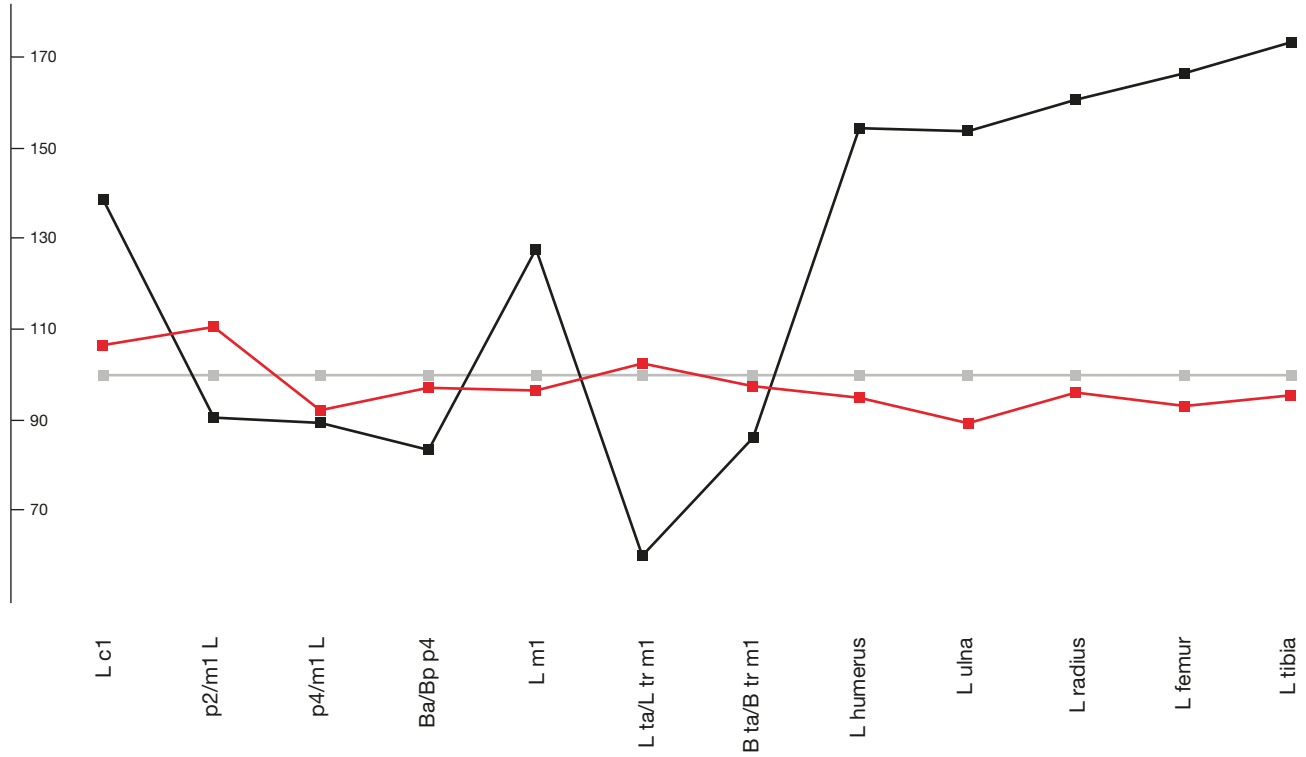

Fig. 10. — A list of selected features of the morphology of small *Mustela* Linnaeus, 1758 males, shown as a percentage of the base population of the extant *Mustela nivalis* Linnaeus, 1766 males (**grey line**), for which the values of all features are presented as 100%. **Black line**, extant *Mustela erminea* Linnaeus, 1758 males; **red line**, *Mustela nivalis* males from Hunas. For citation see the chapter Material.

material, such as *L. lutra*, as well as in the unusual accumulation in one place and in a relatively short time of well-preserved material of *M. nivalis*. Comparing the fauna of mustelids from Hunas with other European localities dated to MIS 11-6, we find a number of analogies in terms of faunal composition, the number of remains of individual species relative to each other and the degree of evolutionary development. Among them, especially noteworthy are sites like French La Fage 1 and 2 (MIS 8-7; Hugueney 1975; Mourer-Chauviré *et al.* 2003; Brugal *et al.* 2020), Deszczowa Cave (layers 1-4, MIS 8-6; Nadachowski *et al.* 2009; Marciszak 2012) and Biśnik Cave (layers 19ad-14, MIS 9-6; Marciszak 2012; Marciszak & Socha 2014) from Poland and Kudaro 1 and 3 Caves from Ossetia (MIS 11-6; Baryshnikov 2009).

The evolutionary lineage *G. g. schlosseri* => *G. g. gulo* is well documented (Kormos 1914). However, the exact timing of derivation of one form from another is not clear. The morphometric differences between *G. g. schlosseri* and *G. g. gulo* were clearly defined and specified and include smaller size, greater diastemas between the lower teeth, less curvature of the lower tooth row, narrower premolars, m1 with proportionally longer and broader talonid and relatively large m2 (Kormos 1914; Dubois & Stehlin 1933; Bonifay 1971; Kolfschoten 2001; Marciszak 2012). However, all these features concern the lower dentition, while the morphology of the upper teeth is generally unknown. Studies of these teeth also showed some differences (Marciszak 2012). The morphology of M1 from Tunel Wielki, with presence of admixture characteristics of both species, suggested an intermediate form. Greater metrical and morphological similarity to *G. g. gulo* tips the balance of classification to this subspecies, making it one of the oldest occurrences in Eurasia (Kot *et al.* 2022).

The transition from *G. g. schlosseri* to *G. g. gulo* took place somewhere during the early part of the late Middle Pleistocene (MIS 12-11). Individuals of *G. g. schlosseri* from the early Middle Pleistocene (MIS 21-17) do not differ morphologically from those from the Early Pleistocene. Specimens from the Middle Pleistocene (MIS 16-13) represent a higher evolutionary level, which is reflected in larger sizes, stronger dental arches, slightly broader p3 and p4 crowns and a stronger reduction of the talonid of m1 (Marciszak 2012). From the German site Mosbach both species were described (Tobien 1957). However, later studies showed that the specimens are of different ages (Brüning 1970; Keller 2004). The smaller mandible with more primitive morphology assigned to *G. g. schlosseri* is a member of an assemblage described as main fauna of Mosbach 2, correlated with the middle level, and dated to MIS 15-13 (von Reichenau 1910; Tobien 1957; Kahlke 1961; Brüning 1970; Döppes 2001, 2005; Keller 2004). Described by Tobien (1957) the right mandible with p2-m1 was found in the upper horizon, later determined as Mosbach 3 and dated to MIS 12-11 (Brüning 1970; Keller 2004). The morphology like strongly expanded distal halves of p3 and p4 and proportions of trigonid and talonid of m1 and size of this specimen (L m1 24 mm) differs only slightly from the Late Pleistocene and extant wolverine and indicate a higher evolutionary level than the first individual.

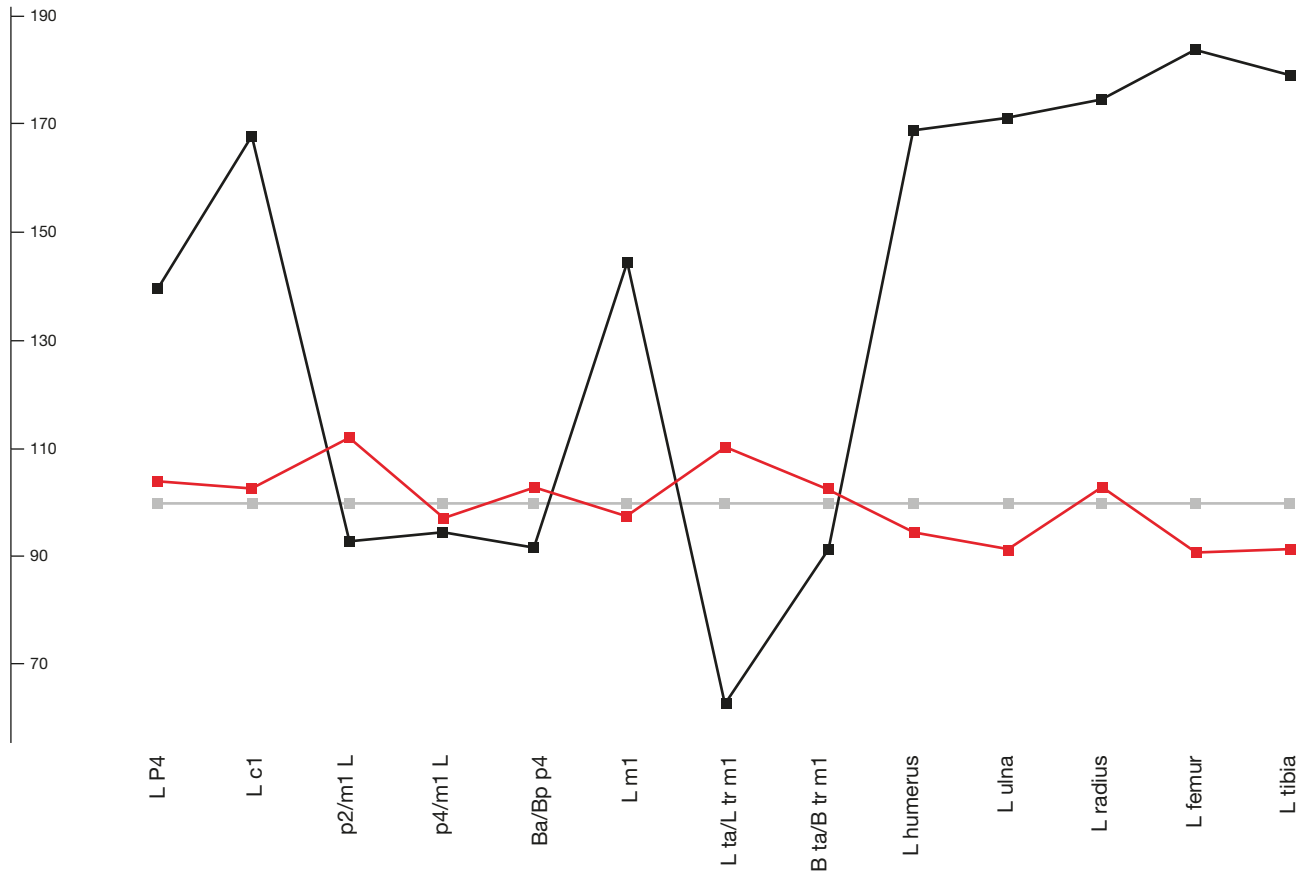

Fig. 11. — A list of selected features of the morphology of small *Mustela* Linnaeus, 1758 males, shown as a percentage of the base population of the extant *Mustela nivalis* Linnaeus, 1766 males (**grey line**), for which the values of all features are presented as 100%. **Black line**, extant *Mustela erminea* Linnaeus, 1758 males; **red line**, *Mustela nivalis* males from Hunas. For citation see the chapter Material.

Pleistocene remains of *L. lutra* are very rare, and relics of this species are mainly known from Holocene deposits (Sommer & Benecke 2004; Mecozzi *et al.* 2022). Among the oldest European records are Hoxne (420-370 kya; England; Mecozzi *et al.* 2022), Maggiore di San Bernardino Cave (240-180 kya, Italy; Cassoli & Tagliacozzo 1994a, b, c; Mecozzi *et al.* 2022), layers 1-4 of Deszczowa Cave (240-180 kya, Poland; Nadachowski *et al.* 2009; Marciszak 2012), Romanelli Cave (150-130 kya, Italy; Mecozzi *et al.* 2022), Pilisszánto 1 (40-30 kya, Hungary; Jánossy 1986) and Skjonghelleren Cave (35-30 kya, Norway; Larsen *et al.* 1987; Willemsen 1992). *L. simplicidens* is a typical species for the Early and Middle Pleistocene sites (1.8-0.4 mya), and is an uncommon but characteristic faunal element of mostly European, but also Asian paleofaunas (Thenius 1948, 1965; Willemsen 1992; Sotnikova & Titov 2009; Cherin & Rook 2014; Cherin *et al.* 2016; Cherin 2017). Finally, characterised by a robust, shellfish-feeding type of dentition, *C. antiqua* is reported from several European localities, dated between 420 and 50 kya (Kurtén 1968; Willemsen 1992; Mecozzi *et al.* 2022).

Martes martes as a species evolved into *M. vetus* during the mid-Middle Pleistocene, probably between 600 and 500 kya (Kurtén 1968; Anderson 1970; Wiszniowska 1989; Marciszak 2012; Marciszak *et al.* 2021). Marten remains from this period (600-430 kya) are mostly described as *M. martes* (Stuart 1974, 1981, 1996; Bon *et al.* 1991; Turner 2009; Stuart & Lister 2010; García & Arsuaga 2011), *Martes* sp. (Kahlke 1961; Kurtén 1968; Wolsan 1993; García *et al.* 1997; García 2003; Ghezzo *et al.* 2014) or even *M. foina* (Koenigswald & Heinrich 1999). Dated to 460-430 kya, marten material from the Spanish site Sima de los Huesos, which shows intermediate features between *M. vetus* and *M. martes*, was classified as *M.* cf. *martes* (García 2003; García *et al.* 2023). *Martes martes* as a species appeared not earlier than *c.* 500 kya (Sutcliffe 1964; Jánossy 1969a, b; Anderson 1970; Koenigswald & Heinrich 1999; Marciszak 2012; Marciszak *et al.* 2021; Kot *et al.* 2022). Specimens from sites like Swanscombe (Great Britain; Sutcliffe 1964) or Draby 3 (Poland; Marciszak *et al.* 2023), both dated to 430-380 kya, already have morphology corresponding to that of *M. martes*. The same was obtained for slightly younger (380-300 kya) materials of *M. martes* from layers 19ad of Biśnik Cave (Marciszak 2012; Marciszak *et al.* 2021) and Kudaro 1 Cave (Baryshnikov 2009).

The evolutionary history of *M. putorius* is relatively poorly documented. Kurtén (1968) stated that this mustelid first appeared in the fossil record from sites like Forest Bed and Mosbach 2 (0.6-0.5 mya). From Mosbach 2 (0.6-0.5 mya), the presence of this species was signalised based on a single radius (von Reichenau 1910; Soergel 1912, 1914; Wenz 1921; Zeuner 1937). Postcranial elements, even complete long bones, are

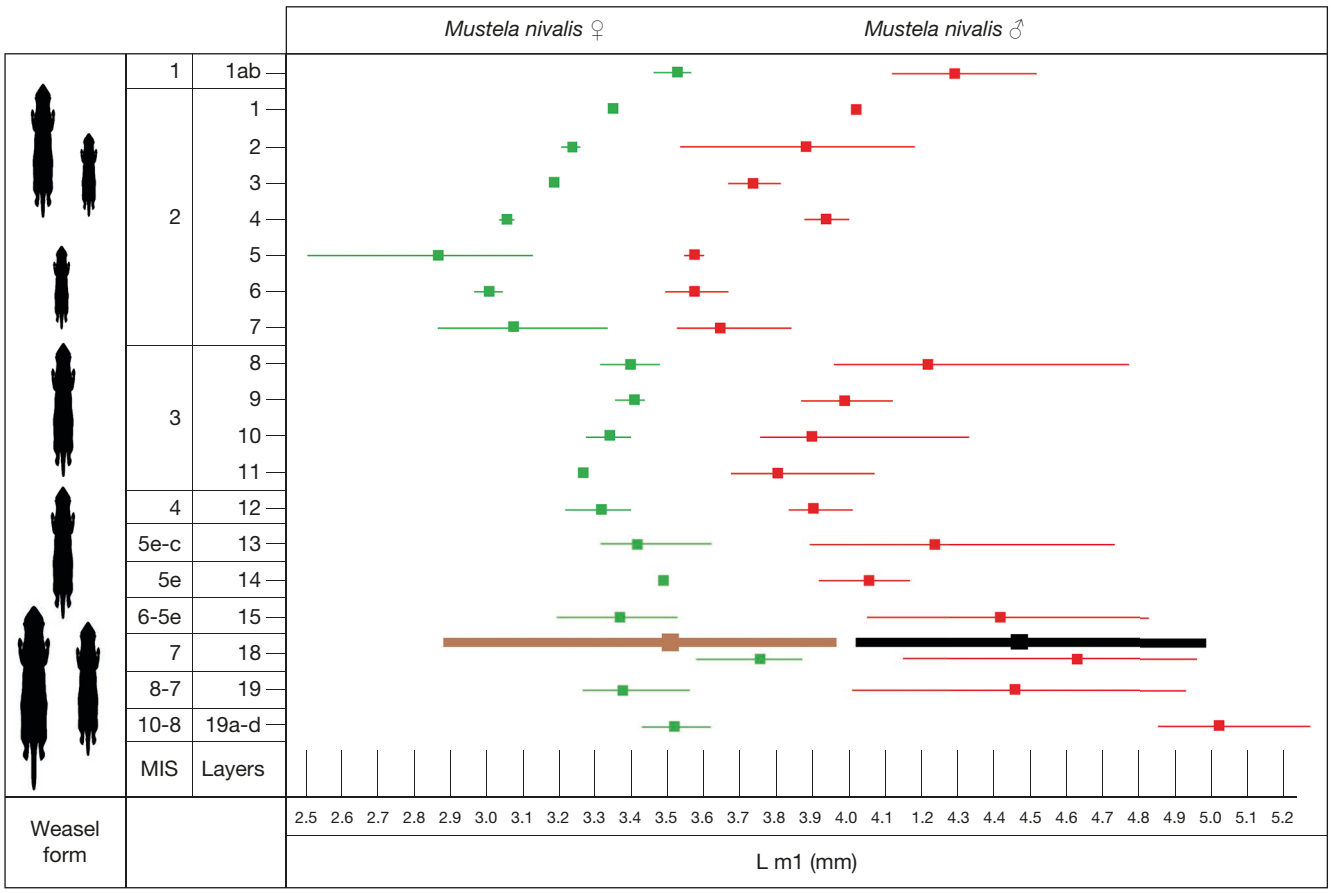

Fig. 12. — Comparison of the *Mustela nivalis* Linnaeus, 1766 m1 length (L m1) from Biśnik Cave (♂♂ **red**; ♀♀ **green**) and Hunas (♂♂ **black**; ♀♀ **brown**). Modified from Marciszak & Socha (2014).

rather vague in polecat determination, so they cannot specify to which species this bone in fact belonged. Additionally, the bone was destroyed during WW2 (Kahlke 1961). From the similarly dated Hundsheim, Freudenberg (1908, 1914) briefly described the presence of a sole hemimandible of ♀ (L m1 6.80 mm). The specimen was personally studied by the authors (A.M.) and we confirmed its primary determination.

Stehlík (1934) described from Stránská Skála (0.9-0.8 mya) seven hemimandibles of variable sizes (L m1 7.00-9.20 mm) and morphology. Some specimens are small and gracile build, with a low mandibular body, while others are distinctly larger, robustly built and characterised by small m2, among others. This material from early excavations (Čapek collection) is clearly heterochronic and comes from at least two different levels. There is no valid reason for assuming that these remains are coeval. The biochronological interpretations for the site should be based on specimens of reliable stratigraphic provenance. This material was studied by A.M. and clearly corresponds to *M. eversmanii* and *M. putorius*. Without a doubt *M. putorius* is well represented in the Spanish site Sima de los Huesos (460-430 kya; García 2003; García *et al.* 2023).

Between 2.4 and 0.7 mya *M. palerminea* and *M. praenivalis* were widespread and commonly represented in European localities (Kormos 1914, 1934; Heller 1930, 1933, 1936, 1958; Brunner 1933; Dehm 1962; Rabeder 1976; Jánossy 1986; Wiszniowska 1989; García 2003; Marciszak 2012; Petrucci *et al.* 2013; Gasparik & Panozyi 2018; Petronio *et al.* 2020; Marciszak *et al.* 2021). Remains of the smallest *Mustela* from 0.6-0.5 mya have morphologies resembling *M. erminea* and *M. nivalis*. Their morphology still has some ancestral characters resembling those of *M. palerminea* and *M. praenivalis*. However, most of their morphological characteristics are typical for *M. erminea* and *M. nivalis*, which allows us to determine them as extant species. Among them are individuals from such localities as Červený Kopec, Château Breccia, Hundsheim, Miesenheim 1, Mosbach 2, Sima de los Huesos, Viatelle and Westbury-sub-Mendip (Freudenberg 1914; Bishop 1982; Turner 1990; Parfitt 1999; García 2003; Marciszak *et al.* 2021; García *et al.* 2023).

The Hunas faunal assemblage is highly diverse, and their exact ages have so far not been fully resolved. Flowstone layers at the base of the sediment stack in Hunas have been dated with 230Th/234U by Hennig *et al.* (1983) with a median age of *c.* 221 kya. A new U-series age for the youngest speleothem generation falls again into a similar time window of *c.* 250 kya (J. Fietzke & M. López Correa pers. comm.), providing a theoretical maximum age constraint for the cave sediments.

More than 90% of the mustelid material came from complex G1-G3. This horizon was differently dated, and the faunal assemblage was characterised as an admixture of cold-adapted

and more thermophilic species (Koenigswald & Heinrich 1999). Adam (1986) dated the whole fauna on the Eemian Interglacial (MIS 5e). In contrast, Carls *et al.* (1988a, b) found that *Arvicola* remains from the whole profile belong to the transitional form between *Arvicola mosbachensis* (Schmidtgen, 1911)/*Arvicola cantianus* (Hinton, 1910) and *Arvicola amphibius* (Linnaeus, 1758), and proposed an age of MIS 8-7. A similar age (Saalian complex) was proposed by most of the authors (Schütt & Hemmer 1978; Carls 1986; Carls *et al.* 1988a, b; Wolsan 1993; Koenigswald & Heinrich 1999; Kowalski 2001; Ambros 2003, 2006; Hilpert 2005, 2006; Ambros *et al.* 2005; Marciszak *et al.* 2019). Böhme, who analysed the amphibian and reptilian skeletal remains as well as fish fauna, clearly pointed out that the faunal assemblages cannot belong to Eemian or Wechselian age (Böhme 2011). The herpetofauna show an early to high glacial sequence, with a short phase of interglacial climate condition at the base of the sediment sequence, directly above the speleothem.

The results obtained for other carnivores corroborated our results. Hilpert (2006) described material of spelaeoid ursids as *Ursus spelaeus* Rosenmüller, 1794, but with a slightly smaller and clearly less complicated occlusal surface. She found distinct differences in the morphology of the postcranial skeleton. According to Hilpert (2006), special local climatic and natural conditions caused the amount of food being relatively more plentiful than in other areas and the ecological pressure was less. Due to this, *U. spelaeus* from Hunas became more generalised and their dentition less specialised. Rabeder (1999) found that the P4/p4 morphodynamic index (54.5) is notably lower than any other characterised Late Pleistocene population (Rabeder 1999). All analysed teeth (90 molars from layers D and E and 563 molars in total were found in Hunas) were smaller, slender and distinctly less complicated than the Late Pleistocene ursids. Rabeder (1999) classified the Hunas ursid as advanced *U. deningeri* Reichenau, 1904.

Also, mustelids pushed the dating of the G1-G3 complex within MIS 7, rather than MIS 5-3. The Central European occurrence of *L. lutra* is more typical for the more moist and thermophilic period MIS 8-5e, than the drier and cooler phase MIS 5d-3 (Sommer & Benecke 2004; Nadachowski *et al.* 2009; Marciszak 2012; Mecozzi *et al.* 2022). Abundant material of *M. nivalis* is also a good marker, which suggested a period of MIS 8-5e instead. When compared L m1 of Hunas material with well stratified and dated material from Biśnik Cave, it showed that their size and massiveness matched the individuals dated to the late Middle Pleistocene (MIS 9-6) (Fig. 12). *Mustela nivalis* from layers 19a-d to 18 are very similar to the large, long-tailed southern weasels of the *boccamela-numidica* group. The weasels of this group are regarded as the closest to the stem-species weasel from the Pliocene and the Early Pleistocene (Abramov & Baryshnikov 2000; Marciszak 2012). In the second period (MIS 6-5c), the size decreases steadily from layer 15 to 13 (with some exceptions), but *M. nivalis* is still quite large, with the L m1 mean of ♂♂ exceeding 4 mm. The climatic conditions and temperature were still quite constant, but some minor fluctuations also occurred. This is the first period that documents more significant climate changes, and the temperature not only dropped sharply, compared to the two preceding periods, but also varied quite strongly. It seems that during that time interval the climate in the neighbourhood of Biśnik Cave was unstable, but overall, the temperature was moderate. Similarity between Biśnik Cave (layers 19ad-12) and the Hunas population could indicate that similar climatic conditions occurred at both sites. The means from both populations notably exceed the means from the younger, Late Pleistocene periods (Fig. 12).

The period between MIS 8-6 in Hunas is also highly probable, since among ♂♂ specimens with L m1 larger than 5 mm are not present. Simultaneously, among ♀♀, there is a sole dwarf individual with L m1 less than 3 mm. The Late Pleistocene dwarf *M. nivalis* is an example of the evolutionary and ecological plasticity of the species (King 1989; Abramov & Baryshnikov 2000; King & Powell 2007; Marciszak & Socha 2014). The Biśnik Cave layers 7-5, dated to MIS 3-2 are the coolest in the whole profile and are characterised by the presence of dwarf *M. nivalis* individuals (Fig. 12). Their morphology corresponded with the smallest short-tailed specimens of the *minuta-rixosa* group (Abramov & Baryshnikov 2000). Apart from a single specimen, their presence was not recorded in the Hunas material, which excluded a Late Pleistocene age of those remains. Additionally, a presence of a weakly to moderately marked longitudinal, lingual furrow of the mandibular body, distinctly stronger developed than in the Late Pleistocene and extant *M. nivalis* is also noteworthy. All the above-mentioned features indicate an age of MIS 7 for the layer complex G1-G3.

Aknowledgements
We are indebted to the Associate Editor L. Rook and two anonymous reviewer for their useful comments and suggestions, which significantly improved the manuscript.We are also to A. Neveu for all the great work and help with the improvement of the manuscript.

Author contributions
Conceptualisation, methodology, software and funding acquisition, A.M.; investigation, A.M., B.H., D.A.; writing-original draft preparation, A.M., B.H., D.A.; visualisation, A.M., B.H.; writing – review and editing, A.M., B.H., D.A. All authors have read and agreed to the published version of the manuscript.

Funding
The research was financed by an internal grant from the Faculty of Biological Sciences, University of Wrocław entitled "The Middle Pleistocene Revolution - how the modern theriofauna of Eurasia was developed", as part of the programme IDUB, grant no. BPIDUB.4610.6.2021.KP.A.

Data availability statement

All information where readers can obtain the research data required to reproduce the work reported in the manuscript, e.g. status of the material, its location, collection numbers etc., are provided within the manuscript and in both appendices. All material, if currently present, is available to study in particular museums and private collections.

REFERENCES

ABRAMOV A. V. & BARYSHNIKOV G. F. 2000. — Geographic variation and intraspecific taxonomy of weasel *Mustela nivalis* (Carnivora, Mustelidae). *Zoosystematica Rossica* 8 (2): 365-402.

ADAM K. D. 1986. — Die Höhlenruine Hunas in der Fränkischen Alb - Reflexionen zum Forschungsstand. *Stuttgarter Beiträge zur Naturkunde, Serie B (Geologie und Paläontologie)* 121: 1-24.

ALT K. W., KAULICH B., REISCH L., VOGEL H. & ROSENDAHL W. 2006. — The Neanderthalian molar from Hunas, Germany. *Homo-Journal of Comparative Human Biology* 57 (3): 187-200. https://doi.org/10.1016/j.jchb.2006.03.002

AMBROS D. 2003. — New finds from the Middle Pleistocene cave ruin Hunas, county Pommelsbrunn, Bavaria, Germany. *Atti del Museo Civico di Storia Naturale di Trieste* 49: 9-14.

AMBROS D. C. 2006. — *Morphologische und metrische Untersuchungen an Phalangen und Metapodien quartärer Musteliden unter besonderer Berücksichtigung der Unterscheidung von Baum- und Steinmarder (*Martes martes *(Linné 1758) und* Martes foina *(Erxleben 1777))*. Der Andere Verlag, Tönning, Lübeck, Marburg, 103 p.

AMBROS D. & HILPERT B. 2005. — Morphologische Unterscheidungsmerkmale an postcranialen Skelettelementen des Baummarders (*Martes martes* (Linné 1758)) und des Steinmarders (*Martes foina* (Erxleben 1777)) (Carnivora, Mustelidae). *Monographien Naturhistorische Gesellschaft Nürnberg* 45: 19-34.

AMBROS D. & HILPERT B. 2023. — Die Steinberg-Höhlenruine bei Hunas (Lkr. Nürnberger Land), *in* UTHMEIER T. & MISCHKA D. (eds), *Steinzeit in Bayern*. Das Handbuch, Band 1: 438-442.

AMBROS D., HILPERT B., KAULICH B., REISCH L. & ROSENDAHL W. 2005. — Steinberg Höhlenruine bei Hunas (HFA A 236). *Abhandlungen der Naturhistorischen Gesellschaft Nürnberg* 45: 325-336.

ANDERSON E. 1970. — Quaternary evolution of the genus *Martes* (Carnivora, Mustelidae). *Acta Zoologica Fennica* 130: 1-132.

ARRIBAS A. & GARRIDO G. 2007. — *Meles iberica* n. sp., a new Eurasian badger (Mammalia, Carnivora, Mustelidae) from Fonelas P-1 (Plio-Pleistocene boundary, Guadix Basin, Granada, Spain). *Comptes Rendus Paleovol* 6 (8): 545-555. https://doi.org/10.1016/j.crpv.2007.06.002

BARYSHNIKOV G. F. 2009. — Pleistocene Mustelidae (Carnivora) from Paleolithic site in Kudaro Caves in the Caucasus. *Russian Journal of Theriology* 8 (2): 75-95. https://doi.org/10.15298/rusjtheriol.08.2.02

BAUMANN CH. 2011. — Kleinsäugerfunde aus drei Profilsäulen (N2, Q1, S2) der mittel- bis spätpleistozänen Höhlenruine Hunas (Mittelfranken). Ein Beitrag zur biostratigraphischen und paläoökologischen Auswertung der Fundstelle. Bachelorarbeit zur Erlangung des akademischen Grades Bachelor of Arts, Friedrich-Schiller-Universität Jena, Philosophische Fakultät, Ur- und Frühgeschichte.

BISHOP M. J. 1982. — The mammal fauna of the early Middle Pleistocene cavern infill site of Westbury-sub-Mendip, Somerset. *Special Papers in Paleontology* 28: 1-108.

BON M., PICCOLI G. & SALA B. 1991. — I giacimenti Quaternari di vertebrati fossili nell'Italia Nord–Orientale. *Memorie degli Instituti di Geologia e Mineralogia dell'Universita di Padova* 47: 185-231.

BONIFAY M.-F. 1971. — *Carnivores quaternaries du Sud-Est de la France*. Muséum national d'Histoire naturelle (Mémoires du Muséum national d'Histoire naturelle, Sér. C – Sciences de la Terre (1950-1992) ; 21 (2)), Paris, 334 p.

BÖHME G. 2011. — Fisch-, Amphibien- und Reptilienreste aus der Höhlenruine Hunas bei Hartmannshof (Mittelfranken). *Quartär* 58: 7-23. https://doi.org/10.7485/QU58_01

BOURGEOIS G. & PHILIPPE M. 2017. — Présence du glouton *Gulo gulo* (Mustelidae, Carnivora) dans le gisement pléistocène moyen de La Fage-Aven II, à Noailles (Corrèze, France). *Paleo* 28: 215-226. https://doi.org/10.4000/paleo.3479

BRUGAL J.-P., ARGANT A., BOUDADI-MALIGNE M., CRÉGUT-BONNOURE E., CROITOR R., FERNANDEZ P., FOURVEL J.-B., FOSSE F., GUADELLI J.-L., LABE B., MAGNIEZ P. & UZUNIDIS A. 2020. — Pleistocene herbivores and carnivores from France: an updated overview of the literature, sites and taxonomy. *Annales de Paléontologie* 106 (2): 102384. https://doi.org/10.1016/j.annpal.2019.102384

BRUNNER G. 1933. — Eine präglaciale Fauna aus dem Windloch bei Sackdilling (Oberpfalz). *Neues Jahrbuch für Mineralogie, Geologie und Paläontologie* 71B: 303-328.

BRÜNING H. 1970. — Zur Klima-Stratigraphie der pleistozänen Mosbacher Sande bei Wiesbaden (Hessen). *Mainzer Naturwissenschaftliches Archiv* 9: 204-256.

CARLS N. 1986. — *Arvicoliden (Rodentia, Mammalia) aus dem Mittel- und Jungpleistozän Süddeutschlands*. Den Naturwissenschaftlichen Fakultäten der Friedrich-Alexander-Universität Erlangen-Nürnberg zur Erlangung des Doktorgrades vorgelegt, Erlangen, 103 p.

CARLS N., GROISS J. T., KAULICH B. & REISCH L. 1988a. — Neue Beobachtungen in der mittelpleistozänen Fundstelle von Hunas im Ldkr. Nürnberger Land, Vorbericht zu den Grabungskampagnen 1983-1986. *Archäologisches Korrespondenzblatt* 18 (2): 109-119.

CARLS N., GROISS J. T. & RABEDER G. 1988b. — Die mittelpleistozäne Höhlenfüllung von Hunas, Fränkische Alb - Chronologische und paläoklimatische Ergebnisse. *Beiträge zur Paläontologie Österreichs* 14: 239-249.

CASSOLI P. F. & TAGLIACOZZO A. 1994a. — I macromammiferi dei livelli tardopleistocenici delle Arene Candide (Savona, Italia): considerazioni paleontologiche e archeozoologiche. *Quaternaria Nova* 4: 101-262.

CASSOLI P. F. & TAGLIACOZZO A. 1994b. — I resti ossei di macromammiferi, uccelli e pesci della Grotta Maggiore di San Bernardino sui Colli Iberici (VI): considerazioni paleoeconomiche, paleoecologiche e cronologiche. *Bullettino di Paletnologia Italiana* 85: 1-71.

CASSOLI P. F. & TAGLIACOZZO A. 1994c. — Considerazioni Paleontologiche, paleoecologiche e archezoologiche sui macromammiferi e gli uccelli dei livelli del Pleistocene Superiore del Riparo Fumane (VR) (Scavi 1988-91). *Bollettino del Museo Civico di Storia Naturale di Verona* 18: 349-445.

CHERIN M. 2017. — New material of *Lutra simplicidens* (Carnivora, Mustelidae, Lutrinae), a key taxon for understanding the evolution of European otters. *Rivista Italiana di Paleontologia e Stratigrafia* 123 (3): 433-441. https://doi.org/10.13130/2039-4942/9024

CHERIN M. & ROOK L. 2014. — First report of *Lutra simplicidens* (Carnivora, Mustelidae, Lutrinae) in the Early Pleistocene of the Upper Valdarno (Italy) and the origin of European otters. *Italian Journal of Geosciences* 133 (2): 200-203. https://doi.org/10.3301/IJG.2013.25

CHERIN M., IURINO D. A., WILLEMSEN G. & CARNEVALE G. 2016. — A new otter from the Early Pleistocene of Pantalla (Italy), with remarks on the evolutionary history of Mediterranean Quaternary Lutrinae (Carnivora, Mustelidae). *Quaternary Science Reviews* 135: 92-102. https://doi.org/10.1016/j.quascirev.2016.01.008

CRÉGUT-BONNOURE E., BOULBES N., DESCLAUX E. & MARCISZAK A. 2018. — New insights into the LGM and LG in southern France (Vaucluse): the mustelids, micromammals and horses from Coulet des Roches. *Quaternary* 1 (3): 1-19.

DEHM R. 1962. — Altpleistozäne Säuger von Schernfeld bei Eichstätt in Bayern. *Mitteilungen der Bayerischen Staatssammlung für Paläontologie und Historische Geologie* 2: 17-61.
DELPECH F. 1989. — Les Mustelides, *in* CAMPY M., CHALINE J. & VUILLEMEY M. (eds), *La Baume de Gigny (Jura)*. Supplement it Gallia Prehistoire 28: 61-68.
DÖPPES D. 2001. — *Gulo gulo* (Mustelidae, Mammalia) im Jungpleistozän Mitteleuropas. *Beiträge zur Paläontologie* 26: 1-95.
DÖPPES D. 2005. — *Gulo gulo* (Mustelidae, Mammalia) im Ober-Pleistozän Deutschlands. *Neues Jahrbuch für Geologie und Paläontologie Abhandlungen* 235 (3): 411-444. https://doi.org/10.1127/njgpa/235/2005/411
DUBOIS A. & STEHLIN H. G. 1933. — La grotte de Cotencher, station mousterienne. *Abhandlungen der Schweizerischen Paläontologischen Gesellschaft* 53: 179-292.
EHRLINGER S. 1997. — *Die Mikromammalier aus Hunas (Quadratmeter O2, Serie 1-33) und deren stratigraphische und paläoökologische Bedeutung*. Unpublished thesis, University Erlangen-Nürnberg, 71 p.
ERLINGE S. 1975. — Feeding habits of the weasel (*Mustela nivalis*) in relation to prey abundance. *Oikos* 26 (3): 378-384. https://doi.org/10.2307/3543510
ERLINGE S. 1979. — Adaptive significance of sexual dimorphism in weasels. *Oikos* 33 (2): 233-245. https://doi.org/10.2307/3544000
ERLINGE S. 1987. — Why do European stoats *Mustela erminea* not follow Bergmann's rule? *Holarctic Ecology* 10: 33-39.
FAGGI A., BARTOLINI-LUCENTI S., MADURELL-MALAPEIRA J., ABRAMOV A. V., PUZACHENKO A. Y., JIANGZUO Q., PEIRAN L. & ROOK L. 2024. — Quaternary Eurasian badgers: intraspecific variability and species validity. *Journal of Mammalian Evolution* 31: 3. https://doi.org/10.1007/s10914-023-09696-y
FETSCHER H. 1996. — *Mikromammalier aus der Höhlenruine von Hunas*. Unpublished thesis, University Erlangen-Nürnberg, 84 p.
FREUDENBERG W. 1908. — Die Fauna von Hundsheim in Niederösterreich. *Jahrbuch der Geologischen Bundesanstalt* 58: 197-222.
FREUDENBERG W. 1914. — Die Säugetiere des älteren Quartärs von Mitteleuropa mit besonderer Berücksichtigung der Fauna von Hundsheim und Deutschaltenburg in Niederösterreich nebst Bemerkungen über verwandte Formen anderer Fundorte. *Geologische und Paläontologische Abhandlungen, Neue Folge* 12 (4): 455-671.
GALIK A. 1997a. — Die Größenvariation der pleistozänen Mauswiesel (*Mustela nivalis* L.) und Hermeline (*Mustela erminea* L.) (Musteliden, Mammalia) aus der Schusterlucke im Kremstal (Waldviertel, Niederösterreich). *Wissenschaftliche Mitteilungen aus dem Niederösterreichischen Landesmuseum, Neue Funde* 10: 45-61.
GALIK A. 1997b. — Die pleistozänen Iltisknochen (Mustelidae, Mammalia) aus der Schusterlucke im Kremstal (Waldviertel, Niederösterreich): *Mustela putorius* L. - *Mustela eversmanni* Less. *Wissenschaftliche Mitteilungen aus dem Niederösterreichischen Landesmuseum, Neue Funde* 10: 63-81.
GARCÍA N. G. 2003. — *Osos y otros carnivoros de la Sierra de Atapuerca*. Fundación Oso de Asturias, Oviedo, 575 p.
GARCÍA N. & ARSUAGA J. L. 2011. — The Sima de los Huesos (Burgos, northern Spain): palaeoenvironment and habitats of *Homo heidelbergensis* during the Middle Pleistocene. *Quaternary Science Reviews* 30 (11-12): 1413-1419. https://doi.org/10.1016/j.quascirev.2010.11.008
GARCÍA N., ARSUAGA J. L. & TORRES T. 1997. — The carnivore remains from the Sima de los Huesos, Middle Pleistocene site (Sierra de Atapuerca, Spain). *Journal of Human Evolution* 33 (2-3): 155-174. https://doi.org/10.1006/jhev.1997.0154
GARCÍA N., JIMENEZ I. J., BLAZQUEZ-ORTA R. & ARSUAGA J. L. 2023. — Updates to the carnivore fauna from the Sima de los Huesos. *The Anatomical Record* 307 (7): 2246-2258. https://doi.org/10.1002/ar.25199
GASPARIK M. & PANOZYI P. 2018. — The macromammal remains and revised faunal list of the Somssich Hill 2 locality (late Early Pleistocene, Hungary) and the Epivillafranchian faunal change. *Fragmenta Palaeontologica Hungarica* 35: 153-178. https://doi.org/10.17111/FragmPalHung.2018.35.153
GHEZZO E., BERTÉ D. F. & SALA B. 2014. — The revaluation of Galerian Canidae, Felidae and Mustelidae of the Cerè Cave (Verona, Northeastern Italy). *Quaternary International* 339-340: 76-89. https://doi.org/10.1016/j.quaint.2012.12.031
GIMRANOV D. & KOSINTSEV P. 2015. — Differentiation of three *Martes* species (*M. martes*, *M. zibellina*, *M. foina*) by tooth morphotypes. *Comptes Rendus Palevol* 14 (8): 647-656. https://doi.org/10.1016/j.crpv.2015.06.007
GROISS J. T. 1983. — Faunenzusammensetzung, Ökologie und Altersdatierung der Fundstelle Hunas, *in* HELLER F. (ed.), Die Höhlenruine Hunas bei Hartmannshof (Landkreis Nürnberger Land). Eine paläontologische und urgeschichtliche Fundstelle aus dem Spät-Riß. *Quartär-Bibliothek* 4: 351-376.
GROISS J. T. 1985. — Hunas - eine quartäre Fundstelle in der Frankenalb. *Mitteilungen des Verbandes der deutschen Höhlen- und Karstforscher* 31: 48-49.
GROISS J. T. 1986. — Erste Funde von Primaten in der Höhlenruine von Hunas/Hartmannshof (Lkrs. Nürnberger Land). *Altnürnberger Landschaft Mitteilungen* 35 (2): 193-197.
HELLER F. 1930. — Eine Forest-Bed-Fauna aus der Sackdillinger Höhle (Oberpfalz). *Neues Jahrbuch für Geologie und Paläontologie B* 63: 247-298.
HELLER F. 1933. — Ein Nachtrag zur Forest Bed Fauna aus der Sackdillinger Höhle (Oberpfalz). *Centralblatt für Mineralogie, Geologie und Paläontologie, Abteilung B* 1933: 60-68.
HELLER F. 1936. — Eine Forest Bed-Fauna aus der Schwäbischen Alb. *Sitzungsberichte der Heidelberger Akademie der Wissenschaften, Mathematisch-naturwissenschaftliche Klasse* 2: 1-29.
HELLER F. 1958. — Eine neue altquartäre Wirbeltierfauna von Erpfingen (Schwäbische Alb). *Neues Jahrbuch für Geologie und Paläontologie Abhandlungen* 107: 1-102.
HELLER F. 1963a. — Hunas, ein neuer bedeutender Quartärfundplatz im Fränkischen Jura. *Quartär* 14: 165-166.
HELLER F. 1963b. — Ein bedeutsames Quartärprofil in einer Höhlenruine bei Hunas/Hartmannshof (Nördliche Frankenalb). 2. Vorbericht. *Eiszeitalter und Gegenwart* 14: 111-116.
HELLER F. 1965. — Ein bedeutsames Profil aus dem fränkischen Höhlendiluvium. *Dritter Internationaler Kongreß für Speläologie. Bearbeitet von H. Trimmel* 4: 27-30.
HELLER F. 1966. — Die Fauna von Hunas (Nördliche Frankenalb) im Rahmen der deutschen Quartärfaunen. *Eiszeitalter und Gegenwart* 17: 113-117.
HELLER F. 1983a (ed.). — Die Höhlenruine Hunas bei Hartmannshof (Landkreis Nürnberger Land). Eine paläontologische und urgeschichtliche Fundstelle aus dem Spät-Riß. Band 4. Ludwig Röhrscheid Verlag, Bonn, 407 p.
HELLER F. 1983b. — Kurze Beschreibung sämtlicher Schichtglieder, *in* HELLER F. (ed.), Die Höhlenruine Hunas bei Hartmannshof (Landkreis Nürnberger Land). Eine paläontologische und urgeschichtliche Fundstelle aus dem Spät-Riß. *Quartär-Bibliothek* 4: 43-45.
HELLER F. 1983c. — Entstehung und Verfüllung der Höhlenruine von Hunas, *in* HELLER F. (ed.), Die Höhlenruine Hunas bei Hartmannshof (Landkreis Nürnberger Land). Eine paläontologische und urgeschichtliche Fundstelle aus dem Spät-Riß. *Quartär-Bibliothek* 4: 46-51.
HELLER F. 1983d. — Vertebrata, *in* HELLER F. (ed.), Die Höhlenruine Hunas bei Hartmannshof (Landkreis Nürnberger Land). Eine paläontologische und urgeschichtliche Fundstelle aus dem Spät-Riß. *Quartär-Bibliothek* 4: 103-263.
HELLER F. 1983e. — Die Fauna von Hunas (Nördliche Frankenalb) im Rahmen der deutschen Quartärfaunen. *Eiszeitalter und Gegenwart* 17: 113-117.

HENNIG G. J., GRÜN R. & BRUNNACKER K. 1983. — Speleothems, travertines, and paleoclimates. *Quaternary Research* 20 (1): 1-29. https://doi.org/10.1016/0033-5894(83)90063-7

HEPTNER V. G. & NAUMOV N. P. 1967. — *Mlekopitayushchije Sovetskogo Soyuza. Part lb. Žinszczinyje (Kunicy; dopolnitelnych widow)*. Vol. II. Vysshaya Shkola, Moscow: 844.

HILPERT B. 2005. — Studies of the morphology of the bears from the Steinberg-Höhlenruine near Hunas. *Naturhistorische Gesellschaft Nürnberg* 45: 117-124.

HILPERT B. 2006. — *Die Ursiden aus Hunas - Revision und Neubearbeitung der Bärenfunde aus der Steinberg-Höhlenruine bei Hunas (Gde. Pommelsbrunn, Mittelfranken, Bayern)*. PhD dissertation, University of Erlangen-Nürnberg, 91 p.

HUGUENEY M. 1975. — Les mustelids (Mammalia, Carnivora) du gisement Pleistocene moyen de la Fage (Correze). *Nouvelle Archiv du Museum de Historie de Naturelle de Lyon* 13: 29-46.

JÁNOSSY D. 1955. — Die Vögel- und Säugetierreste der spätpleistozänen Schichten der Höhle von Istallöskö. *Acta Archaeologica Academiae Scientiarum Hungaricae* 5: 149-181.

JÁNOSSY D. 1969a. — Stratigraphische Auswertung der europäischen mittelpleistozänen Wirbeltierfauna. Teil I. *Berichte der deutschen Gesellschaft für geologische Wissenschaft, Abteilung A, Geologie und Paläontologie* 4: 367-438.

JÁNOSSY D. 1969b. — Stratigraphische Auswertung der europäischen mittelpleistozänen Wirbeltierfauna. Teil II. *Berichte der deutschen Gesellschaft für geologische Wissenschaft, Abteilung A, Geologie und Paläontologie* 5: 573-643.

JÁNOSSY D. 1978. — Larger mammals from the lowermost Pleistocene fauna, Ostramos, loc. 7 (Hungary). *Annales Historico-Naturales Musei Nationalis Hungarici, pars Mineralogica et Palaeontologica* 70: 69-79.

JÁNOSSY D. 1983. — Die Jungmittelpleistozäne Vogelfauna von Hunas (Hartmannshof), *in* HELLER F. (ed.), Die Höhlenruine Hunas bei Hartmannshof (Landkreis Nürnberger Land). *Quartär-Bibliothek* 4: 265-288.

JÁNOSSY D. 1986. — Pleistocene vertebrate faunas of Hungary. *Development in Palaeontology and Stratigraphy* 8: 1-201.

KAHLKE H.-D. 1961. — Revision der Säugetierfaunen der klassischen deutschen Pleistozän-Fundstellen von Süßenborn, Mosbach und Taubach. *Geologie* 10: 493-529.

KARWATH I. 1998. — *Mittelpleistozäne Mikromammalier aus der Höhlenruine von Hunas bei Hartmannshof/Gemeinde Pommelsbrunn im Landkreis Nürnberger Land und deren Bedeutung in Stratigraphie und Ökologie (Quadrant P3, Serie 1-22)*. Unpublised thesis, Uniserty Erlangen-Nürnberg, 190 p.

KELLER T. 2004. — Sedimentology and taphonomy of the Middle Pleistocene Mosbach Sands (Germany), *in* MAUL L. C. & KAHLKE R.-D. (eds), *18th International Senckenberg Conference, VI International Palaeontological Colloquium in Weimar. Late Neogene and Quaternary biodiversity and evolution: regional developments and interregional correlations*. A conference in honour of the 80th birthday of Professor Hans-Dietrich Kahlke, Weimar (Germany), 25th-30th April, 2004: 131-132.

KING C. M. 1989. — The advantages and disadvantages of small size to weasels, *Mustela* species, *in* GITTLEMAN J. (ed.), *Carnivore Behaviour, Ecology, and Evolution*. Cornell University Press, London: 302-334.

KING C. M. & MOORS P. J. 1979. — On co-existence, foraging strategy and the biogeography of the weasels and stoats (*Mustela nivalis* and *M. erminea*) in Britain. *Oecologia* 39: 129-150. https://doi.org/10.1007/BF00348064

KING C. M. & POWELL R. A. 2007. — *The natural history of weasels and stoats. Ecology, behavior, and management.* Oxford University Press, New York: 464 p.

KOENIGSWALD W. V. & HEINRICH W.-D. 1999. — Mittelpleistozäne Säugetierfaunen aus Mitteleuropa - der Versuch einer biostratigraphischen Zuordnung. *Kaupia* 9: 53-112.

KOLFSCHOTEN T. V. 2001. — A fossil wolverine *Gulo schlosseri* (Carnivora, Mustelidae) from Nieuwegein, the Netherlands. *Lynx* 32 (1): 183-191.

KORMOS T. 1911. — Die Pleistozäne Säugetierfauna der Felsnische Puskaporos bei Hamor, *in* CAPEK W., BOLKAY S. V., KADIC O. & KORMOS T. (eds), Die Felsnische Puskaporos bei Hámor im Komitat Borsod und ihre Fauna. *Mitteilungen aus dem Jahrbuche der Königlichen Ungarischen Geologischen Reichsanstalt* 19: 125-147.

KORMOS T. 1914. — Drei neue Raubtiere aus den Präglazial-Schichten des Somlyóhegy bei Püspökfürdő. *Mitteilungen aus der Jahrbuche der Königlichen Ungarischen Geologischen Reichsanstalt* 22: 223-247.

KORMOS T. 1934. — Neue und wenig bekannte Musteliden aus dem ungarischen Oberpliozän. *Folia Zoologica et Hydrobiologica* 5 (2): 129-158.

KOT M., BERTO C., KRAJCARZ M. T., MOSKAL-DEL HOYO M., GRYCZEWSKA N., SZYMANEK M., MARCISZAK A., STEFANIAK K., ZARZECKA-SZUBIŃSKA K., LIPECKI G., WERTZ K. & MADEYSKA T. 2022. — Frontiers of the Lower Palaeolithic expansion in Europe: Tunel Wielki Cave (Poland). *Scientific Reports* 12: 16355. https://doi.org/10.1038/s41598-022-20582-0

KOWALSKI K. 2001. — Pleistocene rodents of Europe. *Folia Quaternaria* 72: 3-389.

KRAJCARZ M. T. 2012. — Small fossil wolverine *Gulo* from Middle Pleistocene of Poland. *Acta Zoologica Cracoviensia* 55 (1): 79-87. https://doi.org/10.3409/azc.55_1.79

KRATOCHVÍL J. 1951. — Kolčavy a kolčavky v Československu. *Sborník Vysoké školy zemědělské v Brně* 1: 61-148.

KRATOCHVÍL J. 1977a. — Sexual dimorphism and status of *Mustela nivalis* in Central Europe (Mamm., Mustelidae). *Acta Scientarum Naturalium Bohemoslovacae Brno* 11: 1-42.

KRATOCHVÍL J. 1977b. — Studies on *Mustela erminea* (Mustelidae, Mamm.) L. variability of metric and mass traits. *Folia Zoologica* 26: 291-304.

KRETZOI M. 1938. — Die Raubtiere von Gombaszög nebst einer Übersicht der Gesamtfauna (Ein Beitrag zur Stratigraphie des Altquartärs). *Annales Musei Nationalis Hungarici, pars mineralogica, geologica, paleontologica* 31: 88-157.

KRETZOI M. 1941a. — Weitere Beiträge zur Kenntnis der Fauna von Gombaszög. *Annales Musei Nationalis Hungarici pars mineralogica, geologica, paleontological* 34: 105-139.

KRETZOI M. 1941b. — Die unterpleistozäne Säugetierfauna von Betfia bei Nagyvarad. *Földtani Közlöny* 71: 308-355.

KURTÉN B. 1968. — *Pleistocene mammals of Europe*. Weidenfeld and Nicolson, London.

LARSEN E., GULLIKSEN S. E., LAURITZEN R., LIE R., LÖVLIE R. & MANGERUD J. 1987. — Cave stratigraphy in western Norway; multiple Weichselian glaciations and interstadial vertebrate fauna. *Boreas* 16 (3): 267-292. https://doi.org/10.1111/j.1502-3885.1987.tb00096.x

MADURELL-MALAPEIRA J., ALBA D. M., MARMI J., AURELL J. & MOYÀ-SOLÀ S. 2011a. — The taxonomic status of European Plio-Pleistocene badgers. *Journal of Vertebrate Paleontology* 31 (5): 885-894. https://doi.org/10.1080/02724634.2011.589484

MADURELL-MALAPEIRA J., MARTÍNEZ-NAVARRO B., ROS-MONTOYA S., ESPIGARES M. P., TORO I. & PALMQVIST P. 2011b. — The earliest European badger (*Meles meles*), from the Late Villafranchian site of Fuente Nueva 3 (Orce, Granada, SE Iberian Peninsula). *Comptes Rendus Palevol* 10 (8): 609-615. https://doi.org/10.1016/j.crpv.2011.06.001

MARCISZAK A. 2012. — *Mustelids (Mustelidae, Carnivora, Mammalia) from the Pleistocene of Poland.* Unpublished PhD thesis, Department of Paleozoology, University of Wrocław, 1076 p.

MARCISZAK A. & SOCHA P. 2014. — Stoat *Mustela erminea* Linnaeus, 1758 and weasel *Mustela nivalis* Linnaeus, 1766 in palaeoecological analysis: A case study of Biśnik Cave. *Quaternary International* 339-340: 258-265. https://doi.org/10.1016/j.quaint.2013.12.058

Marciszak A., Gornig W. & Stefaniak K. 2017a. — Large mammals (carnivores, artiodactyls) from Solna Jama Cave (Bystrzyckie Mts, Southwestern Poland) in the context of faunal changes in the postglacial period of Central Europe. *Palaeontologia Electronica* 20 (3A): 1-37. https://doi.org/10.26879/581

Marciszak A., Lipecki G., Wojtal P. & Zarzecka-Szubińska K. 2017b. — Mustelids (Carnivora, Mammalia) from the Ciemna Cave (southern Poland) as an example of Late Pleistocene small carnivore assemblage. *Acta Zoologica Cracoviensia serie A, Vertebrata* 60 (2): 15-34. https://doi.org/10.3409/azc.60_2.15

Marciszak A., Schouwenburg Ch., Gornig W., Lipecki G. & Mackiewicz P. 2019. — Morphometric comparison of *Panthera spelaea* (Goldfuss, 1810) from Poland with the lion remains from Eurasia over the last 700 ka. *Quaternary Science Reviews* 223: 105950. https://doi.org/10.1016/j.quascirev.2019.105950

Marciszak A., Ambros D. & Hilpert B. 2021. — Mustelids from Sackdilling Cave (Bavaria, Germany) and their biostratigraphic significance. *Geobios* 68: 83-107. https://doi.org/10.1016/j.geobios.2021.04.004

Marciszak A., Gornig W. & Szynkiewicz A. 2023. — Carnivores from Draby 3 (central Poland): the latest record of *Lycaon lycaonoides* (Kretzoi, 1938) and the final accord in the long history of ancient faunas. *Quaternary International* 674-675: 62-86. https://doi.org/10.1016/j.quaint.2023.03.012.

Mecozzi B. 2022. — *Meles meles* from Middle Pleistocene to Early Holocene of the Italian Peninsula within the evolution of European badgers in the Quaternary of Eurasia. *Palaeontographica Abteilung A* 319 (1-6): 133-159. https://doi.org/10.1127/pala/2021/0100

Mecozzi B., Coppola D., Iurino D. A., Sardella R. & De Marinis M. 2019. — The Late Pleistocene European badger *Meles meles* from Grotta Laceduzza (Brindisi, Apulia, Southern Italy): the analysis of the morphological and biometric variability. *The Science of Nature* 106 (5-6): 13. https://doi.org/10.1007/s00114-019-1604-2

Mecozzi B., Iannucci A., Bona F., Mazzini I., Pieruccini P. & Sardella R. 2022. — Rediscovering *Lutra lutra* from Grotta Romanelli (southern Italy) in the framework of the puzzling evolutionary history of Eurasian otter. *Paläontologische Zeitschrift* 96 (3): 161-174. https://doi.org/10.1007/s12542-021-00553-y

Mourer-Chauviré C., Philippe M., Quinif Y., Chaline J., Debard E., Guérin C. & Hugueney M. 2003. — (September): position of the palaeontological site Aven I des Abîmes de La Fage, at Noailles (Corrèze, France), in the European Pleistocene chronology. *Boreas* 32 (3): 521-531. https://doi.org/10.1111/j.1502-3885.2003.tb01232.x

Nadachowski A., Żarski M., Urbanowski M., Wojtal P., Miękinia B., Lipecki G., Ochman K., Krawczyk M., Jakubowski G. & Tomek T. 2009. — *Late Pleistocene Environment of the Częstochowa Upland (Poland) reconstructed on the basis of faunistic evidence from archaeological cave sites*. Institute of Systematics and Evolution of Animals, Polish Academy of Sciences, Cracov, 112 p.

Parfitt S. A. 1999. — Mammalia, *in* Roberts M. B. & Parfitt S. A. (eds), *Boxgrove. A Middle Pleistocene hominid site at Eartham Quarry, Boxgrove*. University College London, London, West Sussex: 197-290.

Pasa A. 1947. — I mammiferi di alcune antiche brecce veronesi. *Memorie del Museo Civico di Storia Naturale di Verona* 1: 1-111.

Petronio C., Angelone C., Atzori P., Famiani F., Kotsakis T. & Salari L. 2020. — Review and new data of the fossil remains from Monte Peglia (late Early Pleistocene, central Italy). *Rivista Italiana di Paleontologia e Stratigrafia* 126 (3): 791-819. https://doi.org/10.13130/2039-4942/14413

Petrucci M., Cipullo A., Martínez-Navarro B., Rook L. & Sardella R. 2013. — The Late Villafranchian (Early Pleistocene) carnivores (Carnivora, Mammalia) from Pirro Nord (Italy). *Palaeontographica Abteilung A* 298 (1-6): 113-145. https://doi.org/10.1127/pala/298/2013/113

Rabeder G. 1976. — Die Carnivoren (Mammalia) aus dem Altpleistozän von Deutsch-Altenburg 2. Mit Beiträgen zur Systematik einiger Musteliden und Caniden. *Beiträge zur Paläontologie von Österreich* 1: 5-119.

Rabeder G. 1999. — Die Evolution des Höhlenbärengebisses. *Mitteilungen der Kommission für Quartärforschung der Österreichischen Akademie der Wissenschaften* 11: 1-102.

Reichstein H. V. 1986. — Beitrag zur Kenntnis des Sexualdimorphismus von *Mustela nivalis* Linné, 1766 und *M. erminea* Linné, 1758 nach Untersuchungen an postcranialen Skeletten aus Schleswig-Holstein. *Annalen des Naturhistorischen Museums in Wien* 88-89B: 293-304.

Rempe U. 1970. — Morphometrische Untersuchungen an Iltisschädeln zur Klärung der Verwandtschaft von Steppeniltis, Waldiltis und Frettchen. Analyse eines "Grenzfalles" zwischen Unterart un Art. *Zeitschrift für Wissenschaftliche Zoologie* 180: 185-367.

Rosendahl W., Ambros D., Hilpert B., Hambach U., Alt K.W., Knipping M., Reisch L. & Kaulich B. 2011. — Neanderthals and monkeys in the Würmian of Central Europe - The Middle Palaeolithic site of Hunas, Southern Germany, *in* Conard N. J. & Richter J. (eds), Neanderthal lifeways, subsistence and technology - one hundred fifty years of Neanderthal study. *Vertebrate Paleobiology and Paleoanthropology* 19 (4): 15-23. https://doi.org/10.1007/978-94-007-0415-2-3

Rosenmüller J. C. 1794. — *Quedam de ossibus fossilibus animalis cuiusdam, historiam eius et cognitionem accuratiorem illustrantia*. Dissertation in October 1794, Leipzig, 34 p.

Schütt G. & Hemmer H. 1978. — Zur Evolution des Löwen (*Panthera leo* L.) im europäischen Pleistozän. *Neues Jahrbuch für Geologie und Paläontologie Monatshefte* 1978 (4): 228-255.

Soergel W. 1912. — Das aussterben diluvialer säugetiere und die jagd des diluvialen menschen. *Z. Ver-erbungslehre* 10: 174-176. https://doi.org/10.1007/BF01943430

Soergel W. 1914. — Die diluvialen Säugetiere Badens. Ein Beitrag zur Paläontologie und Geologie des Diluviums. Teil I: Älteres und mittleres Diluvium. *Mitteilungen der Badischen Geologischen Landesanstalt* 9: 1-254.

Soergel W. 1917. — Der Steppeniltis, *Foetorius Eversmanni* Less. aus dem oberen Travertin des Travertingebietes von Weimar. *Zeitschrift der Deutschen Geologischen Gesellschaft* 69: 139-181.

Sommer R. & Benecke N. 2004. — Late- and postglacial history of the Mustelidae in Europe. *Mammal Review* 34 (4): 249-284. https://doi.org/10.1111/j.1365-2907.2004.00043.x

Sotnikova M. & Titov V. 2009. — Carnivora of the Tamanian faunal unit (the Azov Sea area). *Quaternary International* 201 (1-2): 43-52. https://doi.org/10.1016/j.quaint.2008.05.019

Stadie C. 1983. — Die Amphibien von Hunas, *in* Heller F. (ed.), Die Höhlenruine Hunas bei Hartmannshof (Landkreis Nürnberger Land). Eine paläontologische und urgeschichtliche Fundstelle aus dem Spät-Riß. *Quartär-Bibliothek* 4: 289-307.

Stehlík A. 1934. — Fossilní ssavci ze Stránské skály u Brna. *Práce moravské přírodovědecké společnosti* 6: 1-94.

Stuart A. J. 1974. — Pleistocene history of the British vertebrate fauna. *Biological Reviews* 49 (2): 225-266. https://doi.org/10.1111/j.1469-185X.1974.tb01574.x

Stuart A. J. 1981. — A comparison of the Middle Pleistocene mammal faunas of Voigtstedt (Thuringia, GDR) and West Runton (Norfolk, England). *Quartärpaläontologie* 4: 155-163.

Stuart A. J. 1996. — Vertebrate faunas from the early Middle Pleistocene of East England, *in* Turner A. (ed.), *The early Middle Pleistocene in Europe*. Balkema, Rotterdam: 9-24.

Stuart A. J. & Lister A. M. 2010. — The West Runton Freshwater Bed and the West Runton mammoth: summary and conclusions. *Quaternary International* 228 (1-2): 241-248. https://doi.org/10.1016/j.quaint.2010.07.033

SUTCLIFFE A. J. 1964. — The mammalian fauna, *in* OVEY C. D. (ed.), The Swanscomhe skull: a survey of research on a Pleistocene site. *Occasional Paper of the Royal Anthropological Institute* 20: 85-111.
THENIUS E. 1948. — Fischotter und Bisamspitzmaus aus dem Altquartär von Hundsheim in Niederösterreich. *Sitzungsberichte der Akademie der Wissenschaften mathematisch-naturwissenschaftliche Klasse* 157: 187-196.
THENIUS E. 1965. — Die Carnivoren-Reste aus dem Altpleistozän von Voigtstedt bei Sangerhausen in Thüringen. *Paläontologische Abhandlungen A: Paläozoologie* 2: 539-564.
TOBIEN H. 1957. — *Cuon* Hodg. and *Gulo* Frisch from the early Pleistocene sands of Mosbach near Wiesbaden. *Acta Zoologica Cracoviensia* 18 (2): 433-451.
TURNER E. 1990. — Middle and Late Pleistocene macrofaunas of the Neuwied Basin region (Rhineland-Palatinate) of West Germany. *Jahrbuch des Römisch-Germanisches Zentralmuseum Mainz* 67: 136-403.
TURNER A. 2009. — The evolution of the guild of large Carnivora of the British Isles during the Middle and Late Pleistocene. *Journal of Quaternary Science* 24 (8): 991-1005. https://doi.org/10.1002/jqs.1278
VON REICHENAU W. 1904. — Über eine neue fossile Bären-Art *Ursus deningeri* aus den fluviatilen Sanden von Mosbach. *Jahrbücherdes Nassauischen Vereins für Naturkunde* 57: 1-11.
VON REICHENAU W. V. 1910. — Revision der Mosbacher Säugetierfauna. *Notizblatt des Vereins für Erdkunde und der hessischen geologischen Landesanstalt zu Darmstadt* 31: 118-134.
WENZ W. 1921. — *Das Mainzer Becken und seine Randgebiete. Eine Einführung in die Geologie des Gebietes zwischen Hunsrück, Taunus, Vogelsberg, Spessart und Odenwald*. Verlag W. Ehrig, Heidelberg, 351 p.
WILLEMSEN G. F. 1992. — A revision of the Pliocene and Quaternary Lutrinae from Europe. *Scripta Geologica* 101: 1-115.
WILLEMSEN G. F. 2006. — *Megalenhydris* and its relationships to *Lutra* reconsidered. *Hellenic Journal of Geoscience* 41: 83-87.
WISZNIOWSKA T. 1989. — Middle Pleistocene Carnivora (Mammalia) from Kozi Grzbiet in the Świętokrzyskie Mts, Poland. *Acta Zoologica Cracoviensia* 32 (14): 589-630.
WOLSAN M. 1993. — Evolution des carnivores quaternaires en Europe centrale dans leur contexte stratigraphique et paleoclimatique. *L'Anthropologie* 97: 203-222.
WOLSAN M. 2001. — Remains of *Meles hollitzeri* (Carnivora, Mustelidae) from the Lower Pleistocene site of Untermassfeld. *Monographien des Römisch-Germanisches Zentralmuseum Mainz* 40: 659-671.
ZEUNER F. E. 1937. — A comparison of the Pleistocene of East Anglia with that of Germany. *Proceedings of the Prehistoric Society* 3 (1-2): 136-157. https://doi.org/10.1017/S0079497X00021344

Submitted on 13 April 2024;
accepted on 25 June 2024;
published on 4 September 2024.

APPENDICES

APPENDIX 1. — Description of sediments in profile 13 of Hunas, the area, where more than 95% mustelid remains were found.

Layer	Description
roof	reddish-brown loams with dolomite debris in different size, most of the stones are parts of the former roof of the cave
E	dark-grey dolomite sands with dolomite debris of 2-4 cm diameter, in many parts of the layer big amounts of particles from charcoal
F	yellow-grey dolomite sands with dolomite debris of about 4 cm diameter and particles from charcoal
G1	dolomite debris about 3-20 cm, in the lower part bigger blocks, little amount of light-grey dolomite sands
G2	light to dark reddish-brown, partly loamy and humous dolomite sands with dolomite debris about 2-10 cm diameter, big amounts of particles from charcoal
G3	light to darker brownish-grey dolomite sands with particles from charcoal and dolomite debris
H	brownish-grey to dark grey humous and dolomite sands with dolomite debris of 2-5 cm diameter, in the upper part particles of charcoal, partly big amounts
I	light yellow to light brown-beige loamy dolomite sands, little dolomite debris and only few particles of charcoal
K upper	reddish-yellow to reddish-brown dolomite sands with dolomite debris
K lower	dark grey dolomite sands with dolomite debris, partly big blocks, and often bigger amounts of particles of charcoal
L	light brownish-grey dolomite sands with dolomite debris of 2-5 cm diameter, and partly big blocks, also partly with particles of charcoal
M	big blocks and partly yellow-grey dolomite sands with dolomite debris

APPENDIX 2. — List of taxa from Hunas, compiled from Heller (1963a, b, 1965, 1966, 1983d, e); Schütt & Hemmer (1978); Carls (1986); Groiss (1986); Fetscher (1996); Ehrlinger (1997); Karwath (1998); Ambros (2003, 2006); Hilpert (2005, 2006); Alt *et al.* (2006); Baumann (2011); Böhme (2011); Marciszak *et al.* (2019).

Gastropoda Cuvier, 1795
Discus rotundatus (Müller, 1774)
Discus ruderatus (Hartmann, 1821)
Fruticicola fruticum (Müller, 1774)
Trochulus sericeus (Draparnaud, 1801)
Perforatella incarnata (Müller, 1774)
Helicigona lapicida (Linnaeus, 1758)
Arianta arbustorum (Linnaeus, 1758)
Cepaea hortensis (Müller, 1774)
Cepaea sp.
Clausilia rugosa (Draparnaud, 1801)
Clausilia aff. *bidentata* (Ström, 1765)
Clausilia dubia Draparnaud, 1805
Macrogastra plicatula (Draparnaud, 1801)
Bivalvia Linnaeus, 1758
Pisidium sp.
Teleostei Müller, 1846
Salmo cf. *trutta* Linnaeus, 1758
Thymallus cf. *thymallus* (Linnaeus, 1758)
Phoxinus phoxinus (Linnaeus, 1758)
Lota lota (Linnaeus, 1758)
Cottus cf. *gobio* Linnaeus, 1758
Amphibia Linnaeus, 1758
Rana temporaria Linnaeus, 1758
Rana arvalis Nilsson, 1842
Bufo bufo (Linnaeus, 1758)
Triturus cf. *vulgaris* (Linnaeus, 1758)
Reptilia Laurenti, 1768
Anguis fragilis Linnaeus, 1758
Lacerta agilis Linnaeus, 1758
Lacerta vivipara Jacquin, 1787
Coronella austriaca Laurenti, 1768
Elaphe longissima (Laurenti, 1768)
Vipera berus (Linnaeus, 1758)
Aves Linnaeus, 1758
Anas platyrhynchos Linnaeus, 1758

Appendix 2. — Continuation.

Anas acuta Linnaeus, 1758
Anas penelope Linnaeus, 1758
Anas querquedula Linnaeus, 1758
Aythya nyroca (Güldenstädt, 1770)
Bucephala clangula (Linnaeus, 1758)
Mergus cf. *serrator* Linnaeus, 1758
Lyrurus tetrix (Linnaeus, 1758)
Lagopus lagopus (Linnaeus, 1758)
Lagopus muta (Montin, 1776)
Perdix perdix (Linnaeus, 1758)
Otis tarda Linnaeus, 1758
Crex crex (Linnaeus, 1758)
Porzana porzana (Linnaeus, 1766)
Charadrius aff. *morinellus* Linnaeus, 1758
Gallinago cf. *media* (Latham, 1787)
Asio flammeus (Pontoppidan, 1763)
Aegolius funereus (Linnaeus, 1758)
Surnia ulula (Linnaeus, 1758)
Bubo scandiacus (Linnaeus, 1758)
Dendrocopus major (Linnaeus, 1758)
Eremophila alpestris (Linnaeus, 1758)
Hirundo rustica Linnaeus, 1758
Corvus corax Linnaeus, 1758
Corvus cf. *frugilegus* Linnaeus, 1758
Pyrrhocorax graculus (Linnaeus, 1766)
Garrulus glandarius (Linnaeus, 1758)
Coloeus monedula (Linnaeus, 1758)
Perisoreus sp.
Parus cf. *palustris* Linnaeus, 1758
Cinclus cinclus (Linnaeus, 1758)
Turdus cf. *torquatus* Linnaeus, 1758
Phoenicurus cf. *phoenicurus* (Linnaeus, 1758)
Ficedula cf. *albicollis* (Temminck, 1815)
Anthus spinoletta (Linnaeus, 1758)
Mammalia Linnaeus, 1758
Eulipotyphla Waddell, Okada & Hasegawa, 1999
Erinaceus sp.
Neomys anomalus Cabrera, 1907
Neomys fodiens (Pennant, 1771)
Sorex araneus Linnaeus, 1758
Sorex cf. *subaraneus* Heller, 1958
Sorex runtonensis Hinton, 1911
Sorex aff. *kennardi* Hinton, 1911
Sorex minutus Linnaeus, 1766
Sorex aff. *minutissimus* Zimmermann, 1780
Talpa europaea Linnaeus, 1758
Chiroptera Blumenbach, 1779
Barbastella barbastellus (Schreber, 1774)
Pipistrellus aff. *pipistrellus* (Schreber, 1774)
Eptesicus nilssonii Keyserling & Blasius, 1839
Eptesicus serotinus (Schreber, 1774)
Plecotus auritus (Linnaeus, 1758)
Myotis sp.
Lagomorpha Brandt, 1855
Lepus sp.
Ochotona pusilla (Pallas, 1769)
Rodentia Bowdich, 1821
Sciurus sp.
Marmota marmota primigenia (Kaup, 1839)
Spermophilus sp.
Castor fiber Linnaeus, 1758
Muscardinus avellanarius (Linnaeus, 1758)
Sicista praeloriger Kormos, 1930
Sicista betulina (Pallas, 1779)
Sicista subtilis (Pallas, 1773)
Parapodemus coronensis Schaub, 1938

Appendix 2. — Continuation.

Apodemus sylvaticus (Linnaeus, 1758)
Apodemus sp.
Apodemus cf. *flavicollis* (Melchior, 1834)
Apodemus maastrichtiensis van Kolfschoten, 1985
Cricetus cricetus (Linnaeus, 1758)
Cricetus major Woldřich, 1880
Cricetus sp.
Phodopus cf. *sungorus* (Pallas, 1773)
Allocricetus bursae Schaub, 1930
Dicrostonyx intermedius Heller, 1983
Dicrostonyx gulielmi (Sanford, 1870)
Lemmus lemmus (Linnaeus, 1758)
Myodes glareolus (Schreber, 1780)
Clethrionomys cf. *acrorhiza* (Kormos, 1933)
Clethrionomys esperi (Heller, 1930)
Arvicola mosbachensis (Schmidtgen, 1911)
– *Arvicola amphibius* (Linnaeus, 1758)
Arvicola sp.
Microtus gregalis (Pallas, 1779)
Pitymys gregaloides Hinton, 1910
Pitymys subterraneus (Sélys-Longchamps, 1836)
Microtus anglicus Hinton, 1910
Microtus arvalis (Pallas, 1778)
– *Microtus agrestis* (Linnaeus, 1761)
Chionomys nivalis (Martins, 1842)
Microtus delusorius Heller, 1983
Microtus oeconomus (Pallas, 1776)
Microtus problematicus Heller, 1858
Primates Linnaeus, 1758
Macaca sylvanus pliocena (Owen, 1846)
Homo sapiens neanderthalensis (King, 1864)
Carnivora Bowdich, 1821
Canis lupus Linnaeus, 1758
Vulpes sp.
Vulpes cf. *lagopus* (Linnaeus, 1758)
Ursus spelaeus Rosenmüller, 1794
Ursus arctos ssp.
Gulo gulo (Linnaeus, 1758)
Meles cf. *meles* (Linnaeus, 1758)
Lutra lutra groissii Heller, 1983
Martes martes (Linnaeus, 1758)
Mustela putorius Linnaeus, 1758
Mustela erminea Linnaeus, 1758
Mustela nivalis Linnaeus, 1766
Panthera spelaea ssp.
Crocuta crocuta spelaea (Goldfuss, 1823)
Perissodactyla Owen, 1848
Stephanorhinus kirchbergensis (Jäger, 1839)
Stephanorhinus hemitoechus (Falconer, 1859)
Equus ferus aff. *mosbachensis* (von Reichenau, 1903)
Artiodactyla (Owen, 1848)
Sus scrofa Linnaeus, 1758
Megaloceros giganteus giganteus (Blumenbach, 1803)
Alces sp.
Cervalces latifrons Johnson, 1874
Cervus elaphus Linnaeus, 1758
Rangifer sp.
Capreolus capreolus suessenbornensis (Kahlke, 1956)
Bison priscus (Bojanus, 1825)
Bos primigenius Bojanus, 1825

Appendix 3. — The catalogue of mustelid remains from Hunas.

Material	Coll. no.	Sex	Layer	Previous determination
***Gulo gulo* (Linnaeus, 1758)**				
right metacarpal 4 without distal epiphysis	HHu 3937	–	G	–
right pisiform	HHu 3938	–	G	–
***Meles meles* (Linnaeus, 1758)**				
body fragment of right mandible with p4-m1	HHu 4604	♂	G2	*Meles meles*
distal half of the left metatarsal 3	H XI 23.8.63	♂	G2	*Meles meles*
***Lutra lutra groissii* Heller, 1983**				
fragment of left maxilla with P4-M1	HHu 4020	♂	G	*Lutra lutra*
phalanx 1	HHu 4021	–	G	*Lutra lutra*
***Martes martes* (Linnaeus, 1758)**				
right, worn m1	HHu 4099	♂	G2	*Martes* sp.
proximal epiphysis of right ulna	HHu 4098	♂	G2	*Martes* sp.
distal half of left metapodium	HHu 4525	–	G1	*Martes* sp.
***Mustela putorius* Linnaeus, 1758**				
left C1	HHu 4546	♂	G3	*Putorius* cf. *stromeri*
right C1	HHu 4522	♀	G2/G3	*Putorius* sp.
fragment of left maxilla with P2-M1	HHu 4603	♂	G2	*Martes martes*
left mandible body with p2-m1	HHu 4605	♀	G2	*Mustela putorius*
right mandible body with damaged symphysis, c1 and p4-m1	HHu 4606	♀	G2	*Mustela putorius*
body fragment of right mandible	HHu 4299	♀	G3	*Putorius* cf. *stromeri*
baculum	HHu 4410	♂	G3	*Putorius* cf. *stromeri*
left metacarpal 4	HHu 4534	–	G2	*Putorius* cf. *stromeri*
left metacarpal 4	HHu 4537	–	G2	*Putorius* cf. *stromeri*
left metacarpal 5	HHu 4539	–	G2	*Putorius* cf. *stromeri*
***Mustela erminea* Linnaeus, 1758**				
right humerus	HHu 4207	–	G1	*Mustela* aff. *palerminea*
right ulna	HHu 4297	–	G1	*Mustela erminea*
right metacarpal 4	HHu 4523	–	G1	*Mustela* cf. *palerminea*
baculum	HHu 4439	♂	G3	*Mustela* sp.
left femur	HHu 4205	–	G1	*Mustela* aff. *palerminea*
proximal half of left tibia	HHu 4206	–	G1	*Mustela* aff. *palerminea*
right metatarsal 4	HHu 4538	–	G2	*Mustela* cf. *palerminea*
right metatarsal 5	HHu 4542	–	G2	*Mustela* cf. *palerminea*
***Mustela nivalis* Linnaeus, 1766**				
left palate with P4	HHu 4599	♀	K	*Mustela* cf. *praenivalis*
left C1	HHu 4082a	♂	G2	*Mustela*
left C1	HHu 4089d	♂	G2	–
left C1	HHu 4089e	♂	G2	–
left C1	HHu 4403	♂	G2	*Mustela* sp.
left C1	HHu 4404	♂	G2	*Mustela* sp.
right C1	HHu 4094a	♂	G2	–
right C1	HHu 4437	♀	G3	*Mustela* sp.
left P4	HHu 4059a	♀	G2	*Mustela*
left mandible with damaged ramus and with c1-m1	HHu 4033	♂	G2	*Mustela* sp.
body of left mandible without symphysis and with p3 and m1	HHu 4034	♂	G2	*Mustela* sp.
body of left mandible without symphysis, with damaged ramus and with p2-m2	HHu 4035	♀	G2	*Mustela* sp.
left mandible with c1-m2	HHu 4038	♂	G2	*Mustela* sp.
body of left mandible without symphysis and with p4-m1	HHu 4039	♂	G2	*Mustela* sp.
body of left mandible without symphysis and with p2-m2	HHu 4042	♂	G2	*Mustela* sp.
left mandible with damaged symphysis, with p2-p3 and m1-m2	HHu 4043	♂	G2	*Mustela* sp.
posterior half of left mandible with damaged ramus and with m1-m2	HHu 4044	♂	G2	*Mustela* sp.
posterior half of left mandible with damaged ramus and with m1-m2	HHu 4045	♂	G2	*Mustela* sp.
body of left mandible without symphysis and with m1	HHu 4050	♂	G2	*Mustela*
body of left mandible with damaged ramus and symphysis and with p2-p3 and m1-m2	HHu 4051	♂	G2	*Mustela*
body of left mandible without symphysis and with p3 and m1	HHu 4053	♂	G2	*Mustela*
left mandible with p3-m2	HHu 4057	♀	G2	*Mustela*
posterior half of left mandible with m2	HHu 4063	♂	G2	*Mustela*
body of left mandible without symphysis and with m1	HHu 4064	♂	G2	*Mustela*
posterior half of left mandible with worn m1	HHu 4065	♀	G2	*Mustela*
body of left mandible without symphysis ramus and with p4-m2	HHu 4066	♂	G2	*Mustela*
left mandible with m1	HHu 4067	♂	G2	*Mustela*

Appendix 3. — Continuation.

left mandible without symphysis and with m1	HHu 4070	♂	G2	*Mustela*
body of left mandible without symphysis, with damaged ramus, c1 and m1	HHu 4071	♂♂	G2	*Mustela*
body of left mandible fragment with p4-m1	HHu 4072	♂♂	G2	*Mustela*
left mandible with damaged symphysis, ramus and with m1	HHu 4073	♂♂	G2	*Mustela*
left mandible with damaged symphysis and with p2 and p4-m1	HHu 4074	♀	G2	*Mustela*
body of left mandible and ramus fragment with p4-m2	HHu 4075	♂♂	G2	*Mustela*
body of left mandible fragment with p3-m1	HHu 4077	♂♂	G2	*Mustela*
body of left mandible with symphysis and ramus fragment and with p2-p3 and m1-m2	HHu 4080	♂	G2	*Mustela*
body of left mandible without symphysis and ramus and with p4-m1	HHu 4081	♂♂	G2	*Mustela*
body of left mandible with damaged symphysis and ramus and with p4-m2	HHu 4082	♂♂	G2	*Mustela*
body fragment of left mandible with m1	HHu 4083	♂♂	G2	*Mustela*
body of left mandible without symphysis, with damaged ramus and with p2-m2	HHu 4088	♂♂	G2	*Mustela*
anterior half of left mandible with p2-p4	HHu 4093	♂♂	G2	*Mustela*
body of left mandible without symphysis, with damaged ramus and m2	HHu 4094	♂♂	G2	*Mustela*
body and ramus fragment of left mandible with m1-m2	HHu 4095	♂♂	G2	*Mustela* aff. *palerminea*
body of left mandible without symphysis, with damaged ramus and m1	HHu 4096	♂♂	G2	*Mustela*
body of left mandible without symphysis and with p3-m1	HHu 4102	♂♀	G2	*Mustela* aff. *praenivalis*
left mandible	HHu 4104	♂♀	G2	*Mustela* aff. *praenivalis*
left mandible with damaged ramus and with p3-m1	HHu 4105	♂♀	G2	*Mustela* aff. *praenivalis*
left mandible with p4-m1	HHu 4106	♂♂	G2	*Mustela nivalis* group
posterior half of left mandible	HHu 4107	♂♀	G2	*Mustela praenivalis*
body of left mandible without symphysis and with m1	HHu 4113	♂♀	G2	*Mustela* aff. *praenivalis*
body of left mandible without symphysis and with p3 and m1	HHu 4115	♀♀	G2	*Mustela nivalis* group
body of left mandible without symphysis, with damaged ramus and with p2-p3 and m1	HHu 4116	♀	G2	*Mustela nivalis* group
body of left mandible without symphysis, with damaged ramus and m1	HHu 4117	♂	G2	*Mustela nivalis* group
body of left mandible without symphysis and with p4-m2	HHu 4118	♀♀	G2	*Mustela* aff. *praenivalis*
left mandible with damaged ramus and p4-m1	HHu 4119	♀♀	G2	*Mustela* aff. *praenivalis*
body of left mandible without symphysis and with p4-m1	HHu 4120	♂♀	G2	*Mustela* aff. *praenivalis*
fragment of body of left mandible with p4	HHu 4126	♂♂	G2	*Mustela* sp.
left mandible with damaged symphysis and m1	HHu 4219	♂♂	G1	*Mustela*
left mandible with damaged ramus and p4-m2	HHu 4220	♂♂	G1	*Mustela*
posterior half of left mandible with m1-m2	HHu 4221	♂♂	G1	*Mustela*
body of left mandible with c1-m2	HHu 4268	♂♂	G1	*Mustela*
left mandible with damaged ramus	HHu 4269	♂♂	G1	*Mustela*
body of left mandible without symphysis, with damaged ramus and m1-m2	HHu 4270	♂♂	G1	*Mustela*
body of left mandible without symphysis	HHu 4300	♂♀	G1	*Mustela* sp.
left mandible without symphysis	HHu 4411	♂♂	I+K	*Mustela* sp.
body fragment of left mandible	HHu 4436	♂♂	G3	*Mustela* sp.
left mandible with damaged ramus and p2-m1	HHu 4454	♂♀	G2	*Mustela nivalis* group
left mandible with damaged ramus and p3-m2	HHu 4455	♂♀	G2	*Mustela nivalis* group
left mandible with c1-m2	HHu 4543	♂♂	G2	*Mustela* sp.
left mandible with damaged symphysis and m1	HHu 4545	♂♂	G2	*Mustela* sp.
anterior fragment of left mandible with p3-p4	HHu 4547	♂♂	G1	*Mustela* aff. *palerminea*
left mandible without symphysis and with p2-m1	HHu 4548	♂♂	G1	*Mustela* aff. *palerminea*
left mandible with c1-p2 and p4-m1	HHu 4549	♂♂	G1	*Mustela* aff. *palerminea*
left mandible with c1-m2	HHu 4550	♂♂	G1	*Mustela* aff. *palerminea*
left mandible with p3-m2	HHu 4551	♂♂	G1	*Mustela* aff. *palerminea*
left mandible with damaged symphysis and m1	HHu 4552	♂♂	G1	*Mustela* aff. *palerminea*
body of left mandible without symphysis and with p3 and m1	HHu 4553	♂♂	G1	*Mustela* aff. *palerminea*
left mandible with damaged ramus and c1-m2	HHu 4554	♂♂	G1	*Mustela* aff. *palerminea*
left mandible with m1-m2	HHu 4556	♂♂	G1	*Mustela* aff. *palerminea*
left mandible with p2 and p4-m1	HHu 4557	♂♂	G1	*Mustela* aff. *palerminea*
posterior half of left mandible with damaged ramus and m1-m2	HHu 4559	♂♂	G1	*Mustela* aff. *palerminea*
left mandible with p2 and p4-m1	HHu 4565	♂♂	K	*Mustela* sp.
body of left mandible without symphysis and with c1 and p3-m1	HHu 4566	♂♂	K	*Mustela* sp.
left mandible with damaged ramus and p4-m1	HHu 4567	♂♂	K	*Mustela* sp.
left mandible with p3-m1	HHu 4581	♂♀	G1	*Mustela* aff. *praenivalis*
left mandible with p3 and m2	HHu 4582	♂♀	G1	*Mustela* aff. *praenivalis*
body of left mandible without symphysis, with damaged ramus and p4-m2	HHu 4588	♂♂	G1	*Mustela nivalis* group
body of left mandible without symphysis, with damaged ramus and p4-m1	HHu 4590	♂♀	G1	*Mustela nivalis* group
left mandible with m1	HHu 4598	♂♀	K	*Mustela* cf. *praenivalis*
left mandible with p4-m1	HHu 4600	♂♀	K	*Mustela* cf. *praenivalis*
body of left mandible without symphysis, with damaged ramus and m1-m2	HHu 4601	♂♀	K	*Mustela* cf. *praenivalis*
body of left mandible without symphysis, with damaged ramus and m1	HHu 4602	♂♀	K	*Mustela* cf. *praenivalis*
posterior half of left mandible with p4-m2	HHu 4047	♂♂	G2	*Mustela* aff. *erminea*
posterior half of left mandible with m1-m2	HHu 4055	♂♂	G2	*Mustela*
body of left mandible without symphysis, with damaged ramus and c1-p3 and m1-m2	HHu 4558	♀	G1	*Mustela* aff. *palerminea*

APPENDIX 3. — Continuation.

right mandible with c1 and p4-m2	HHu 4036	♂	G2	*Mustela* sp.
right mandible with p4-m1	HHu 4037	♂	G2	*Mustela* sp.
right mandible with p4-m1	HHu 4040	♂	G2	*Mustela* sp.
right mandible with p2-m2	HHu 4041	♂	G2	*Mustela* sp.
right mandible with p2-m2	HHu 4046	♂	G2	*Mustela* sp.
right mandible with c1-m2	HHu 4048	♂	G2	*Mustela*
body of right mandible without symphysis and with p4-m1	HHu 4049	♂	G2	*Mustela*
body of right mandible without symphysis and ramus, with p4-m1	HHu 4052	♂	G2	*Mustela*
posterior half of right mandible with p4-m2	HHu 4054	♂	G2	*Mustela*
right mandible without symphysis and with p3-m1	HHu 4056	♂	G2	*Mustela*
body of right mandible without symphysis, with damaged ramus and p4-m2	HHu 4058	♂	G2	*Mustela*
body fragment of right mandible with m1	HHu 4059	♂	G2	*Mustela*
body of right mandible without symphysis, with damaged ramus and with p3-m1	HHu 4060	♂	G2	*Mustela*
posterior half of right mandible	HHu 4061	♂	G2	*Mustela*
body of right mandible without symphysis, with damaged ramus and with m1-m2	HHu 4062	♂	G2	*Mustela*
body of right mandible without symphysis, with damaged ramus and with p3-m2	HHu 4068	♂	G2	*Mustela*
body of right mandible with m1	HHu 4069	♂	G2	*Mustela*
body of right mandible fragment with p4-m1	HHu 4076	♂	G2	*Mustela*
body of right mandible without symphysis, with damaged ramus and with m1	HHu 4078	♀	G2	*Mustela*
body of right mandible with ramus fragment and m1-m2	HHu 4079	♂	G2	*Mustela*
body of right mandible without symphysis, with damaged ramus and with p4-m2	HHu 4084	♂	G2	*Mustela*
body right of mandible without symphysis, with damaged ramus and with p4-m2	HHu 4085	♂	G2	*Mustela*
body of right mandible without symphysis, with damaged ramus and m1	HHu 4086	♂	G2	*Mustela*
body fragment of right mandible with p3-p4	HHu 4087	♂	G2	*Mustela*
body of right mandible without symphysis and with p2-m2	HHu 4089	♀	G2	*Mustela*
body of right mandible with p3-m2	HHu 4090	♂	G2	*Mustela*
body of right mandible without symphysis, with damaged ramus and with p3-m1	HHu 4091	♂	G2	*Mustela*
body of right mandible with damaged ramus and with p2-m2	HHu 4092	♂	G2	*Mustela*
body of right mandible with m1	HHu 4097	♀	G2	*Mustela*
body of right mandible without symphysis, with damaged ramus and with p4-m2	HHu 4100	♀	G2	*Mustela*
right mandible with p3-m2	HHu 4101	♀	G2	*Mustela*
body of right mandible without symphysis, with damaged ramus and with p4-m1	HHu 4103	♂	G2	*Mustela nivalis* group
body of right mandible without symphysis, with damaged ramus and with p4-m2	HHu 4108	♀	G2	*Mustela nivalis* group
body of right mandible without symphysis, with damaged ramus and with m1-m2	HHu 4109	♀	G2	*Mustela nivalis* group
body of right mandible without symphysis, with damaged ramus and with p3 and m1	HHu 4110	♀	G2	*Mustela nivalis* group
body of right mandible with damaged ramus and with p3-m1	HHu 4111	♀	G2	*Mustela nivalis group*
body of right mandible without symphysis, with damaged ramus and with p4-m2	HHu 4112	♀	G2	*Mustela* aff. *praenivalis*
body fragment of right mandible	HHu 4114	♀	G2	*Mustela* aff. *praenivalis*
posterior half of right mandible with m1	HHu 4123	♀	G2	*Mustela nivalis* group
body of right mandible without symphysis and with damaged ramus	HHu 4124	♀	G2	*Mustela* sp.
body of right mandible without symphysis and with p3-m1	HHu 4125	♀	G2	*Mustela* aff. *praenivalis*
body of right mandible without symphysis, with damaged ramus and with p3-m2	HHu 4130	♂	G2/G3	*Mustela* aff. *praenivalis*
right mandible without symphysis and with p4-m2	HHu 4222	♂	G1	*Mustela*
body of right mandible with p2-m1	HHu 4223	♂	G1	*Mustela*
body of right mandible without symphysis, with damaged ramus and m1	HHu 4224	♂	G1	*Mustela*
body of right mandible with p4-m2	HHu 4225	♂	G1	*Mustela*
body of right mandible without symphysis and ramus and with m1	HHu 4271	♂	G1	*Mustela*
body of right mandible without symphysis and with c1-p4	HHu 4272	♂	G1	*Mustela*
body of right mandible without symphysis, with damaged ramus and with p4-m2	HHu 4273	♂	G1	*Mustela*
body of right mandible without symphysis, with ramus fragment and p3-m2	HHu 4274	♂	G1	*Mustela*
anterior half of right mandible with c1 up to the trigonid of m1	HHu 4275	♂	G1	*Mustela*
body of right mandible fragment with p3-m1	HHu 4276	♂	G1	*Mustela*
body of right mandible and ramus fragment with m1-m2	HHu 4277	♂	G1	*Mustela*
body of right mandible without symphysis, with damaged ramus and p4-m2	HHu 4278	♂	G1	*Mustela*
body of right mandible fragment without symphysis and with p3-m1	HHu 4278	♂	G1	*Mustela*
body of right mandible with p2-m1	HHu 4279	♂	G1	*Mustela*
right mandible with p3 and m1	HHu 4284	♂	G1	*Mustela nivalis* group
damaged ramus of right mandible	HHu 4285	♂	G1	*Mustela nivalis* group
right mandible with p4-m2	HHu 4286	♂	G1	*Mustela*
body fragment of right mandible	HHu 4298	♂	G2	*Mustela* sp.
right mandible with damaged symphysis and p3-m2	HHu 4452	♀	G2	*Mustela nivalis* group
body of right mandible without symphysis, with damaged ramus and p2-m2	HHu 4453	♀	G2	*Mustela nivalis* group
body of right mandible fragment with p4-m1	HHu 4456	♂	G2	*Mustela nivalis* group
body and ramus fragment of right mandible with m1	HHu 4504	♀	G3	*Mustela nivalis* group
right mandible with damaged ramus and p4-m1	HHu 4505	♀	G2/G3	*Mustela praenivalis*
body of right mandible without symphysis and ramus, with m1	HHu 4544	♂	G2	*Mustela* sp.
body of right mandible without symphysis and with p3 and m1	HHu 4555	♂	K	*Mustela* sp.
right mandible with p2-m1	HHu 4560	♂	G1	*Mustela* aff. *palerminea*
right mandible with damaged ramus and p2-m2	HHu 4561	♀	G1	*Mustela* aff. *palerminea*
right mandible with p2-m2	HHu 4562	♂	G1	*Mustela* aff. *palerminea*

Appendix 3. — Continuation.

right mandible with damaged ramus, p2 and p4-m1	HHu 4563	♂♀	G1	*Mustela* aff. *palerminea*
body of right mandible without symphysis and with p2-m1	HHu 4564	♂	G1	*Mustela* aff. *palerminea*
body fragment of right mandible with p4-m2	HHu 4568	♂	K	*Mustela* sp.
right mandible with p2-m2	HHu 4583	♀	G1	*Mustela* aff. *praenivalis*
right mandible with m1	HHu 4584	♀	G1	*Mustela* aff. *praenivalis*
right mandible with p2-m2	HHu 4585	♀	G1	*Mustela* aff. *praenivalis*
right mandible with damaged ramus and p3 and m1	HHu 4586	♀	G1	*Mustela* aff. *praenivalis*
right mandible with p4-m1	HHu 4587	♀	G1	*Mustela nivalis* group
right mandible with damaged ramus and p3-m2	HHu 4593	♀	G1	*Mustela* sp.
body of right mandible without symphysis and with p3-m2	HHu 4594	♀	G1	*Mustela* sp.
right mandible with damaged ramus and p4-m1	HHu 4595	♀	G1	*Mustela* sp.
left c1	HHu 4089c	♀	G2	–
left c1	HHu 4108a	♀	G2	*Mustela nivalis* group
left c1	HHu 4122	♂	G2	*Mustela* sp.
left c1	HHu 4564a	♂	G1	*Mustela* aff. *palerminea*
right c1	HHu 4089a	♂	G2	–
right c1	HHu 4089b	♂	G2	–
right c1	HHu 4121	♂	G2	*Mustela* sp.
right c1	HHu 4128	♀	G2	*Mustela praenivalis*
right m1	HHu 4129	♂	G2	*Mustela praenivalis*
atlas	HHu 4391	–	G2	*Mustela* sp.
atlas	HHu 4476	–	K	*Mustela*sp. (*nivalis* group)
axis	HHu 4333	–	G2	*Mustela* sp.
axis	HHu 4334	–	G2	*Mustela* sp.
axis	HHu 4589	–	G1	*Mustela* sp.
damaged, right scapula	HHu 4392	–	G2	*Mustela* sp.
distal epiphysis of left humerus	HHu 4161	♂	G2	*Mustela nivalis* group
distal half of left humerus	HHu 4166	♀	G2	*Mustela nivalis* group
distal half of left humerus	HHu 4169	♀	G2	*Mustela nivalis* group
proximal half of left humerus	HHu 4171	♂	G2	*Mustela praenivalis*
distal half of left humerus	HHu 4178	♂	G2	*Mustela nivalis* group
distal half of left humerus	HHu 4186	♀	G2	*Mustela nivalis* group
left humerus	HHu 4210	♂	G1	*Mustela nivalis* group
proximal half of left humerus	HHu 4217	♂	G1	*Mustela nivalis* group
left humerus	HHu 4218	♂	G1	*Mustela nivalis* group
proximal half of left humerus	HHu 4230	♂	G1	*Mustela*
proximal half of left humerus	HHu 4247	♂	G1	*Mustela*
left humerus	HHu 4254	♂	G1	*Mustela nivalis* group
distal half of left humerus	HHu 4264	♂	G1	*Mustela nivalis* group
distal epiphysis of left humerus	HHu 4323	♂	G2	*Mustela* sp.
left humerus	HHu 4325	♂	G2	*Mustela* sp.
proximal epiphysis of left humerus	HHu 4326	♂	G2	*Mustela* sp.
proximal epiphysis of left humerus	HHu 4343	♂	G2	*Mustela* sp.
distal epiphysis of left humerus	HHu 4352	♂	G2	*Mustela* sp.
proximal half of left humerus	HHu 4353	♂	G2	*Mustela* sp.
distal half of left humerus	HHu 4354	♂	G2	*Mustela* sp.
proximal half of left humerus	HHu 4356	♂	G2	*Mustela* sp.
distal epiphysis of left humerus	HHu 4366	♂	G2	*Mustela* sp.
distal epiphysis of left humerus	HHu 4367	♂	G2	*Mustela* sp.
distal epiphysis of left humerus	HHu 4368	♂	G2	*Mustela* sp.
left humerus	HHu 4371	♂	G2	*Mustela* sp.
proximal half of left humerus	HHu 4387	♂	G2	*Mustela* sp.
proximal half of left humerus	HHu 4388	♂	G2	*Mustela* sp.
distal half of left humerus	HHu 4396	♂	G2	*Mustela* sp.
distal epiphysis of left humerus	HHu 4398	♂	G2	*Mustela* sp.
proximal half of left humerus	HHu 4418	♀	G2	*Mustela* sp.
proximal half of left humerus	HHu 4420	♀	G2	*Mustela* sp.
proximal half of left humerus	HHu 4428	♀	G2	*Mustela* sp.
distal half of left humerus	HHu 4429	♀	G2	*Mustela* sp.
left humerus	HHu 4450	♀	G1	*Mustela* smaller than *Mustela nivalis*
left humerus	HHu 4473	♂	K	*Mustela nivalis* group
proximal half of left humerus	HHu 4478	♀	K	*Mustela praenivalis*
left humerus	HHu 4492	♂	K	*Mustela nivalis* group
distal half of left humerus	HHu 4494	♀	K	*Mustela* sp. (*Mustela nivalis pusilla* group)
shaft of left humerus	HHu 4497	♂	K	*Mustela* sp. (*Mustela nivalis* group)
left humerus	HHu 4360	♂	G2	*Mustela* sp.

Appendix 3. — Continuation.

damaged, left humerus	HHu 4499	♂	K	*Mustela* sp. (*Mustela nivalis* group)
proximal half of left humerus	HHu 4509	♀	G3	*Mustela nivalis* group
left humerus	HHu 4518	♂	G3	*Mustela nivalis* group
left humerus	HHu 4569	♂	G1	*Mustela* aff. *praenivalis*
left humerus	HHu 4570	♂	G1	*Mustela* aff. *praenivalis*
distal half of left humerus	HHu 4592	♀	G1	*Mustela* sp.
proximal half of right humerus	HHu 4131	♂	G2/G3	*Mustela* aff. *praenivalis*
right humerus	HHu 4132	♂	G2/G3	*Mustela* aff. *praenivalis*
distal half of right humerus	HHu 4146	♂	G2	*Mustela* aff. *praenivalis*
proximal half of right humerus	HHu 4155	♀	G2	*Mustela nivalis* group
distal epiphysis of right humerus	HHu 4162	♀	G2	*Mustela nivalis* group
proximal half of right humerus	HHu 4180	♀	G2	*Mustela nivalis* group
right humerus	HHu 4195	♀	G2	*Mustela nivalis* group
proximal half of right humerus	HHu 4208	♂	G1	*Mustela erminea* group
right humerus	HHu 4213	♂	G1	*Mustela nivalis* group
right humerus	HHu 4214	♂	G1	*Mustela nivalis* group
distal half of right humerus	HHu 4235	♂	G1	*Mustela*
proximal half of right humerus	HHu 4240	♂	G1	*Mustela*
distal epiphysis of right humerus	HHu 4242	♂	G1	*Mustela*
distal half of right humerus	HHu 4244	♂	G1	*Mustela*
right humerus	HHu 4251	♂	G1	*Mustela nivalis* group
distal half of right humerus	HHu 4252	♂	G1	*Mustela nivalis* group
distal half of right humerus	HHu 4257	♂	G1	*Mustela nivalis* group
distal half of right humerus	HHu 4259	♂	G1	*Mustela nivalis* group
distal half of right humerus	HHu 4267	♂	G1	*Mustela nivalis* group
right humerus	HHu 4294	♀	G1	*Mustela* smaller than *Mustela nivalis*
proximal epiphysis of right humerus	HHu 4324	♂	G2	*Mustela* sp.
right humerus	HHu 4338	♂	G2	*Mustela* sp.
right humerus	HHu 4345	♂	G2	*Mustela* sp.
proximal epiphysis of right humerus	HHu 4347	♂	G2	*Mustela* sp.
distal half of right humerus	HHu 4355	♂	G2	*Mustela* sp.
distal epiphysis of right humerus	HHu 4362	♂	G2	*Mustela* sp.
distal epiphysis of right humerus	HHu 4364	♂	G2	*Mustela* sp.
distal half of right humerus	HHu 4378	♂	G2	*Mustela* sp.
proximal half of right humerus	HHu 4386	♂	G2	*Mustela* sp.
proximal epiphysis of right humerus	HHu 4389	♂	G2	*Mustela* sp.
right humerus	HHu 4393	♂	G2	*Mustela* sp.
proximal epiphysis of right humerus	HHu 4399	♂	G2	*Mustela* sp.
proximal half of right humerus	HHu 4423	♀	G2	*Mustela* sp.
right humerus	HHu 4431	♀	G2	*Mustela* sp.
right humerus	HHu 4441	♀	G1	*Mustela* smaller than *Mustela praenivalis*
right humerus	HHu 4442	♀	G1	*Mustela* smaller than *Mustela praenivalis*
right humerus	HHu 4447	♀	G1	*Mustela* smaller than *Mustela nivalis*
distal half of right humerus	HHu 4449	♀	G1	*Mustela* smaller than *Mustela nivalis*
proximal half of right humerus	HHu 4457	♀	G2	*Mustela nivalis* group
proximal half of right humerus	HHu 4461	♀	G2	*Mustela nivalis* group
proximal half of right humerus	HHu 4465	♀	G2	*Mustela nivalis* group
proximal half of right humerus	HHu 4468	♀	G2	*Mustela nivalis* group
right humerus	HHu 4481	♀	K	*Mustela nivalis* group
right humerus	HHu 4482	♀	K	*Mustela nivalis* group
right humerus	HHu 4483	♀	K	*Mustela nivalis* group
right humerus	HHu 4484	♀	K	*Mustela nivalis* group
proximal half of right humerus	HHu 4500	♀	K	*Mustela* sp. (*Mustela nivalis* group)
right humerus	HHu 4507	♂	G3	*Mustela nivalis* group
right humerus	HHu 4508	♂	G3	*Mustela nivalis* group
right humerus	HHu 4514	♀	G3	*Mustela nivalis* group
right humerus	HHu 4517	♀	G3	*Mustela nivalis* group
proximal half of right humerus	HHu 4591	♀	G1	*Mustela* sp.
proximal half of right humerus	HHu 4596	♀	G1	*Mustela* sp.
proximal half of right humerus	HHu 4597	♀	G1	*Mustela* sp.
right humerus	HHu 4187	♀	G2	*Mustela nivalis* group
proximal half of right humerus	HHu 4488	♀	K	*Mustela nivalis* group
left radius	HHu 4159	♀	G2	*Mustela nivalis* group

Appendix 3. — Continuation.

left radius	HHu 4167	♀	G2	*Mustela nivalis* group
left radius	HHu 4168	♂	G2	*Mustela*
left radius	HHu 4170	♂	G2	*Mustela nivalis* group
left radius	HHu 4181	♂	G2	*Mustela* aff. *praenivalis*
distal half of left radius	HHu 4196	♀	G2	*Mustela nivalis* group
left radius	HHu 4250	♂	G1	*Mustela*
left radius	HHu 4310	♂	K	*Mustela* sp.
shaft fragment of left radius	HHu 4330	♂	G2	*Mustela* sp.
proximal half of left radius	HHu 4336	♂	G2	*Mustela* sp.
left radius	HHu 4405	♂	G2	*Mustela* sp.
proximal half of left radius	HHu 4407	♂	G2	*Mustela* sp.
left radius	HHu 4516	♂	G3	*Mustela* sp.
left radius	HHu 4519	♂	G3	*Mustela nivalis* group
proximal half of left radius	HHu 4511	♂	G3	*Mustela* sp.
damaged, left radius	HHu 4281	♀♂	G1	*Mustela nivalis* group
right radius	HHu 4174	♂	G2	*Mustela nivalis* group
right radius	HHu 4283	♂	G1	*Mustela nivalis* group
right radius	HHu 4406	♂	G2	*Mustela* sp.
right radius	HHu 4409	♂	G2	*Mustela* sp.
right radius	HHu 4434	♀	G2	*Mustela* sp.
proximal epiphysis of left ulna	HHu 4287	♂	G1	*Mustela*
proximal half of left ulna	HHu 4412	♂	G2/G3	*Mustela praenivalis*
left ulna	HHu 4425	♀	G2	*Mustela* sp.
left ulna	HHu 4487	♀	K	*Mustela nivalis* group
left ulna	HHu 4160	♂	G2	*Mustela nivalis* group
left ulna	HHu 4309	♂	K	*Mustela* sp.
proximal half of left ulna	HHu 4467	♀	G2	*Mustela nivalis* group
proximal epiphysis of left ulna	HHu 4175	♀	G2	*Mustela nivalis* group
proximal half of left ulna	HHu 4184	♀♂	G2	*Mustela nivalis* group
distal half of right ulna	HHu 4193	♂	G2	*Mustela nivalis* group
distal half of right ulna	HHu 4203	♂	G2	*Mustela nivalis* group
distal half of right ulna	HHu 4204	♂	G2	*Mustela nivalis* group
right ulna	HHu 4296	♀	G1	*Mustela* smaller than *Mustela nivalis*
proximal half of right ulna	HHu 4314	♂	G2	*Mustela* sp.
right ulna	HHu 4383	♂	G2	*Mustela* sp.
proximal epiphysis of right ulna	HHu 4384	♂	G2	*Mustela* sp.
proximal half of right ulna	HHu 4385	♂	G2	*Mustela* sp.
right ulna	HHu 4408	♂	G2	*Mustela* sp.
right ulna	HHu 4426	♀♂	G2	*Mustela* sp.
proximal half of right ulna	HHu 4438	♂	G3	*Mustela* sp.
right ulna	HHu 4510	♂	G3	*Mustela nivalis* group
proximal half of right ulna	HHu 4249	♀	G1	*Mustela*
proximal half of right ulna	HHu 4342	♂	G2	*Mustela* sp.
distal half of right ulna	HHu 4335	♂	G2	*Mustela* sp.
fragment of left pelvis	HHu 4153	–	G2	*Mustela nivalis* group
left pelvis	HHu 4173	–	G2	*Mustela nivalis* group
left pelvis	HHu 4179	–	G2	*Mustela nivalis* group
damaged, left pelvis	HHu 4241	–	G1	*Mustela*
left pelvis	HHu 4243	–	G1	*Mustela*
damaged, left pelvis	HHu 4248	–	G1	*Mustela*
damaged, left pelvis	HHu 4308	–	K	*Mustela* sp.
damaged, left pelvis	HHu 4313	–	G2	*Mustela* sp.
damaged, left pelvis	HHu 4340	–	G2	*Mustela* sp.
fragment of left pelvis	HHu 4358	–	G2	*Mustela* sp.
damaged, left pelvis	HHu 4370	–	G2	*Mustela* sp.
fragment of left pelvis	HHu 4397	–	G2	*Mustela* sp.
fragment of left pelvis	HHu 4414	–	L	*Mustela praenivalis-nivalis* group
left pelvis	HHu 4440	–	G1	*Mustela* smaller than *Mustela praenivalis*
damaged, left pelvis	HHu 4463	–	G2	*Mustela nivalis* group
damaged, left pelvis	HHu 4471	–	G2	*Mustela nivalis* group
left pelvis	HHu 4491	–	K	*Mustela* smaller than *Mustela praenivalis*
left pelvis	HHu 4503	–	G3	*Mustela* sp.
damaged right pelvis	HHu 4149	–	G2	*Mustela* aff. *praenivalis*
fragment of right pelvis	HHu 4150	–	G2	*Mustela* aff. *praenivalis*
right pelvis	HHu 4154	–	G2	*Mustela nivalis* group
right pelvis	HHu 4172	–	G2	*Mustela nivalis-praenivalis*

Appendix 3. — Continuation.

right pelvis	HHu 4177	–	G2	*Mustela nivalis* group
damaged, right pelvis	HHu 4190	–	G2	*Mustela* sp. (*Mustela nivalis* group)
right pelvis	HHu 4197	–	G2	*Mustela nivalis* group
damaged, right pelvis	HHu 4237	–	G1	*Mustela*
damaged, right pelvis	HHu 4307	–	K	*Mustela* sp.
right pelvis	HHu 4315	–	G2	*Mustela* sp.
fragment of right pelvis	HHu 4359	–	G2	*Mustela* sp.
right pelvis	HHu 4376	–	G2/G3	*Mustela* sp.
right pelvis	HHu 4379	–	G2	*Mustela* sp.
right pelvis	HHu 4475	–	K	*Mustela nivalis* group
damaged, right pelvis	HHu 4480	–	K	*Mustela nivalis* group
left femur	HHu 4137	♂	–	*Mustela nivalis* group
left femur	HHu 4142	♂	G2	*Mustela* aff. *praenivalis*
proximal half of left femur	HHu 4148	♂	G2	*Mustela* aff. *praenivalis*
proximal half of left femur	HHu 4156	♂	G2	*Mustela nivalis* group
proximal half of left femur	HHu 4157	♀	G2	*Mustela nivalis* group
distal half of left femur	HHu 4176	♀	G2	*Mustela nivalis* group
proximal half of left femur	HHu 4189	♀	G2	*Mustela nivalis* group
proximal half of left femur	HHu 4191	♂	G2	*Mustela nivalis* group
proximal half of left femur	HHu 4211	♀	G1	*Mustela nivalis* group
left femur	HHu 4216	♂	G1	*Mustela nivalis* group
left femur	HHu 4227	♂	G1	*Mustela*
left femur	HHu 4228	♂	G1	*Mustela*
distal half of left femur	HHu 4234	♂	G1	*Mustela*
proximal half of left femur	HHu 4238	♂	G1	*Mustela*
proximal half of left femur	HHu 4253	♀	G1	*Mustela nivalis* group
left femur	HHu 4256	♂	G1	*Mustela nivalis* group
proximal half of left femur	HHu 4263	♂	G1	*Mustela nivalis* group
shaft of left femur	HHu 4266	♀	G1	*Mustela nivalis* group
damaged, left femur	HHu 4282	♀	G1	*Mustela nivalis* group
proximal half of left femur	HHu 4289	♀	G1	*Mustela* smaller than *Mustela nivalis*
distal half of left femur	HHu 4291	♀	G1	*Mustela* smaller than *Mustela nivalis*
left femur	HHu 4295	♀	G1	*Mustela* smaller than *Mustela nivalis*
damaged, left femur	HHu 4302	♂	K	*Mustela*
proximal half of left femur	HHu 4304	♂	K	*Mustela*
proximal half of left femur	HHu 4319	♂	G2	*Mustela* sp.
proximal half of left femur	HHu 4321	♂	G2	*Mustela* sp.
proximal half of left femur	HHu 4331	♀	G2	*Mustela* sp.
proximal end of left femur	HHu 4357	♂	G2	*Mustela* sp.
proximal half of left femur	HHu 4361	♂	G2	*Mustela* sp.
proximal half of left femur	HHu 4363	♂	G2	*Mustela* sp.
proximal half of left femur	HHu 4365	♂	G2	*Mustela* sp.
left femur	HHu 4373	♂	G2	*Mustela* sp.
left femur	HHu 4380	♂	G2	*Mustela* sp.
left femur	HHu 4381	♂	G2	*Mustela* sp.
proximal half of left femur	HHu 4382	♂	G2	*Mustela* sp.
left femur	HHu 4390	♂	G2	*Mustela* aff. *palerminea*
damaged, left femur	HHu 4416	♀	G2/G3	*Mustela* sp.
damaged, left femur	HHu 4419	♀	G2	*Mustela* sp.
left femur	HHu 4443	♀	G1	*Mustela* smaller than *Mustela praenivalis*
damaged, left femur	HHu 4479	♂	K	*Mustela nivalis* group
damaged, left femur	HHu 4493	♀	K	*Mustela* sp. (*Mustela nivalis pusilla* group)
proximal half of left femur	HHu 4501	♀	K	*Mustela* sp.
proximal half of left femur	HHu 4512	♀	G3	*Mustela nivalis* group
proximal end of left femur	HHu 4513	♂	G3	*Mustela nivalis* group
proximal half of left femur	HHu 4515	♂	G3	*Mustela nivalis* group
damaged, left femur	HHu 4521	♀	G3	*Mustela nivalis* group
left femur	HHu 4572	♂	G1	*Mustela* aff. *praenivalis*
left femur	HHu 4573	♂	G1	*Mustela* aff. *praenivalis*
shaft fragment of right femur	HHu 4127	♂	G2	*Mustela* sp.
shaft of right femur	HHu 4136	♂	G1	*Mustela nivalis* group
right femur	HHu 4138	♂	G	*Mustela nivalis* group
distal end of right femur	HHu 4139	♀	G2	*Mustela nivalis* group
distal half of right femur	HHu 4140	♂	G3	*Mustela nivalis* group
proximal half of right femur	HHu 4143	♂	G2	*Mustela* aff. *praenivalis*

Appendix 3. — Continuation.

proximal half of right femur	HHu 4144	♂	G2	*Mustela* aff. *praenivalis*
right femur	HHu 4145	♂	G2	*Mustela* aff. *praenivalis*
distal end of right femur	HHu 4158	♂	G2	*Mustela nivalis* group
proximal half of right femur	HHu 4164	♀	G2	*Mustela nivalis* group
proximal half of right femur	HHu 4183	♀	G2	*Mustela nivalis* group
distal half of right femur	HHu 4185	♀	G2	*Mustela nivalis* group
distal end of right femur	HHu 4188	♀	G2	*Mustela nivalis* group
distal half of right femur	HHu 4209	♀	G1	*Mustela erminea* group
proximal half of right femur	HHu 4215	♂	G1	*Mustela nivalis* group
right femur	HHu 4226	♂	G1	*Mustela*
right femur	HHu 4232	♂	G1	*Mustela*
shaft of right femur	HHu 4233	♂	G1	*Mustela*
distal half of right femur	HHu 4236	♀	G1	*Mustela*
proximal half of right femur	HHu 4239	♂	G1	*Mustela*
right femur	HHu 4260	♂	G1	*Mustela nivalis* group
shaft of right femur	HHu 4261	♀	G1	*Mustela nivalis* group
right femur	HHu 4288	♀	G1	*Mustela* smaller than *Mustela nivalis*
right femur	HHu 4292	♀	G1	*Mustela* smaller than *Mustela nivalis*
right femur	HHu 4293	♀	G1	*Mustela* smaller than *Mustela nivalis*
right femur	HHu 4311	♂	G2	*Mustela* sp.
proximal half of right femur	HHu 4316	♂	G2	*Mustela* sp.
proximal half of right femur	HHu 4318	♂	G1	*Mustela* sp.
right femur	HHu 4320	♂	G2	*Mustela* sp.
proximal half of right femur	HHu 4322	♂	G2	*Mustela* sp.
right femur	HHu 4337	♂	G2	*Mustela* sp.
proximal half of right femur	HHu 4369	♀	G2	*Mustela* sp.
damaged proximal end of right femur	HHu 4372	♂	G2	*Mustela* sp.
damaged, right femur	HHu 4417	♀	G2/G3	*Mustela* sp.
damaged, right femur	HHu 4421	♀	G2	*Mustela* sp.
proximal half of right femur	HHu 4424	♀	G2	*Mustela* sp.
damaged, right femur	HHu 4427	♀	G2	*Mustela* sp.
right femur	HHu 4432	♀	G2	*Mustela* sp.
damaged, right femur	HHu 4433	♀	G2	*Mustela* sp.
damaged, right femur	HHu 4451	♀	G1	*Mustela* smaller than *Mustela nivalis*
proximal half of right femur	HHu 4460	♀	G2	*Mustela nivalis* group
damaged, right femur	HHu 4462	♀	G2	*Mustela nivalis* group
right femur	HHu 4472	♂	K	*Mustela nivalis* group
right femur	HHu 4477	♀	K	*Mustela nivalis* group
right femur without distal epiphysis	HHu 4485	♀	K	*Mustela nivalis* group
right femur without distal epiphysis	HHu 4486	♀	K	*Mustela nivalis* group
damaged, right femur	HHu 4490	♂	K	*Mustela* smaller than *Mustela praenivalis*
proximal half of right femur	HHu 4495	♀	K	*Mustela* sp. (*Mustela nivalis pusilla* group)
proximal half of right femur	HHu 4496	♀	K	*Mustela* sp. (*Mustela nivalis* group)
right femur	HHu 4520	♂	G3	*Mustela nivalis* group
right femur	HHu 4571	♂	G1	*Mustela* aff. *praenivalis*
right femur	HHu 4574	♂	G1	*Mustela* aff. *praenivalis*
left tibia	HHu 4141	♂	G2	*Mustela* aff. *praenivalis*
distal half of left tibia	HHu 4147	♂	G2	*Mustela* aff. *praenivalis*
left tibia	HHu 4151	♂	G2	*Mustela nivalis* group
left tibia	HHu 4163	♂	G2	*Mustela nivalis* group
proximal half of left tibia	HHu 4192	♂	G2	*Mustela nivalis* group
distal end of left tibia	HHu 4198	♂	G2	*Mustela nivalis* group
left tibia	HHu 4212	♂	G1	*Mustela nivalis* group
left tibia	HHu 4229	♂	G1	*Mustela*
proximal half of left tibia	HHu 4245	♂	G1	*Mustela*
distal half of left tibia	HHu 4246	♀	G1	*Mustela*
proximal half of left tibia	HHu 4258	♂	G1	*Mustela nivalis* group
left tibia	HHu 4290	♀	G1	*Mustela* smaller than *Mustela nivalis*
proximal half of left tibia	HHu 4303	♂	K	*Mustela*
distal half of left tibia	HHu 4305	♂	K	*Mustela*
left tibia	HHu 4306	♂	K	*Mustela* sp.
proximal half of left tibia	HHu 4317	♂	G1	*Mustela* sp.

Appendix 3. — Continuation.

proximal end of left tibia	HHu 4332	♂	G2	*Mustela* sp.
left tibia	HHu 4339	♂	G2	*Mustela* sp.
proximal end of left tibia	HHu 4346	♂	G2	*Mustela* sp.
proximal end of left tibia	HHu 4351	♂	G2	*Mustela* sp.
distal end of left tibia	HHu 4374	♂	G2/G3	*Mustela* sp.
damaged proximal end of left tibia	HHu 4375	♂	G2/G3	*Mustela* sp.
distal half of left tibia	HHu 4400	♂	G2	*Mustela* sp.
proximal half of left tibia	HHu 4401	♂	G2	*Mustela* sp.
distal half of left tibia	HHu 4413	♀	H	*Mustela nivalis* group
distal half of left tibia	HHu 4415	♀	L	*Mustela praenivalis-nivalis* group
left tibia	HHu 4446	♀	G1	*Mustela* smaller than *Mustela praenivalis*
left tibia	HHu 4448	♀	G1	*Mustela* smaller than *Mustela nivalis*
proximal half of left tibia	HHu 4459	♂	G2	*Mustela nivalis* group
left tibia	HHu 4464	♂	G2	*Mustela nivalis* group
proximal half of left tibia	HHu 4474	♂	K	*Mustela nivalis* group
proximal half of left tibia	HHu 4498	♂	K	*Mustela* sp. (*Mustela nivalis* group)
left tibia	HHu 4576	♂	G1	*Mustela* aff. *praenivalis*
left tibia	HHu 4579	♂	G1	*Mustela* aff. *praenivalis*
left tibia	HHu 4580	♂	G1	*Mustela* aff. *praenivalis*
proximal end of right tibia	HHu 4133	♂	G2/G3	*Mustela* aff. *praenivalis*
right tibia	HHu 4134	♂	G2	*Mustela nivalis* group
shaft fragment of right tibia	HHu 4135	♂	G3	*Mustela nivalis* group
proximal half of right tibia	HHu 4152	♂	G2	*Mustela nivalis* group
distal half of right tibia	HHu 4165	♂	G2	*Mustela nivalis* group
distal half of right tibia	HHu 4182	♂	G2	*Mustela* aff. *praenivalis*
proximal half of right tibia	HHu 4194	♂	G2	*Mustela nivalis* group
distal end of right tibia	HHu 4199	♂	G2	*Mustela nivalis* group
distal half of right tibia	HHu 4200	♂	G2	*Mustela nivalis* group
distal half of right tibia	HHu 4201	♂	G2	*Mustela nivalis* group
proximal half of right tibia	HHu 4202	♀	G2	*Mustela nivalis* group
proximal half of right tibia	HHu 4231	♂	G1	*Mustela*
proximal half of right tibia	HHu 4255	♂	G1	*Mustela nivalis* group
proximal half of right tibia	HHu 4262	♂	G1	*Mustela nivalis* group
proximal half of right tibia	HHu 4265	♀	G1	*Mustela nivalis* group
right tibia	HHu 4280	♀	G1	*Mustela nivalis* group
distal end of right tibia	HHu 4301	♂	K	*Mustela erminea*
right tibia	HHu 4312	♂	G2	*Mustela* sp.
right tibia	HHu 4327	♂	G2	*Mustela* sp.
proximal end of right tibia	HHu 4328	♂	G2	*Mustela* sp.
shaft of right tibia	HHu 4329	♂	G2	*Mustela* sp.
distal half of right tibia	HHu 4341	♂	G2	*Mustela* sp.
right tibia	HHu 4344	♂	G2	*Mustela* sp.
proximal end of right tibia	HHu 4348	♂	G2	*Mustela* sp.
distal end of right tibia	HHu 4349	♂	G2	*Mustela* sp.
distal end of right tibia	HHu 4350	♂	G2	*Mustela* sp.
right tibia	HHu 4377	♂	G2	*Mustela* sp.
distal half of right tibia	HHu 4394	♂	G2	*Mustela* sp.
proximal half of right tibia	HHu 4395	♂	G2	*Mustela* sp.
distal half of right tibia	HHu 4402	♂	G2	*Mustela* sp.
right tibia	HHu 4422	♀	G2	*Mustela* sp.
shaft of right tibia	HHu 4430	♀	G2	*Mustela* sp.
distal half of right tibia	HHu 4435	♀	G2	*Mustela* sp.
right tibia	HHu 4444	♀	G1	*Mustela* smaller than *Mustela praenivalis*
right tibia	HHu 4445	♀	G1	*Mustela* smaller than *Mustela praenivalis*
distal half of right tibia	HHu 4458	♂	G2	*Mustela nivalis* group
right tibia	HHu 4466	♀	G2	*Mustela nivalis* group
distal half of right tibia	HHu 4469	♀	G2	*Mustela nivalis* group
distal half of right tibia	HHu 4470	♀	G2	*Mustela nivalis* group
right tibia	HHu 4489	♀	K	*Mustela nivalis* group
proximal half of right tibia	HHu 4502	♀	K	*Mustela* sp.
proximal half of right tibia	HHu 4506	♂	G3	*Mustela* sp.
right tibia	HHu 4575	♂	G1	*Mustela* aff. *praenivalis*
right tibia	HHu 4577	♂	G1	*Mustela* aff. *praenivalis*
right tibia	HHu 4578	♂	G1	*Mustela* aff. *praenivalis*

Appendix 4. — Scheme of measurements of mustelids mandible: **A**, buccal view; **B**, lingual view; **C**, occlusal view. The abbreviations can be found in Appendix 5.

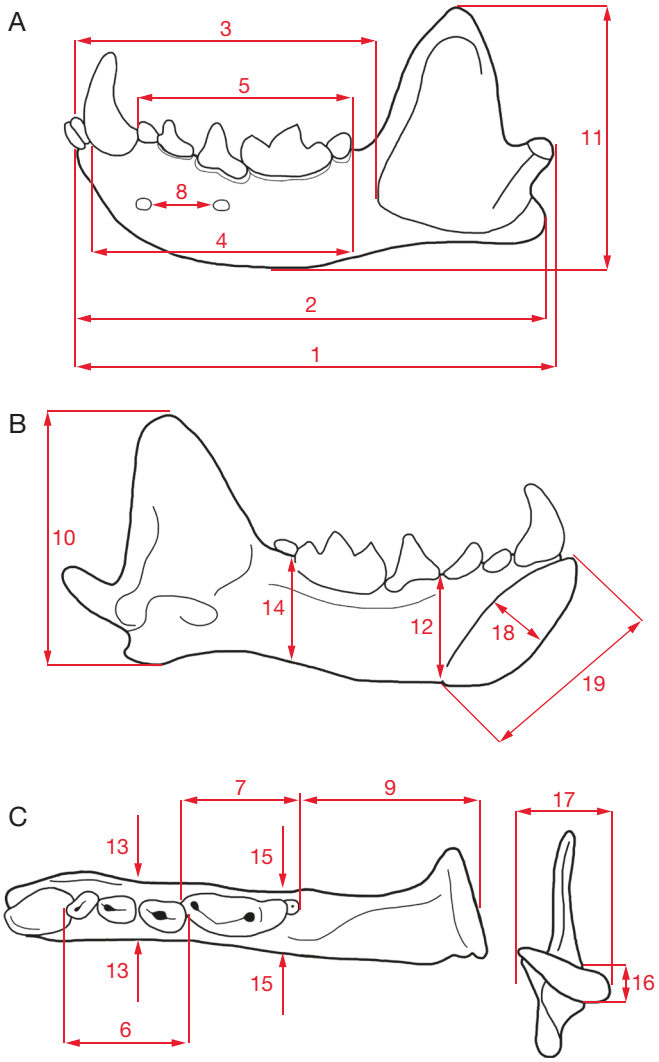

Appendix 5. — Abbreviations of the scheme of measurements of mustelids mandible available in Appendix 4.

No.	The mandibular measurements
1	total length (infradentale to condyle)
2	length from infradentale to angular process
3	length infradentale to mesial margin of masseteric fossa
4	c1-m2 length (mesial margin of c1 to distal margin of m2)
5	p2-m2 length (mesial margin of p1 to distal margin of m2)
6	p2-p4 length (mesial margin of p2 to distal margin of p4)
7	m1-m2 length (mesial margin of m1 to distal margin of m2)
8	distance between mental foramina
9	length from distal margin of m2 to condyle
10	ramus height (from the base of angular process to the apex of coronoid process)
11	mandible maximum height
12	mandibular body height between p3 and p4
13	mandibular body thickness between p3 and p4
14	mandibular body height between m1 and m2
15	mandibular body thickness between m1 and m2
16	condyle height
17	condyle breadth
18	symphysis maximum diameter
19	symphysis minimum diameter

Appendix 6. — The scheme of measurements and cusp terminology of mustelid teeth: **A**, **B**, m1; **C**, P4; **D**, M1. The abbreviations can be found in Appendix 7.

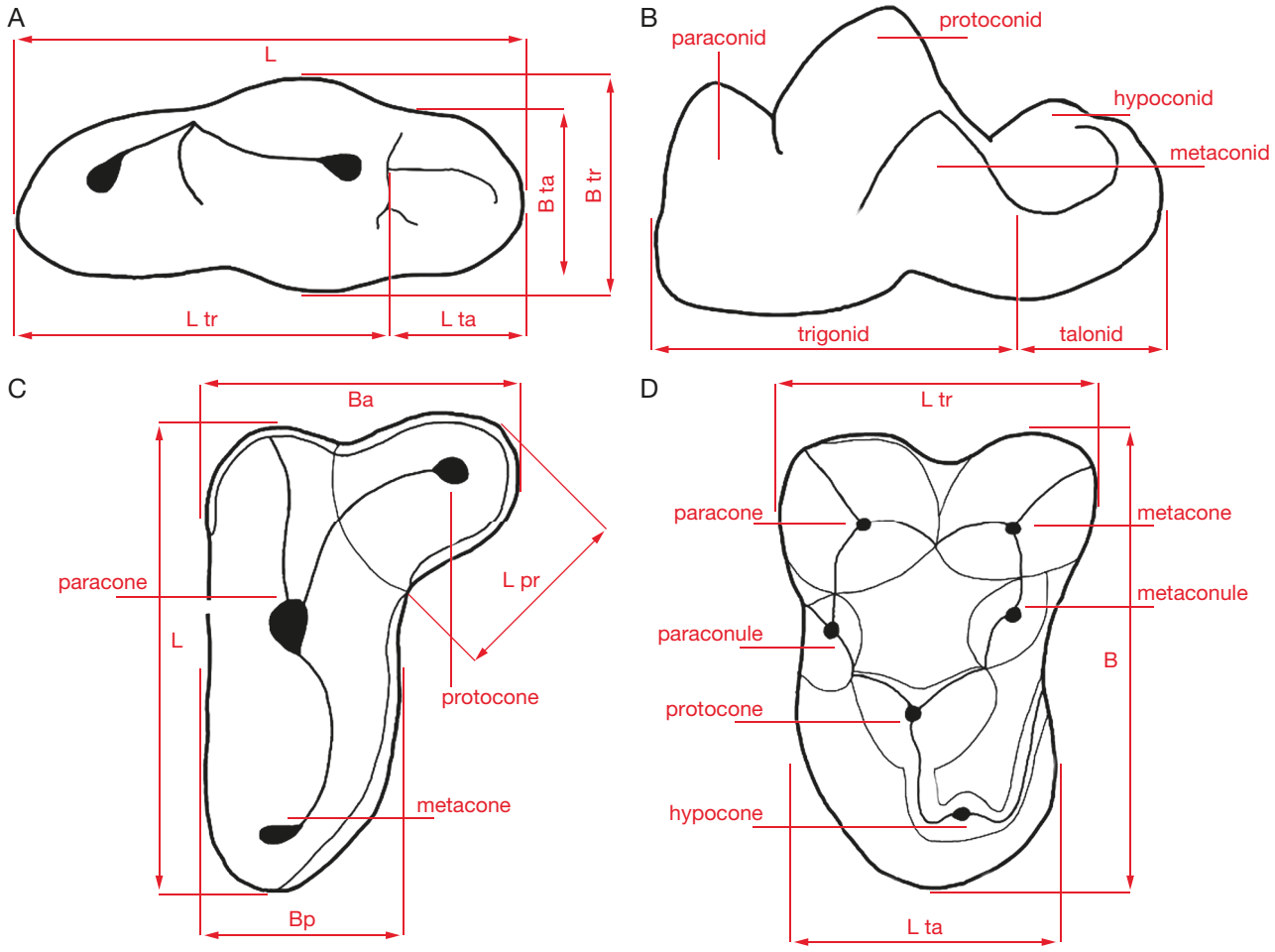

Appendix 7. — Abbreviations of the scheme of measurements and cusp terminology of mustelid teeth available in Appendix 6.

Abbreviations	The teeth measurements
L	total length
L pr	protocone length of P4
L tr	trigon/trigonid length
L ta	talon/talonid length
B	total breadth
Ba	mesial breadth
Bp	distal breadth
B tr	trigonid breadth
B ta	talonid breadth

Appendix 8. — The scheme of measurements of mustelid postcranial bones: **A**, humerus; **B**, ulna; **C**, radius; **D**, femur; **E**, tibia; **F**, fibula; **G**, mc 1; **H**, mc 2; **I**, mc 3; **J**, mc 4; **K**, mc 5; **L**, mt 1; **M**, mt 2; **N**, mt 3; **O**, mt 4; **P**, mt 5. Abbreviations: **dtr**, trochlea breadth; **dB**, breadth of the distal epiphysis; **dL**, length of the distal epiphysis; **L**, total length; **mB**, minimal breadth of the shaft; **mL**, minimal length of the shaft; **pB**, breadth of the proximal epiphysis; **pL**, length of the proximal epiphysis. The abbreviations can be found in Appendix 9.

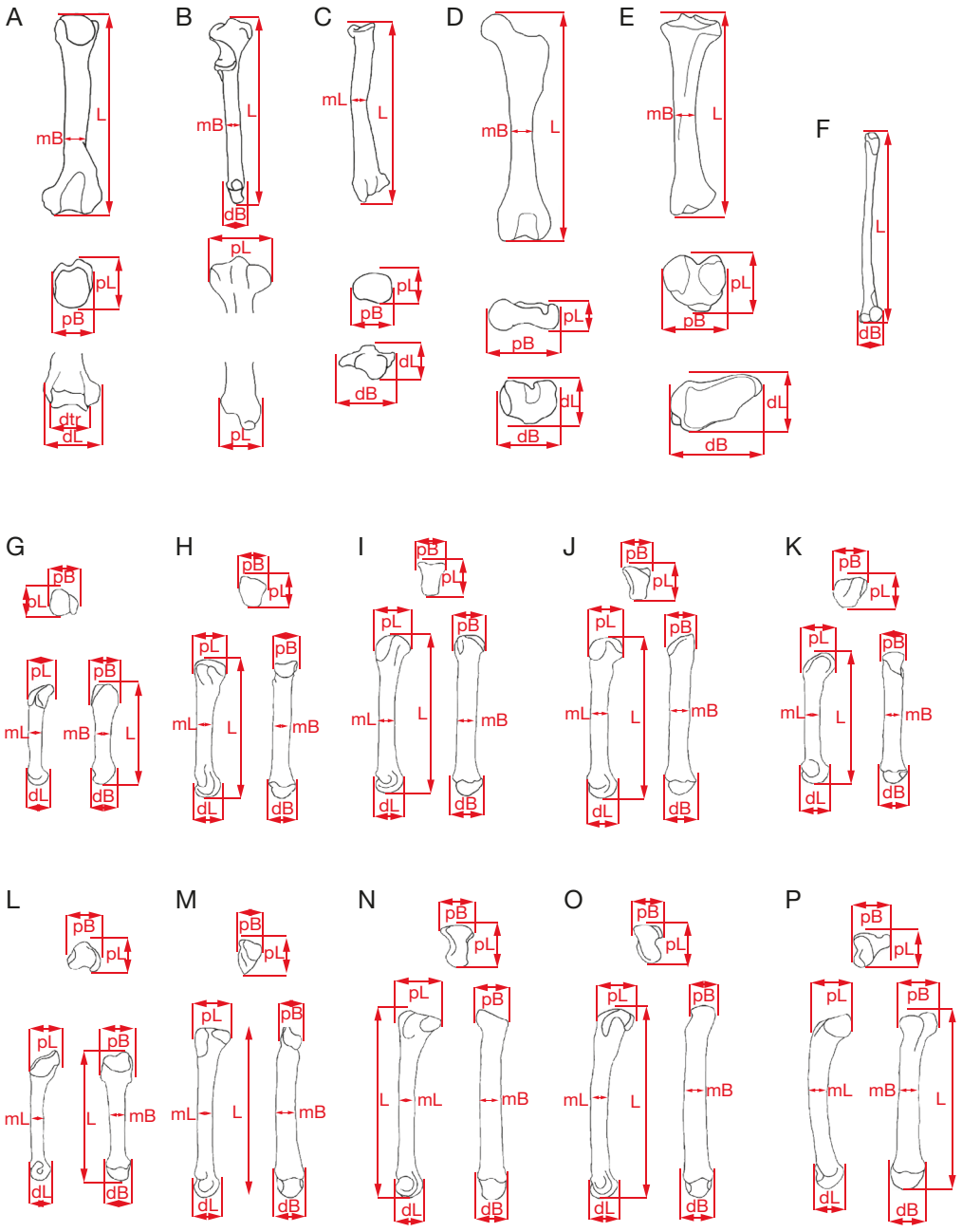

Appendix 9. — Abbreviations of the scheme of measurements of mustelid postcranial bones available in Appendix 8.

Abbreviations	The postcranial bone measurements
L	total length
pL	proximal epiphysis depth
pB	proximal epiphysis breadth
mL	mesial-distal shaft diameter
mB	minimum shaft diameter
dL	distal epiphysis depth
dB	distal epiphysis breadth
B tr	trochlear breadth

Appendix 10. — Raw measurement data of mustelid mammals from Hunas and indexes calculated on their basis, which are one of the basis for marking the remains. All measurements are in mm. Available at: https://doi.org/10.5852/cr-palevol2024v23a23_1

Appendix 11. — Schematic visualisation of p3, p4 and m1 morphotypes of the genus Mustela (modified from Rabeder 1976): **A**, p3: **A1**, oval-shaped outline, not broadened distally (morphotype A1); **A2**, also not widened distally, but with a mesio-buccal projection of the crown edge, which can be developed into a buccal indentation (morphotype A2); **A3**, wider distally than mesial, without buccal bulging (morphotype A3); **A4**, considerably widened distally, the broadening mainly affects the disto-lingual part, the crown outline is strongly asymmetrical (morphotype A4); **B**, p4: **B1**, mesial and distal halves of the crown almost equally wide ((morphotype A); **B2**, crown distally widened, with straight buccal margin and weak to moderate lingual bulging of the lingual margin (morphotype B); **B3**, crown distally considerably widened, with strong bulging of the lingual margin and moderate bulging of the buccal margin (morphotype C); **C**, m1: **C1**, narrow crown, talonid of the same width as trigonid, a poorly marked edge in place of the absent metaconid (morphotype A); **C2**, narrow crown, talonid of the same or almost the same width as trigonid (morphotype B); **C3**, moderate wide crown, with weak to moderate bulging of the buccal margin and straight lingual margin (morphotype C); **C4**, wide crown, with moderate to strong bulging of the buccal margin and moderate bulging of the lingual margin, moderate reduction of the talonid, sometimes with internal, median root located on the lingual margin (morphotype D); **C5**, robust crown, with considerable bulging of the buccal and lingual margins, regularly present internal, median root located on the lingual margin, strongly reduced talonid (morphotype E).